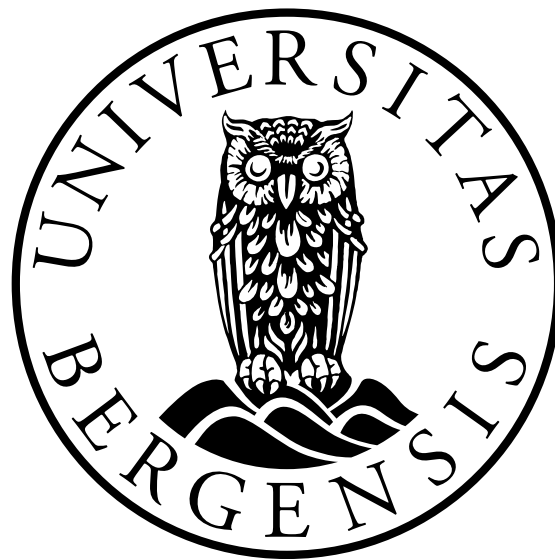# Hydrogen Consumption by Halophilic Microorganisms - Implications for Underground Hydrogen Storage

by

Kelly Ngoc Nguyen

Master in Energy

Integrated Master's Program in Energy at Geophysical Institute

June 2023

Supervised by Prof. Martin Fernø, Dr. Nicole Dopffel and Dr. Na Liu

Department of Physics and Technology

University of Bergen

Acknowledgement

The past five years at the University of Bergen have been an incredible journey, and I am deeply grateful to the individuals who have made it truly memorable and enjoyable. Without their presence, support, and camaraderie, my experience would not have been the same.

First and foremost, I would like to thank my supervisor, Prof. Martin Fernø at the Department of Physics and Technology at the University of Bergen, for his invaluable guidance, support, and the opportunity to undertake this exciting thesis. I would also like to thank my co-supervisor. Dr. Na Liu, for her availability and willingness to address the small and big questions that arose during the completion of this thesis. I express my sincere gratitude and special thanks to my co-supervisor, Dr. Nicole Dopffel at NORCE, for her invaluable guidance, support, and extensive expertise in this exciting field of study. Her profound knowledge, insightful feedback, and dedication have played a crucial role in shaping this thesis.

For my fellow students at the Integrated Master's in Energy, We did it! I am grateful for all the memories and the joyful times in and outside the studies during these five years. A special thanks to my friends in Sal 526, Alicia E. Bang, Marte B. Nåmdal, and occasionally Alexander Flem, for their daily support, encouragement, and fun company upon completing this thesis.

Last but not least, I want to thank my dear family; my mom, dad, and brother, for their endless support and unconditional love. I am truly grateful for everything you have provided me.

Kelly Ngoc Nguyen
Bergen, June 2023

Abstract

Underground Hydrogen Storage (UHS) in reservoirs and caverns is a possible solution for large-scale and long-term storage of hydrogen (H_2) in the subsurface. As the cost of technology installation and electricity from renewable energy, such as solar and wind energy, continues to decrease, utilization and storage of H_2 can accelerate the energy transition. H_2 and UHS can also contribute to energy security and a more sustainable energy system. However, it is essential to understand the potential implications the microbial processes in the subsurface can cause in the UHS.

This thesis quantifies and studies the impacts of different H_2 concentrations and pressures on the microbial H_2 consumption by two metabolic groups; sulfate-reducers and methanogenesis. The sulfate-reducing bacterium (SRB) and the methanogen used in this experiment are *Desulfohalobium retbaense* and *Methanocalculus halotolerans*, respectively. In addition, the microbial H_2 consumption by the SRB was also studied in the micromodel experiment to observe the behavior in porous media.

The metabolic processes of the SRB were inhibited by the high pH of 9.0 in the higher H_2 concentrations and pressures. The highest maximum consumption rate was at 100%H_2 with 0.05 mmoles/day and at 90%H_2 with 0.22 mmoles/day for the SRB and methanogen, respectively. For the different pressures, the maximum consumption rate for the SRB was stable at 0.04 mmoles/day, while for the methanogen was at 2 barg with 0.59 mmoles/day. In the micromodel at 35 barg, the consumption rate for the SRB was $1.23 \cdot 10^{-6}$ mmoles/day. The lower consumption rate could be due to the pore geometry, fewer microbial cells, and unfavorable environments caused by waste and byproducts. The production of H_2S by the SRB was influenced by the high pH, resulting in a dominant sulfide concentration in the form of HS^-. Meanwhile, the microbial activity of the methanogen did not encounter limiting factors, leading to the highest CH_4 concentration of 29.92% at 2 barg.

The SRB was able to inhibit their microbial activity and poses a lower risk for H_2 loss, corrosion, and clogging in UHS. However, the methanogen had effective metabolic processes and consumed the available H_2 regardless and produced CH_4. Therefore, more studies should be conducted to control the microbial activity in the subsurface to ensure safe and stable UHS.

List of Figures

List of Tables

Nomenclature

P	Pressure	[bar]
V	Volume	[m^3]
n	Number of moles	[mol]
R	Gas constant	[m$^3 \cdot$ Pa $\cdot$ K$^{-1} \cdot$ mol^{-1}]
T	Temperature	[K] or [°C]
C	Concentration	[mol/m^3]

Abbreviations

barg	Bar gauge
CCS	Carbon Capture and Storage
CH$_4$	Methane
CO$_2$	Carbon dioxide
DSMZ	Deutsche Sammlung von Mikroorganismen und Zellkulturen
GHG	Greenhouse gas
H$_2$	Hydrogen
H$_2$S	Hydrogen sulfide
IEA	International Energy Agency
LNG	Liquified natural gas
mbarg	Millibar gauge
mmoles	Millimoles
NH$_3$	Ammonia
O$_2$	Oxygen
PV	Photovoltaic
SMR	Steam Methane Reforming
SRB	Sulfate-reducing bacterium (singular) or Sulfate-reducing bacteria (plural)
UHS	Underground Hydrogen Storage
wt%	Weight percent

Contents

Chapter 1

Introduction

1.1 Motivation

The global energy transition is accelerating, driven by increasingly ambitious energy and climate policies, technological developments, and economic considerations. Despite the rapid advancements in clean energy technologies, the majority of the world's energy supply still comes from fossil fuels [1], [2]. In developing countries, the share of fossil fuels in the total primary energy mix increased from 77% in 2000 to 80% in 2021, mainly due to an increase in coal use. In developed countries, the share of fossil fuels decreased from 82% to 77% [1]. Consequently, the global share of energy from fossil fuels remained relatively constant at around 80% [1], [2].

Anthropogenic emissions of carbon dioxide (CO_2) and other greenhouse gas (GHG) emissions over the last decade are at a historic high, which already led to significant changes in the climate system [3], [4], [5]. This includes observed impacts such as an increase in the frequency and intensity of heatwaves across most regions, as well as an increase in the frequency and duration of marine heatwaves. Furthermore, there is an increase in the occurrence, magnitude, and amount of heavy precipitation events globally. Similarly, the Mediterranean region is facing an increased risk of drought. The loss of certain ecosystems and biodiversity may have permanent or long-term consequences [3].

Significant progress still needs to be made to mitigate the emissions and limit global warming to well below 2 °C pre-industrial levels, preferably to limit to 1.5 °C, corresponding to the Paris Agreement from 2015. Over the past decade, the costs of renewable energy technologies

and electricity prices from solar and wind energy have been decreasing. For example, the global weighted-average total installed cost for large-scale solar photovoltaic (PV) installations decreased from 4731 USD/kW to 883 USD/kW, which is a substantial cost reduction of 81% [6]. Similarly, onshore wind and offshore wind experienced declines of 31% and 34%, respectively [6]. During the same time period, the cost of electricity from large-scale solar PV, onshore wind, and offshore wind had a significant decrease of 85%, 56%, and 48%, respectively [6]. The reduction is mainly driven by improvements in technology, an increase in the economy of scale, and the growing demand for renewable energy [6]. The advancement in renewable energy technology and a decrease in costs have made it more viable as an alternative to fossil fuels.

Energy generated from renewable sources like solar and wind energy are highly unpredictable, as it depends on sun light and wind velocity. Therefore, hydrogen (H_2) has been considered an important energy carrier in the energy transition and with a major potential to decarbonize the energy system [7]. The declining electricity costs from solar power and wind power can enhance the competitiveness of green H_2 [6]. As H_2 production increases, large-scale storage solutions are needed to balance fluctuations in the availability of renewable energy, variation in demand, and ensure supply security [8], [9]. One of the options for large-scale and long-term storage of H_2 is in geological formations, such as depleted oil and gas reservoirs, aquifers, and salt caverns [9]. Low-emission H_2, underground hydrogen storage (UHS), and other renewable energy sources have the opportunity to reduce the dependence on fossil fuels. Figure 1.1 illustrates the concept of UHS in the mentioned possible reservoirs and caverns. This transition can reduce the negative associated impacts of burning fossil fuels, in addition to creating a more sustainable energy system and contributing to energy security [8].
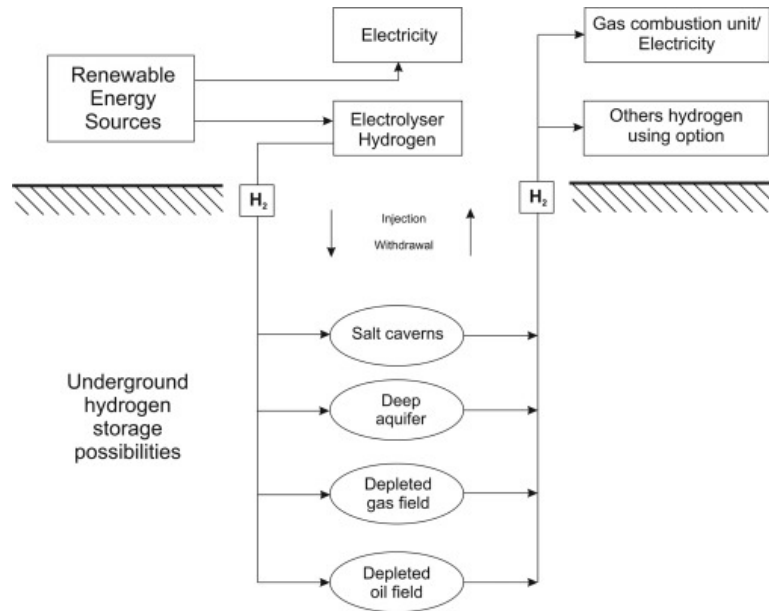
Figure 1.1: Schematic representation of UHS facility including the possible reservoirs and caverns [10].

In the mentioned storage above exists a diversity of microorganisms [11]. H_2 injection in the subsurface artificially increases the H_2 concentration, which the microorganisms can use as a source of energy by consuming the H_2 and stimulating their growth [12], [13], [14]. Additionally, this elevated H_2 concentration can lead to implications such as undesired gas production of hydrogen sulfide (H_2S) and methane (CH_4), corrosion and alteration in stored gas volume [14].

Understanding the microbial process occurring in the subsurface and their implications is crucial for the successful large-scale storage of hydrogen underground.

1.2 Literature Review

With the increasing interest in H_2 production, usage, and storage, there is also growing literature. Several case studies of UHS have been conducted, including in the Netherlands, Spain, Poland, and China [15], [16], [17], [18], [19]. In 2021, there were six sites operating for UHS in the United States (salt dome), the United Kingdom (bedded salt), Czechia (aquifer), and Austria (depleted gas reservoir) [20]. In the scientific community, there is a general consensus about the concerns due to microbial activity in the subsurface for UHS. Among these are H_2 loss, corrosion, and formation of undesirable and unfavorable gases such as H_2S and CH_4 [11], [14], [20], [21], [22].

Dopffel *et al.* [11] highlighted the potential side effects of microorganisms in UHS, namely H_2 loss, corrosion, and formation of undesirable and unfavorable gases such as H_2S and CH_4. The authors conclude that the likelihood of microbial activity is lower for salt caverns compared with aquifers and gas reservoirs. However, it strongly depends on the conditions and other factors such as temperature, pressure, and nutrient availability in each specific reservoir. Furthermore, the authors suggest gaining more experience on the field site to make general predictions on microbial risks.

Thaysen *et al.* [22] published an overview, and the results indicated that there was significant microbial growth and a small H_2 consumption in reservoirs with low salinity and low temperature, which also may increase with repeated storage cycles. Therefore, reservoirs with more extreme conditions, such as high temperature and high salinity, may be preferred in terms of microbial proliferation.

Fournier *et al.* [23] found that the majority of the microbial activity occurred at the beginning of the H_2 injection with the use of a mathematical model. The activity was also correlated to the availability of aqueous CO_2 and $SO_4{}^{2-}$, which sulfate-reducing bacteria and methanogen use in their metabolic process. Furthermore, their laboratory scale model found that the H_2 consumption was at 5% at the end of the experiment. However, the authors highlighted that the laboratory experiment results may not always be directly applicable on a field-scale due to expected differences in behavior.

Dohrmann and Krüger [24] showed that H_2 consumption immediately occurred by microorganisms in a formation fluid from a gas field, without any additional nutrients. This indicated that the microbial H_2 consumption was solely supported by the nutrients already present in the formation fluid. However, the H_2 consumption rate was affected by the availability of H_2

and strongly on sulfate as a terminal electron acceptor. Hence, with insufficient availability of essential nutrients, H_2 consumption will stop. The study demonstrated that there is a significant connection between H_2 consumption and the chemistry of both the rock and fluid in UHS.

The studies presented in this section are related to microbial H_2 consumption based on models and experimental research in the laboratory. Currently, there are no to very few available studies on the impact of different H_2 concentrations and the effect of different pressures on H_2 consumption by halophilic microorganisms. Additionally, there is a need for more research on the quantitative data on the microbial impact of increased H_2 concentrations in the subsurface [11], [25].

1.3 Main Objective

The main objective of this thesis is to study and quantify H_2 consumption of two different groups, specifically sulfate-reducers, and methanogens. Furthermore, the implications of halophilic microorganisms on UHS will be discussed. Halophilic microorganisms are relevant to study for large-scale H_2 storage in salt caverns and saline aquifers.

Two separate experiments were conducted with their own specific objective to address the main objective. The first experiment investigates the impact on the microbial H_2 consumption with different H_2 concentrations over time, while the second experiment studies the impact of different pressures affects the microbial H_2 consumption.

Numerous scientific reports and research papers emphasize the importance of large-scale energy storage for future energy systems. As a result, UHS is identified as a popular option for large-scale storage of H_2. However, several knowledge gaps need to be addressed, including microbial abundance, activity, the effect of elevated H_2 concentration, and the impact of different pressures in the subsurface. Therefore, as the popularity of UHS continues to grow, it is important to research further to fill these gaps and ensure safe and viable storage options for the future.

Chapter 2

Background

2.1 Hydrogen

H_2 is the most abundant element in the universe and is the lightest in the periodic table. H_2 can rarely be found naturally in its free state, as it is usually found in compound form with other elements in liquid, gas, or solids. In the industry, pure H_2 and gaseous H_2-mixtures are essential in oil refineries and the production of methanol and ammonia (CH_4)(mainly for fertilizers) [26]. H_2 is a chemical energy carrier, which is not a source of energy like solar and wind and, therefore, must be produced. There are various energy sources and technologies for the production of H_2. To distinguish between different methods and energy sources of H_2 production, a color categorization has thus been implemented, as seen in Figure 2.1.
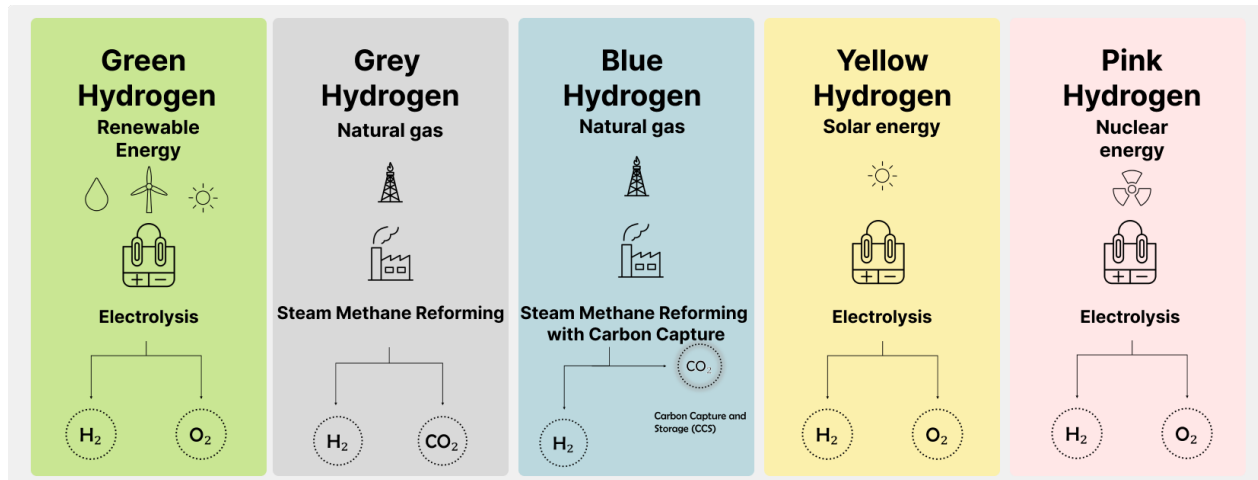
Figure 2.1: Illustration of the colors of H_2 with corresponding production methods and energy sources. Green, yellow, and pink H_2 are produced through the process of electrolysis using renewable energy sources, which include wind, solar and nuclear. Grey and blue H_2 are generated by steam methane reforming (SMR) from natural gas. Blue H_2 includes carbon capture and storage (CCS) to mitigate GHG emissions. Modified from [27] and [28].

The chemical reactions for green H_2 (Equation 2.2) and grey H_2 (Equation 2.2) show that the former will not release any emissions, thus making it a clean and sustainable source of energy. On the other hand, grey H_2 will emit CO_2 in the reformation process and contribute to global warming [26].

$$2\,H_2O \longrightarrow 2\,H_2 + O_2 \tag{2.1}$$

$$CH_4 + 2\,H_2O + \text{heat} \longrightarrow 4\,H_2 + CO_2 \tag{2.2}$$
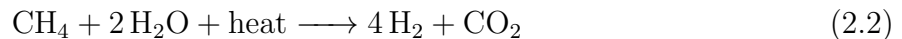
To fully leverage the strengths of H_2, it is essential to have a comprehensive understanding of its physical and chemical properties (see Table 2.1), as well as health and safety concerns. These properties determine its behavior and usage in a wide range of applications. H_2 is non-toxic, colorless, and odorless. However, it is highly flammable and can form explosive mixtures with air. Furthermore, it has a high gravimetric energy density, which refers to the energy stored in a unit of mass. It is three times higher than natural gas, with 140 MJ/kg compared to 54 MJ/kg. However, the volumetric energy density, representing energy stored per unit of mass, is relatively low. The energy content of liquid H_2 is 10 MJ/L, whereas

that of liquid natural gas (LNG) is 22 MJ/L [29]. Energy from H_2 can be released through combustion or electrochemical reactions in a fuel cell.

Table 2.1: A selection of H_2 properties [29], [30].

Property	Value
Atomic weight	1.008 g/mol
Density at 0 °C	0.090 kg/m^3
Liquid density	70.08 kg/m^3
Boiling point	-253 °C
Melting point	-259.14 °C
Flammability range in air	4-75% vol
Minimum ignition energy	0.017 MJ

The behavior of H_2 gas in UHS can be influenced by various factors such as salinity, temperature, pressure, and the presence of other solvents and gases. An increasing temperature leads to a decrease in solubility in water, as indicated in Figure 2.3 [31]. However, the H_2 solubility in brine is different due to the presence of salt affecting the properties. H_2 solubility in brine is less studied compared to pure water [32]. As subsurface reservoirs, such as salt caverns and saline aquifers, are in direct contact with residual brine and formation water, it is important to understand the behavior of H_2 in contact with brine. Similar to all gases, the presence of salt decreases the solubility. Therefore, the H_2 solubility in brine is expected to decrease proportionally with increasing concentrations of salt, known as the "salting-out effect" [32]. The H_2 solubility in brine is determined by the temperature, pressure, salinity, and composition of salt. Figure 2.2 illustrates the measured solubility of H_2 in brine for 50 °C and 100 °C with pressure. The highest salt concentrations of 5M have the lowest solubility with increasing pressure compared to 3M, 1M, and pure water.
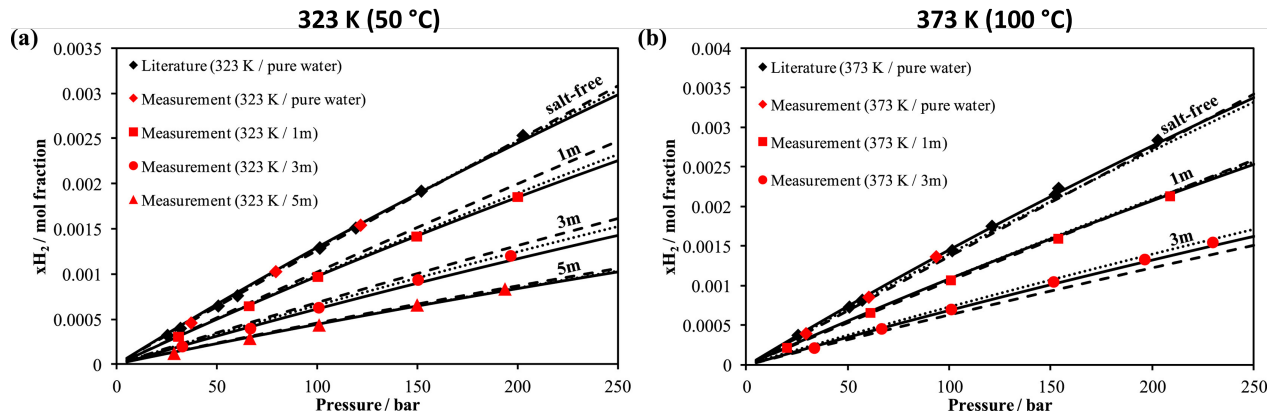
Figure 2.2: The measured solubility of H_2 gas in brine for a) 323 K or 50 °C and b) 373 K or 100 °C. Modified from [33].

The temperature and pressure depend on the type and location of the subsurface storage, and the solubility varies depending on the specific gas. At standard conditions, the solubility of H_2 is 0.0014 g H_2 per kg water at 37 °C. H_2 has a very low solubility compared to gases like H_2S (approx. 2.5 g H_2/kg water) and CO_2 (approx. 1 g CO_2/kg water) [34].
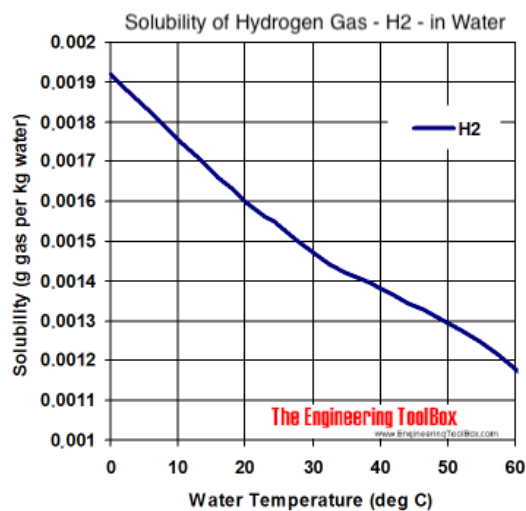
Figure 2.3: The solubility of H_2 gas in water [34].

Increasing the partial pressure will result in a higher gas solubility in the liquid. The high pressure increases the concentration in the gas phase, and the collision frequency is higher, which causes gas molecules to dissolve in the liquid to achieve dynamic equilibrium [31]. This relationship can be observed in the ideal gas law, as shown in Equation 3.1.
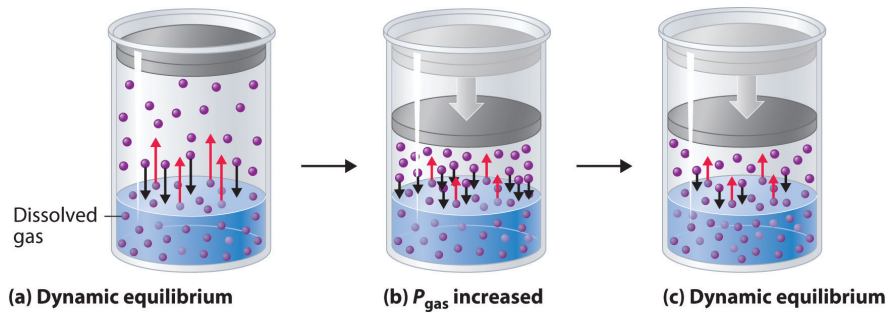
Figure 2.4: The effect of gas pressure on the solubility of gas in a liquid [31].

2.2 Hydrogen Storage

The advantages of H_2 stem from its adaptability and versatility. As mentioned above, there are different technologies and methods to produce H_2. H_2 can be transported as a gas by pipelines or in liquid form by ships. Moreover, it can also be transformed into electricity and methane to power homes and feed industry and into fuels for vehicles [26]. Several methods exist to store H_2 for transportation and later use. The most mature and common approaches to storing H_2 are physical storage as compressed gas and cryogenic liquid H_2. The initial method involves compressing H_2 at high pressure and storing it as pressurized gas in cylinders, containers, or underground caverns [35]. Depending on the type of storage, duration, and end-use, the pressure for compressed H_2 may vary. It is typically stored in high-pressure tanks with a range of 250-700 bar [36].

Meanwhile, liquid H_2 is stored in cryogenic tanks at extremely low temperatures (-253 °C). To maintain the liquid state, it is necessary to lower its temperature to the critical temperature of -240 °C, after which it can be stored below boiling point (-253 °C at 1 atm). As liquid H_2 is stored in cryogenic temperatures, equipment in direct contact must be specifically designed and manufactured to withstand these extreme conditions. Failure to do so could lead to material rupture in components such as valves, vents, and pipes due to ice formation [37]. Moreover, liquid H_2 (at -253 °C) has a significantly higher density with 70.85 kg/m^3 compared to 0.08987 kg/m^3 for compressed H_2 (at 0 °C and 1 atm) [37].

Another challenge is a phenomenon called boil-off. Boil-off arises when heat leaks through the thermal insulation of the storage and supporting elements. As a result, the liquid H_2 will evaporate in the tanks, and the pressure increases [7]. To avoid pressure buildup and not let the pressure exceed the tank's upper limit, the boil-off is released through a relief valve [38]. The boil-off rate refers to the amount of hydrogen lost over time and is expressed as

a percentage of the total amount of hydrogen in storage [39]. The boil-off rate depends on thermal insulation, tank size, shape, and dimensions. According to [40], the rate is 1.5-3% per day, while [7] states 0.1-1% per day.

Chemically storing H_2 in NH_3 is considered an attractive and promising method. NH_3 has a high H_2 density with 17.7 wt% gravimetrically, while liquid NH_3 at 10 bar is 123 kg/m^3 volumetrically [39]. Furthermore, the infrastructure for production, transport, and storage is already mature and prevalent on an industrial scale for manufacturing fertilizers [41]. Compared to liquid H_2, storing liquid NH_3 does not require extremely high pressures. Liquid NH_3 can be stored at ambient temperature and moderate pressure of 25 °C and 9.9 bar, which reduces the complexity and cost of the storage system and makes it less expensive to store than H_2 [42].

The flammability range of NH_3 is narrow, ranging from 15 to 28 percent in air. By comparison, the flammability range is broader, with a range of 4 to 75 percent, as seen in Table 2.1. Thus, NH_3 can be a fire hazard if exposed to an ignition source and the concentration is within the flammability range. However, NH_3 has a low reactivity at a stoichiometric concentration of 22%, making it less prone to fire or explosion. The risk of explosion is significant in confined spaces with concentrations close to stoichiometry [43].

Other challenges associated with the storage of NH_3 include the major drawback and primary concern of its toxicity. Prolonged exposure to NH_3 levels above 2500 ppm (0.25%) can be fatal, whereas exposure to 40 000 ppm (4%) can result in immediate fatality [43]. Hence, handling NH_3 with proper safety measures and sufficient training is crucial.

2.3   Underground Hydrogen Storage

The concept of storing large quantities of gases in the subsurface has existed for some time. According to Taylor *et al.* [44], natural gas has been stored underground since 1916. Some parts of the process of storing H_2 are similar to the storage of natural gas, such as site specifications and storage operation. The skills related to characterization and knowledge about geological formations are transferable, indicating that the knowledge and experience gained from natural gas storage can be directly applied to hydrogen storage [20]. However, the difference in physiochemical properties between H_2 and natural gas is crucial in terms of subsurface storage, such as the high diffusivity of H_2 poses the risk of leakage [45]. The chemical affinity of H_2 can react with the surrounding rocks and cause mineral dissolution,

changing the permeability and porosity in the carbon-containing reservoir [11]. Porosity is defined as the fraction of the void space of the bulk volume of the reservoir, and the rock's ability to allow for fluid flow through the interconnected pores is the permeability [46]. The microorganisms in the subsurface can utilize H_2 in their metabolism, which can cause H_2 loss [11], [20], [22]. As for now, the practical experience with underground hydrogen storage in geological formations is limited. Although this subject has been up for discussion for over three decades, it continues to generate interest, reflected by an increasing number of articles and studies [17]. The major long-term effects of H_2 storage are mainly untested. Further research is therefore needed to understand these challenges [21], [47], [48]. Nevertheless, the expectations for UHS as energy storage are high.

As previously mentioned, the idea of UHS is not new but has increased in popularity due to the energy transition and strategy associated with net-zero emissions. In addition to the potential to store a large amount of hydrogen for later use as an energy source [49]. Several objectives that UHS can contribute to are regulating the balance between energy supply and demand during times of excess energy production, regulating energy prices, overcoming challenges affecting renewable methods, providing a hydrogen backup supply to industry for increased energy security, and supporting the transition towards a low carbon economy [49].

Underground storage of gases in geological sites may be divided into porous media and cavern storage. The former stores the gas in the pore space within carbonate or sandstone formations, while the latter stores gas in underground cavities created either through excavation or naturally formed by the dissolution of rock [20]. According to Heinemann *et al.* [21], experience with UHS in porous rock formations is very limited. Currently, the predominant use of this technology is for the storage of town gas, which is composed of a gas mixture containing 25-60% H_2, 10-33% of CH_4, less than 30% of N_2, and 12-20% of CO and CO_2 [21].

For H_2 storage in the subsurface, several types are available such as depleted gas/oil reservoirs, artificial salt caverns, deep aquifers, hard rock caverns, and abandoned mines. Figure 2.5 illustrates the three main types of underground gas storage that have been proposed, which are depleted oil/gas reservoirs, saline aquifers, and salt caverns [11], [20], [48].
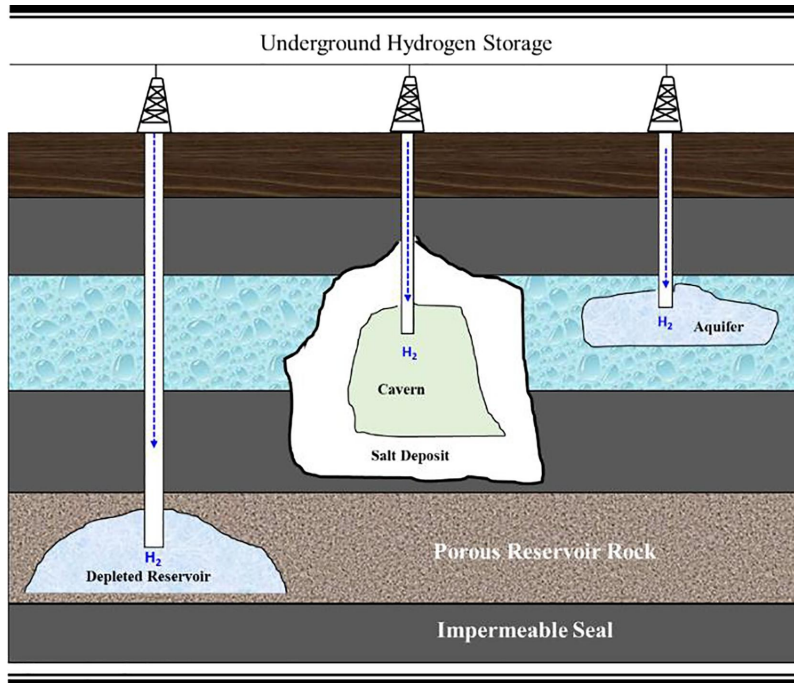
Figure 2.5: UHS in a depleted reservoir, salt cavern, and aquifer [48].

2.3.1 Depleted Oil/Gas Reservoirs

Due to their long existence, the most widespread underground porous media in the geological subsurface are depleted oil and gas reservoirs. Properties such as substantial pore space, high permeability, integrity and tightness of cap rock, and well-characterized geological structures make them a popular option for gas storage [20], [50]. Therefore, it is crucial to have a solid cap rock to prevent leakage of the stored gas [50]. In porous rock, such as depleted oil/gas reservoirs and aquifers, the operating pressure can be up to 200 bar [51].

Given that the infrastructure is well-implemented and exists for gas storage, it is considered to be economically viable for the storage of hydrogen [25]. Storing H_2 in the geological subsurface consists of the pre-injection of cushion gas before injecting hydrogen [20]. The cushion gas is injected to maintain sufficient operating pressure in the storage [21]. Depleted gas reservoirs are more commonly used in underground storage. In storing hydrogen, such reservoirs already have the necessary installation on the surface and subsurface. Furthermore, residual gas is advantageous because it can be used as cushion gas. However, it may also influence the purity of H_2 gas in storage [20]. A considerable presence of sulfate has been found in depleted oil and gas wells, which microorganisms can utilize in their metabolisms to enhance microbial proliferation [45]. The interaction between residual oil and H_2 can also cause

undesired reactions. Overall, these reactions may lead to the dissolution of H_2, microbial H_2 consumption, and microbial production of H_2S and CH_4. Furthermore, alteration and loss of H_2 in the storage can occur [10], [11], [45].

2.3.2 Saline Aquifers

Saline aquifers are porous and permeable rock formations where the pore space is occupied by water or brine at a great depth [10], [20]. The porous and permeable rocks are mostly sandstone or carbonate [45], [52].

To store H_2 in the pore space of the aquifer, the H_2 needs to displace the water or brine present in the pores to create storage space, mainly in the near-well region. The H_2-injection increases the pressure in the aquifer. A pressure exceeding the limit of the aquifer can cause cracks in the formation, which result in leakage of H_2 [53]. Upon H_2 withdrawal, the pressure will drop and can cause some of the displaced water or brine to move upwards the well and mix with the gas. The movement of gas and water or brine during the injection and withdrawal can cause shifting of the gas/water boundary. Consequently, causing the water or brine to trap the gas and the residual gas cannot be recovered later [10], [49], [54], [55]. The residual fluid can also interact with the H_2 and may cause undesired production of H_2S [49]. Figure 2.6 illustrates the trapping mechanisms of H_2 storage in geological formations.
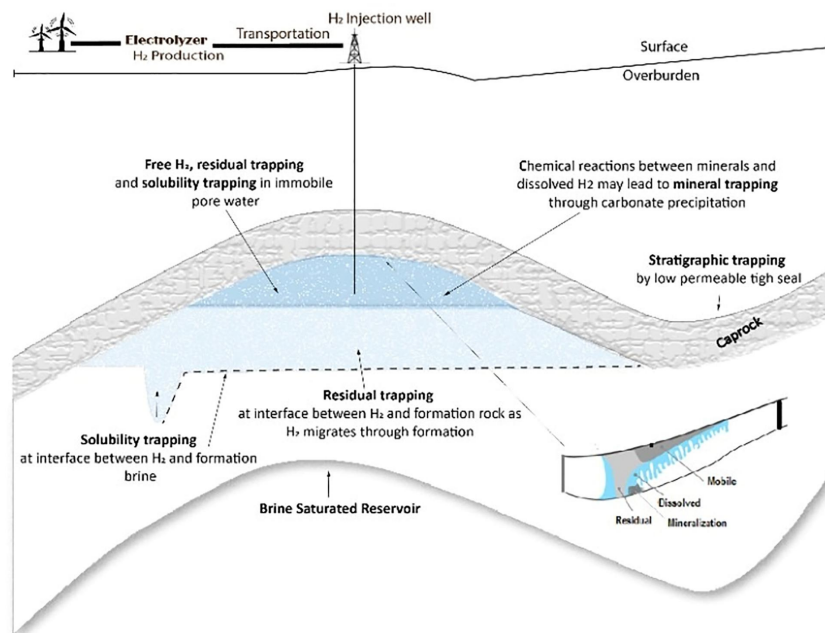
Figure 2.6: Overview of trapping mechanisms in underground hydrogen storage within geological reservoirs, such as depleted oil/gas reservoirs and aquifers [49].

Saline aquifers are common and can be found in most parts of the world. Their widespread occurrence makes them a good option in areas where depleted reservoirs or salt caverns are unavailable [10], [20]. Furthermore, saline aquifers often have a large storage capacity. However, the volume of stored gas depends on factors such as the reservoir's volume and porosity, as well as the temperature and pressure of the storage [10], [56].

Several factors can determine storage efficiencies, such as biochemical reactions, chemical reactions, leakage, and cushion gas [20], [54]. The presence of microorganisms has been reported in saline aquifers, which can utilize the injected H_2 in the metabolism and produce gases such as CH_4 and H_2S. The increased hydrogen concentration injected into the storage could stimulate the microorganisms. This results in H_2 loss, corrosion, alteration of the original gas mixture, and pore space clogging [14], [54]. Saline aquifers require large cushion gas volume to main the operational pressure and maintain a desired production rate [45], [54]. A study by Heinemann *et al.* [54] revealed the importance of cushion gas in saline aquifers. The study found that the cushion gas directly impacts the storage capacity and controls both injectivity and productivity of H_2 [54].

2.3.3   Salt Caverns

Salt caverns are artificially created in the subsurface by solution mining or leaching, as illustrated in Figure 2.7. This technique involves injecting fresh water or seawater from the surface into a well in the salt deposits [51], [57]. Subsequently, the water is withdrawn before filling the cavern with H_2 for storage [45], [51]. During this process, water may be trapped at the bottom of the cavern [45], [58]. Furthermore, the process is performed in a controlled manner on typically salt domes or bedded formations, which are considered to be ideal for salt caverns [50], [59]. Salt caverns are mostly cylindrical and are appropriate for gas storage under high pressure. The operating pressure in a more than 1000 meter deep cavern may exceed 200 bar [51], [57]. The storage capacity is affected by the depth of the cavern. A greater cavern depth leads to high pressure and increased capacity for compressed gas storage. However, a lower depth requires less cushion gas and therefore reduces the operation cost [20].
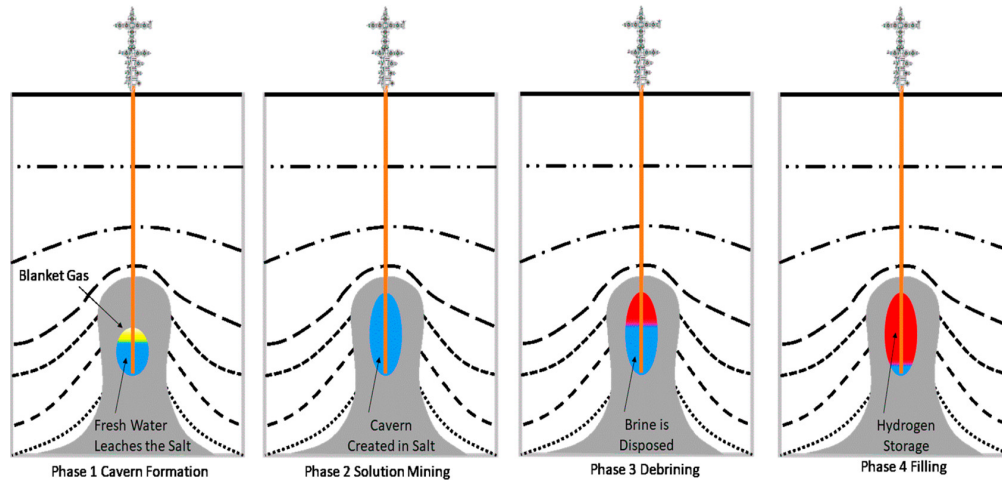
Figure 2.7: The process of salt mining in the four phases of identifying a suitable cavern formation, solution mining/leaching, debrining, and filling with H_2 for subsurface storage [45].

According to International Energy Agency (IEA) [26] and Raza *et al.* [49], salt caverns are recognized as the best option for underground hydrogen storage compared to depleted oil and gas reservoirs and aquifers. Advantages such as their tightness and lower risk of contamination compared to others are contributors. The high salinity environment causes osmotic stress for the present microorganisms, reducing diversity and abundance. However, halophilic (salt-loving) and halotolerant (salt-tolerant) microorganisms are commonly found in high-salt conditions [11], [60]. H_2 consumption can, therefore, also occur in these extreme conditions (high stress and high salinity) and does not necessarily lower the risk. However, the risk of microbial activity is lower in salt caverns than in aquifers and depleted gas reservoirs. In addition, a cavern has a smaller surface area than porous media and therefore is less prone to biofilm formation and clogging [11].

Successful storage of hydrogen in salt caverns has been conducted in the United States of America, the United Kingdom, and Germany [10], [49]. However, the salt cavern's storage capacity is lower than aquifers and depleted oil and gas reservoirs [45].

2.4 Microorganisms

To thoroughly study the impact of microorganisms in UHS, it is essential to have a comprehensive understanding of the behavior of various microorganisms, their metabolic processes, and their corresponding effects on the subsurface environment. In the subsurface, the diverse community of microbial organisms includes two significant groups of unicellular organisms,

namely Archaea and Bacteria. They are responsible for many biochemical and geochemical reactions [11], [50], [61].

In the subsurface, molecular hydrogen is considered a central electron donor for various microbial respiration processes [11]. This is because H_2 contains a low reduction potential, meaning it has a high capacity to donate electrons [14]. According to Zivar *et al.* [20], the reaction rate can be influenced by the concentration of H_2. The high concentration of H_2 in storage sites can thus accelerate the reaction. In addition, different groups of organisms can use H_2 in their metabolic processes [11]. Two processes in the subsurface contribute to H_2 consumption and generation; abiotic and biotic [14], [20], [50]. Abiotic refers to non-living components like water, rock minerals, and gases. While biotic refers to living components, such as microorganisms [20], [50]. Abiotic processes can operate at temperatures up to 600 °C, whereas biotic processes require cooler environments where conditions are more optimal for supporting life [14], [20]. Methanogenesis, sulfate reduction, acetogenesis, and iron (III) reduction are typical biotic processes known for hydrogen consumption in underground gas storage wells [20], [50]. They have been observed to occur at temperatures up to 90 °C and at very high salinities of around 340-350 g/L [11], [62]. To compare the high salinity, the salt concentration in seawater is 35 g/L [63]. Only the two metabolic processes of sulfate-reduction and methanogenesis will be further addressed as they are more relevant in this thesis.

2.4.1 Sulfate-reducing bacteria

In the presence of sulfate, sulfate-reducing microorganisms are recognized for utilizing H_2 and producing H_2S, seen in Equation 2.3. The role of sulfate-reducing bacteria (SRB) is significant in H_2 storage in porous media and salt caverns [45]. Their metabolism or sulfate-reduction is highly efficient, whereby small quantities can result in a substantial amount of H_2S [11]. Additionally, the gas formation is toxic and can pose serious health concerns for humans or be fatal when exposed. An exposure of 500 ppm H_2S in the air causes severe poisoning, while 900 ppm leads to immediate fatality [33]. Furthermore, this byproduct from the SRB has a corrosive effect on the equipment in the facility and can contribute to catalyzing H_2 embrittlement. The purity of the H_2 storage can also be altered with the presence of H_2S [45]. The presence of sulfide can reduce the pH in porous media and cause mineral dissolution and clogging [45].

The chemical equation for sulfate reduction is the following [14]:

$$\frac{1}{4}\,SO_4{}^{2-} + H_2 + \frac{1}{4}\,H^+ \longrightarrow \frac{1}{4}\,HS^- + H_2O \tag{2.3}$$
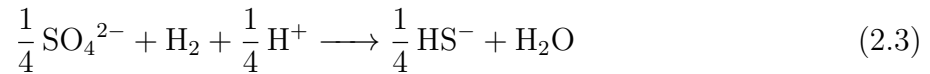
The pH is a crucial factor affecting the metabolism and growth of the SRB. Changes in pH can destroy cell homeostasis, which is important for the balance of the internal environment within the SRB [64].

Alteration in pH can also affect the surrounding substances in the solution, thereby impacting the SRB. The presence of sulfide species (H_2S, HS^- and S^{2-}) is dependent on the pH as it can affect the chemical balance, as illustrated in Figure 2.8 [64], [65], [66]. In acidic solutions (pH < 7.0), the sulfides exist mainly in the form of H_2S. However, H_2S is a volatile gas likely to exist in the gaseous form, which can cause loss of H_2S to the air [66]. In alkaline solutions (pH > 7), the sulfides primarily exist as HS^-. The sulfide concentration is higher because HS^- is more stable in alkaline conditions [66]. Kushkevych *et al.* [67] found that acidic and alkaline pH outside their optimum range inhibited metabolic activity and growth of SRB. The rate of inhibition was higher towards lower or higher pH. Thus, the production of H_2S by the SRB also affects their growth.

Changes in the pH can also affect the metabolism of competing and collaborating microorganisms in the solution, especially methanogens. SRB and methanogens are known for competing for the same substrates, mainly acetate and H_2, under anaerobic conditions [68]. In sulfate-rich environments, the SRB generally outperforms the methanogen. However, the coexistence depends on the conditions and the present substrates [68]. A high initial pH inhibits the competition between SRB and methanogen and promotes the latter's growth [64]. However, these mentioned findings are from wastewater. Therefore, conditions like pH, temperature, and nutrient availability may differ from those in underground gas storage.
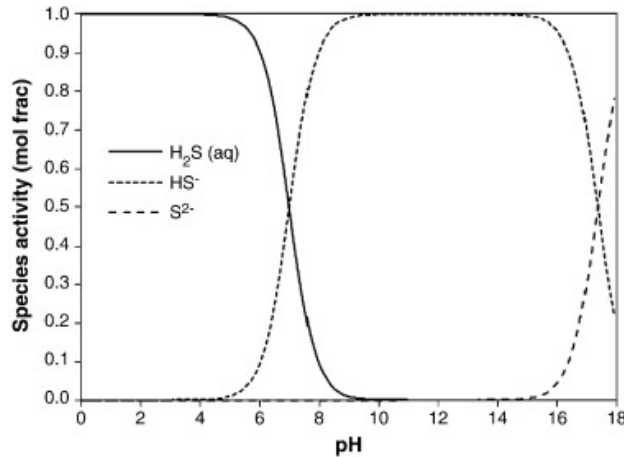
Figure 2.8: The relationship between sulfide (H_2S, HS^- and S^{2-}) and pH. In acidic conditions (low pH), the concentration of H_2S is higher than HS^-. As the pH increases and alkaline conditions occur, sulfide primary exists as HS^-. S^{2-} is dominating at very high pH [69].

2.4.2   Methanogens

Methanogens belong to the Archaea domain and are highly sensitive to oxygen. Therefore require strictly anaerobic conditions for their survival and growth [70]. They are known for reducing CO_2 to produce CH_4 by oxidizing H_2, as illustrated in Equation 2.4. This metabolic process is called methanogenesis [22]. The CH_4 formation may result in the loss of H_2 in UHS and increased CH_4 concentration. CH_4 is the second most important greenhouse gas after CO_2, which significantly contributes to global warming [70]. Furthermore, this gas alteration may reduce the efficiency of the storage system, and less H_2 would be available for utilization [47].

The following chemical equation is the process of methanogenesis [11].

$$\frac{1}{4}\,HCO_3^- + H_2 + \frac{1}{4}\,H^+ \longrightarrow \frac{1}{4}\,CH_4 + \frac{3}{4}\,H_2O \tag{2.4}$$
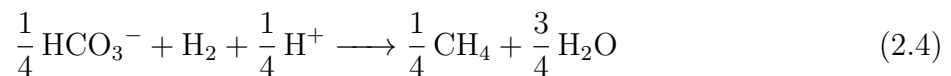
As mentioned in Section 2.4.1, the methanogen can co-exist and compete with the SRB. Methanogenesis can still occur in the presence of sulfate, but the SRB outcompetes the methanogen in high-sulfate environments [14].

Methanogens are capable of occurring in extreme conditions, such as high salinity. The high salt concentration can lead to osmotic stress. Therefore, they have developed two mechanisms to withstand the osmotic pressure and achieve osmotic balance. The first strategy is the

"salt-in" strategy, which accumulates high ionic concentrations, while the other is to exclude the salt from their cells and use another solute that does not interfere with other processes [22], [71].

Chapter 3

Methods

The following chapter will introduce and describe the experimental methods used in the experiments. Four experiments were conducted in the Norwegian Research Center (NORCE) laboratory in Bergen. Imaging of the microbial H_2 consumption in micromodel was performed by Dr. Na Liu in the laboratory at the Department of Physics and Technology at the University of Bergen. The strains used in the experiments are *Desulfohalobium retbaense* (DSM 5692) and *Methanocalculus halotolerans* (DSM 14092), which were ordered from Deutsche Sammlung von Mikroorganismen und Zellkulturen (DSMZ) website.

3.1   The Strains and Growth Conditions

Desulfohalobium retbaense (DSM 5692) is a halophilic sulfate-reducing bacterium. It was first isolated from saline sediment in a hypersaline lake in Senegal [72]. This bacterium requires acetate and vitamins for growth, but can also be replaced with Biotrypcase or yeast extract. The SRB can also use different electron acceptors to reduce to H_2S, such as sulfate, sulfite, thiosulfate, and elemental sulfur [72].

According to Ollivier *et al.* [72], the growth for *Desulfohalobium retbaense* occurs at pH between 5.5 and 8.0, while the optimum growth is at pH between 6.5 and 7.0. The optimum temperature for growth is 37 °C to 40 °C. The strain grows up to a NaCl concentration of 24% in the growth medium. However, when the concentration in the medium increased to 20%, the activity was greatly reduced. The optimum growth occurs when the NaCl concentration is around 10%.

Methanocalculus halotolerans (DSM 14092) is a halotolerant methane-producing archaeon or methanogen. It was first isolated from saline oil field water in France [73]. The methanogen required acetate in addition to an 80% H_2 and 20% CO_2 mixture to produce methane, similar to Strain SEBR 4845^T described in [73]. They observed that the growth occurred at a pH between 7.0 and 8.5, with an optimum pH of 7.6. The optimum growth temperature is 38 °C, and no growth occurred at temperatures below 24 °C or above 50 °C. The growth occurs in NaCl concentration ranging between 0 % and 12.5%, with optimum growth at 5%. Furthermore, this strain is highly sensitive to oxygen (O_2) and does not grow in an oxidized medium [73].

Desulfohalobium retbaense and *Methanocalculus halotolerans* thrive in environments with high salt concentrations, although the latter is not strictly halophilic. Moreover, they are anaerobic microorganisms, which implies their ability to survive and grow without O_2.

3.2   Preparing the Media

When studying microorganisms in a laboratory, growing them in controlled conditions is crucial. They need certain nutrients and environmental conditions, such as optimum temperature and pH, to grow. Microorganisms are remarkably diverse and require different types of growth media. The growth media are prepared with specific nutrients that are stated in the media sheet for microorganisms.

To make the growth media for *Desulfohalobium retbaense*, DSMZ Medium 499 recipe was followed with some modifications. Despite being specified in the media sheet, the carbon sources of lactate, yeast extract, and trypticase peptone were not added to the media. These modifications were made to have complete control over the carbon sources and nutrients for experimental purposes. The Medium 499 provides the nutrients to prepare the optimal growth medium for the SRB. By adding lactate, the SRB would have used it as an electron donor instead of H_2, and the purpose of this thesis is to study the utilization of H_2. The content in Trypticase peptone is unknown and, therefore, not included. The selenite-tungstate solution was also excluded because it was unavailable in the laboratory's inventory. Table 3.1 shows the media sheet with the modifications. The medium was sparged with 100% N_2 to create an anoxic environment. The pH of the medium should be between 6.8 and 7.0.

Table 3.1: Modified DSMZ Medium 499 recipe for *Desulfohalobium retbaense*.

Media for *Desulfohalobium retbaense*		
Ingredients	Amount	Unit
NH_4Cl	1.00	g
K_2HPO_4	0.30	g
KH_2PO_4	0.30	g
$MgCl_2$ x $6\,H_2O$	20.0	g
NaCl	100.00	g
$CaCl_2$ x $2\,H_2O$	2.70	g
KCl	4.00	g
Na_2SO_4	3.00	g
Trace element solution SL-10	1.00	mL
Sodium resazurin (0.1% w/v)	0.50	mL
Na_2S x $9\,H_2O$	0.30	g
Distilled water	1000.00	mL

The growth media for *Methanocalculus halotolerans* was made by following the recipe for DSMZ Medium 905. Similar to the previous strain, the media for *Methanocalculus halotolerans* also excluded the carbon sources yeast extract and trypticase, in alignment with the abovementioned reason. L-Cysteine HCl x H_2O was also not included due to unavailability. Table 3.2 shows the added nutrients in the medium. The medium was sparged with 80% N_2 and 20% CO_2 mixture to create an anoxic environment. In addition, the pH should be in the range between 7.2 and 7.6.

Table 3.2: Modified DSMZ Medium 905 recipe for *Methanocalculus halotolerans*.

Media for *Methanocalculus halotolerans*		
Ingredients	Amount	Unit
NH_4Cl	1.00	g
K_2HPO_4	0.30	g
KH_2PO_4	0.30	g
KCl	0.17	g
NaCl	50.00	g
Modified Wolin's mineral solution	10.00	mL
Sodium resazurin (0.1% w/v)	0.50	mL
$NaHCO_3$	2.00	g
$CaCl_2$ x $2\,H_2O$	0.60	g
$MgCl_2$ x $6\,H_2O$	3.20	g
Na_2S x $9\,H_2O$	0.30	g
Distilled water	1000.00	mL

To ensure consistent volumes for all the small bottles, they were marked at a volume of 25 mL (Figure 3.1) of the 50 ml bottles and 50 mL of the 100 ml bottles prior to preparation.

Figure 3.1: 50 mL bottles used in experiments filled with 25 mL medium, in addition to nutrients.

The procedure to prepare media for the microorganisms was as follows:

1. Weighted the nutrients as stated in the specific media recipe in Table 3.1 and Table 3.2. Poured them into a bottle with a screw cap.

2. Measured distilled water as stated in the media recipe and added into the same bottle.

Shook the bottle to mix the nutrients with the distilled water.

3. Poured the media into the Widdel flask (Figure 3.2) with a funnel to avoid spillage.
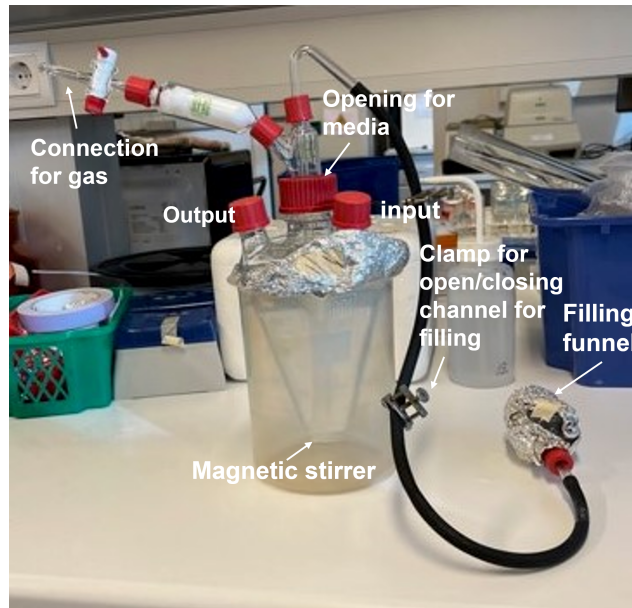
Figure 3.2: The Widdel flask was utilized to prepare media for the experiments. The two red lids (input and output) on the front were slightly open during autoclaving.

4. Autoclaved the Widdel flask with the media inside. The two red lids on the front were not entirely closed to prevent an explosion. The rest was closed. Placed bottles (Figure 3.1) that were used in the experiments in a beaker to autoclave.

5. While the bottles were autoclaved, the setup (seen in Figure 3.3) was prepared under the fume hood with the two lines of the stated gas mixture, a magnetic stir bar, a magnetic stirrer, and a stand to stabilize the Widdel flask. Flushed the gas lines for one minute to ensure no contamination of other gases.

Figure 3.3: The experimental setup for preparing media under the fume hood.

6. Removed the Widdel flask from the autoclave before it was reduced to 80 ℃. It was crucial because temperatures over 80 ℃ removes the O_2 from the media and sterilize it. Installed the Widdel flask as seen in Figure 3.3 under the fume hood. Connected the stated gas mixture (100% N_2 for SRB and 80% N_2 + 20% CO_2 for methanogen) to the Widdel flask and open the lines to make it anoxic (see Figure 3.2). The red front lids were slightly open. The whole process of removing the Widdel flask from the autoclave and connecting it to the gas mixture under the fume hood lasted less than three minutes to avoid contamination of O_2.

7. Cooled down the media by showering the Widdel flask with cold water and drained the hot water into a separate beaker until the media had a comfortable temperature.

8. The burner was turned on to make the area sterile when adding and removing into the media. The red lid to the right was for input or adding, and the left was for output or removing. Add vitamin, resazurin, and carbonate through the red lid on the right.

9. Extracted 1000 µL with an Eppendorf pipette from the medium to measure the pH. The machine used the pH measurements was Inolab 720 from WTW ($\pm$ 0.01 pH). Adjusted the pH to ensure it was within the target range, which was pH 6.8-7.0 for the SRB and pH 7.2-7.6 for the methanogen. Decreased the pH by adding HCl if it was too high and added NaOH if the pH was too low.

10. The initial 100 mL of the medium was discarded. This was to ensure that all the medium was adjusted to the desired pH stated above.

11. Prepared the line with the stated gas mixture (N_2 or N_2+CO_2) in the recipe. Turned on the burner, closed the red lids, and opened the water line.

12. Removed the foil of the autoclaved bottles and moved it through the flame to sterilize. Poured the media into the bottles through the filling funnel until the marked line of the bottles (25 ml for the 50 ml bottle or 50 ml for the 100 ml bottle).

13. Flushed with the gas mixture for 30-60 seconds to remove the O_2. Closed the opening of the bottles with a stopper and a crimp seal. Secured the crimp seal with a manual vial crimper.

3.3 Preculture

Preculture was prepared separately to initially promote the growth of the microorganisms before inoculating them to the experimental bottles.

The preculture for *Desulfohalobium retbaense* included 50 mL medium 499, 500 µL from 10% stock solution yeast extract, 500 µL from 10% stock solution peptone, 600 µL from 2M stock solution lactate, 300 µL from 2M stock solution acetate, and 2 mL culture. The preculture was stored in an incubator at 37 °C. For the experiments with different H_2 concentrations, the preculture was allowed to grow for seven days. The preculture had a concentration of 13.53% H_2S at the end of the cultivation period. The preculture was grown for eight days for the experiments with different pressures, and the amount of H_2S was 12.57%

The preculture for *Methanocalculus halotolerans* was prepared by combining the following components: 50 mL media 905, 500 µL from 2M stock solution acetate, 2 mL from 1M stock solution formate, 250 µL from 10% stock solution yeast extract, and 10 mL culture. In addition, a gas mixture of 80% H_2 gas and 20% CO_2 gas was added to the headspace to create an anaerobic environment and encourage growth. This preculture was also stored in an incubator at 37 °C. For the experiments with different H_2 concentrations, the preculture was allowed to grow for 13 days. While for the experiment with different pressures, the preculture grew for 12 days.

3.4   Working with Hydrogen

Hydrogen is a highly flammable gas, as previously mentioned in Section 2.1. Therefore, it was crucial to take the necessary precautions. Three key rules must be kept in mind and followed when working with hydrogen:

- No flames nearby due to the explosion risk by ignition.

- Low volume of gas because hydrogen gas mixed with air can cause an explosion.

- Good ventilation to prevent a build-up of potential explosive concentration in the air.

3.5   Method for Measuring Pressure

Pressure measurements were conducted at the start and the end of the sampling day using a pressure transducer. Unfortunately, information about the uncertainty of the pressure transducer was not found. Figure 3.4 illustrates the setup, and the software used for the measurements was Flexlogger.

The method was as follows:

1. Cleaned the cap of the bottle with ethanol to sterilize and placed the needle into the rubber center of the bottle in a straight motion. It was important to avoid bending the needle to minimize the risk of incorrect measurement.

2. Read the measurement from the Flexlogger. Finally, the needle was removed slowly from the rubber to minimize pressure loss.
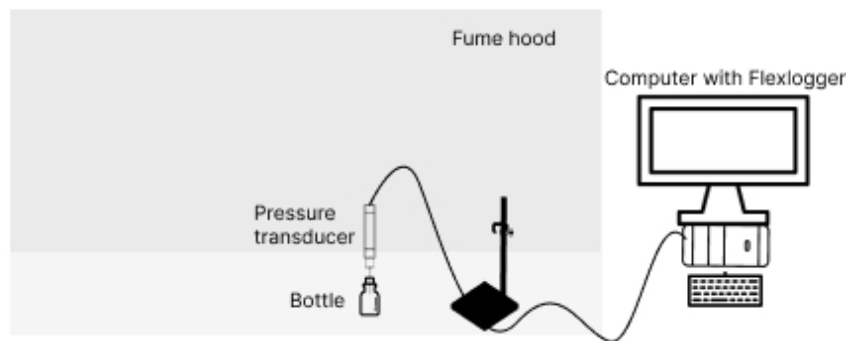
Figure 3.4: A simple illustration of the setup to measure the pressure with the pressure transducer.

3.6   Method for Measuring Gas Composition

Micro gas chromatography (microGC) measured the gas composition in the different bottles. A machine from Agilent Technologies called Agilent 490 Micro GC was used with the software Soprane CDS. The setup is illustrated in Figure 3.5. To measure the gas composition, the instrument extracted a small sample from the headspace of the bottles. The machine had an uncertainty of $\pm$ 0.5% (mole%). Some pressure would be lost during these measurements due to the extraction of the gas from the headspace and removing the needle from the bottles.

It is important to note that the machine required the pressure in the bottles to be over 25 millibar gauge (mbarg) and below 1 bar gauge (barg) to measure the gas composition.

1. Placed the needle into the rubber center of the bottle in a straight motion to avoid bending and incorrect measurement.

2. Waited until the extraction was complete. The needle was slowly removed from the rubber to prevent pressure loss.
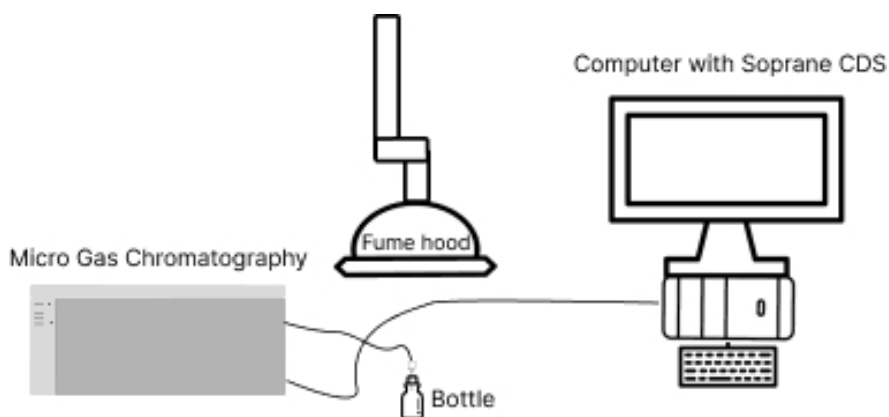
Figure 3.5: A simple illustration of the setup to measure the gas composition with microGC.

3.7   Method for Measuring pH

A pocket pH meter of the brand Horiba LAQUAtwin pH-11 was used to measure the pH. The measurements were performed at the start and the end of the experiments to compare the results. The uncertainty of the apparatus is $\pm$ 0.1 pH. It was important to measure until the pH value was stable.

The procedure was as follows:

1. The bottle cap was sterilized by cleaning it with ethanol. Afterward, the bottle was shaken to ensure that the liquid was homogeneous.

2. Placed the needle into the rubber center and turned the bottle upside-down to extract directly from the liquid and avoid gases in the syringe. Used the syringe to withdraw 200 µL liquid from the bottle. Turned the bottle upright and slowly removed the needle from the rubber to avoid pressure loss.

3. Transferred the liquid from the syringe to the pH meter (see Figure 3.6).
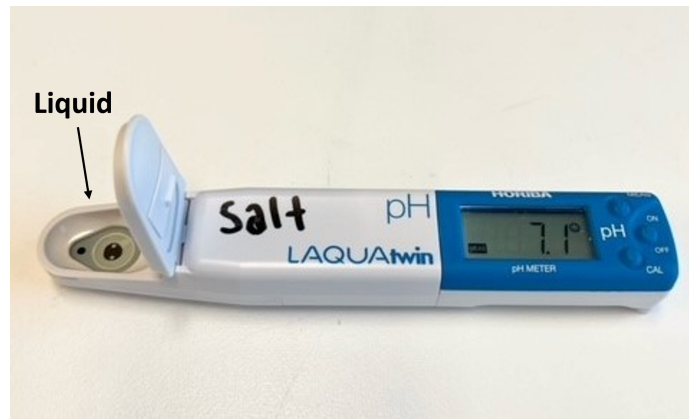
Figure 3.6: Pocket pH meter (Horiba LAQUAtwin pH-11) for measurement of the pH. The liquid had to cover the dots and measure until the pH was stable to ensure correct measurements.

3.8 Method for Liquid Sampling

The purpose of the liquid sample was to measure the residual acetate after the experiments. Liquid samples were taken at the experiments' beginning and end. The liquid samples can be stored in the freezer for later use, such as DNA analysis.

1. The area of use was cleaned with ethanol to sterilize the surface. Sterile Eppendorf tubes were used and labeled. Half of the tubes were designated for the supernatants and the other half for the pellets.

2. The bottle cap was wiped with ethanol, and the bottle was shaken to ensure homogeneity.

3. The needle was placed into the rubber center of the bottle in a straight motion to avoid bending the needle and ensure correct measurement.

4. The bottle was turned upside-down without bending the needle to extract directly from the liquid and avoid gases in the syringe. Exactly 1 mL of liquid was withdrawn into the syringe. The bottle was turned upright, and the needle was slowly removed from the rubber to avoid gas leakage.

5. The needle was discarded, and the liquid was transferred into the Eppendorf tubes. The Eppendorf tubes were closed and placed evenly distributed in the centrifuge machine (Heaeus Biofuge pico). The machine separated the pellet from the supernatant by centrifuging at 13000 rpm for 20 minutes. Removed the tubes from the machine when finished.

6. An Eppendorf pipette on 1000 µL was used to withdraw as much supernatant as possible without touching the pellet.

7. The supernatant was transferred to a sterile Eppendorf tube and placed in a box before storing them in the freezer.

3.9   Method for DNA Analysis

The purpose of DNA analysis was to extract DNA from the bottles to measure cell numbers, but this was not included in the thesis due to time constraints. However, measuring the cell numbers can be performed in future work.

DNA-extraction

Pre-treatment was initially conducted to break up the cells and extract the DNA. The procedure was as follows:

1. The ultrasonic cleaner (VWR Ultrasonic Cleaning Bath) was filled with distilled water below the line.

2. The frozen Eppendorf tubes with the pellets were placed in the floaters. Followed by placing the floater in the ultrasonic cleaner for five minutes.

3. After five minutes, the Eppendorf tubes were placed in a box and into a freezer at −80 °C for five minutes to shock-freeze.

4. The Eppendorf tubes were placed back in the floater and back into the ultrasonic

cleaner again for five more minutes.

For DNA extraction, the DNeasy Blood & Tissue Kit (50) manufactured by QIAGEN was utilized. Eppendorf pipettes with PCR-clean and sterile tips were utilized. The manufacturer's manual was followed with some adjustments in the procedure.

The following modifications were made to the manufacturer's protocol during the DNA extraction procedure:

- Turned on at 13000 rpm instead of 14000 rpm in the centrifuge.

- Used 50 µL DNA-free water instead of 200 µL buffer AE.

Adjustments were made because the centrifuge at the laboratory had a maximum rate of 13000 rpm. Moreover, information about the composition of buffer AE was not provided, making it uncertain whether it could affect subsequent chemical processes. DNA-free water was chosen as a substitute to avoid potential alternations because it is known to be pure.

Qubit 4 Fluorometer Invitrogen was used to measure DNA quantification in the samples. The quantification requires the use of Qubit Assay Tubes, which are specifically designed to fit the machine. To obtain precise measurements, it was important to calibrate the machine before analyzing the samples, which involved the measurement of standards containing known concentrations of DNA, typically one low and one high concentration.

1. An Eppendorf pipette was used to withdraw 190 µL of working solution and transferred to the Qubit Assay Tubes.

2. 10 µL of the low-concentration standard solution was transferred into the Qubit Assay Tubes. The tubes were vortexed (IKA MS1 S1 Vortex Shaker) for a few seconds to mix the liquids.

3. The tubes were incubated for two minutes at room temperature before being placed in the Qubit 4 Fluorometer Invitrogen to read the value.

4. The steps above were repeated with the high-concentration standard solution

The procedure from the manufacturer was followed for the samples

1. Qubit Assay Tubes were placed into a tube rack and labeled for easier tracking

2. 199 µL of the working solution was drawn out with an Eppendorf pipette with PCR-clean tip and transferred to the Qubit Assay Tubes. This was done for all samples without changing the tip.

3. 1 µL of each sample was drawn out with an Eppendorf pipette and transferred to the respective Qubit Assay Tube. A new tip was used for each sample to prevent contamination.

4. The tubes were vortexed for a few seconds to ensure homogeneity.

5. The tubes were incubated for two minutes at room temperature before placing them in the machine to read the values.

3.10   Method for Acetate Measurement

The purpose of the acetate measurements was to determine the extent of the acetate utilization by the microorganisms at the start and the end of the experiments. It was described that *Desulfohalobium retbaense* and *Methanocalculus halotolerans* used acetate as a carbon source [72], [73].

To measure the amount of acetate, the liquid samples with the supernatant were analyzed using the apparatus named Agilent 1260II HPLC for liquid chromatography.

The preparation of the samples before analysis was as follows:

1. The Eppendorf tubes with the supernatant were defrosted overnight in the fridge.

2. Prepared new Eppendorf tubes and labeled them for easier identification.

3. Used the Eppendorf pipette to withdraw 500 µL of the supernatant and transferred to the new Eppendorf tubes. 1000 µL of 14 mM sulfuric acid (H_2SO_4) was also transferred to the Eppendorf tubes.

4. Prepared vials and labeled them for easier identification.

5. Used a syringe to withdraw all the diluted samples from the Eppendorf tubes, removed

the needle, and filtered the diluted sample through a 0.45 µm RC (Regenerated Cellulose) syringe filter.

6. Put the vials in the liquid chromatography (Agilent 1260II HPLC)

The HPLC procedure is described in Appendix A.

3.11   Experiments with Different Hydrogen Concentrations

The experiments involved taking measurements of pressure, gas composition, and pH at both the beginning and the end and collecting liquid samples. Furthermore, acetate was measured at the end of the experiment, as the initial amount is already known from the preparation of the bottles in Table 3.3 and Table 3.4.

Each H_2 concentration in this study was measured as duplicates. Duplicates are useful to compare the development and ensure consistent results. Furthermore, it can help to identify unexpected or unusual behavior due to contamination or procedure errors. The result is the average of the two measurements. Error bars are used to decide the deviation of the duplicates.

3.11.1   *Desulfohalobium retbaense*

A total of 14 bottles were prepared for this experiment. Eight bottles were unsterile, and the remaining six were sterile controls. 300 µL from 2M stock solution acetate, 350 µL vitamin, and 2.5 mL from 10% stock solution inoculum were injected into the unsterile bottles (see Table 3.3).

Four different microbial setups were prepared, each with duplicate samples and a different H_2 concentrations in the headspace of $0\%H_2$, $10\%H_2$, $40\%H_2$, and $100\%H_2$. The remaining headspace was occupied by N_2. The hydrogen gas line was flushed for one minute, and subsequently, the syringe was flushed with H_2 three times to eliminate any traces of O_2. To inject H_2 gas into the headspace of the bottles, a volume of 5 mL of H_2 gas corresponded to 10% H_2 concentration, while 20 mL of H_2 gas corresponded to 40% H_2 concentration. 100% H_2 required flushing the bottle with H_2 gas for a duration of one minute. During the experiment, when the pressure level was below the lower limit (< 25 mbarg) for microGC, the pressure was re-added in the bottles by using a syringe filled with $100\%N_2$.

The bottles were stored upside down in the incubator at 37 °C to prevent H_2 leakage.

Table 3.3: The experimental plan for the experiments with different H_2 concentrations with *Desulfohalobium retbaense*.

H_2 (%)	Acetate 2M (μl)	Vitamin (μl)	Inoculum 10% (mL)
0	300	350	2.5
0	300	350	2.5
10	300	350	2.5
10	300	350	2.5
40	300	350	2.5
40	300	350	2.5
100	300	350	2.5
100	300	350	2.5
10	-	-	-
10	-	-	-
40	-	-	-
40	-	-	-
100	-	-	-
100	-	-	-

3.11.2   *Methanocalculus halotolerans*

Similar to the previous strain, this experiment also had 14 bottles prepared. Eight of them were unsterile, while the remaining six were sterile. The unsterile bottles had the following nutrients added: 250 µL from 2M stock solution acetate, 150 µL from 10% stock solution yeast extract, and 2.5 mL from 10% stock solution inoculum (see Table 3.4).

This experiment consisted of four microbial setups, each with a different H_2 concentration in the headspace: 0%H_2, 10%H_2, 40%H_2, and 90%H_2, with duplicates of each setup. Before adding the H_2, the headspace was occupied with 80% N_2 and 20% CO_2. The procedures for achieving 0%, 10%, and 40% H_2 concentrations in the headspace are the same as described above in *Desulfohalobium retbaense*. The 90% H_2 concentration requires a few more steps. Initially, the headspace was flushed with H_2 gas for one minute to attain 100% H_2. A syringe extracted 5 mL of H_2 gas from the headspace. Subsequently, the CO_2 line was flushed for

one minute to remove any remaining O_2 traces. The syringe was also flushed three times to eliminate any residual gases. To achieve a 90% H_2 concentration, 5 mL of CO_2 was injected into the bottle. The bottles were re-added with 80%N_2+20%CO_2 using a syringe when the pressure was too low for the microGC.

The bottles were stored upside down in the incubator at 37 °C to prevent H_2 leakage.

Table 3.4: Experimental plan for the experiments with different H_2 concentrations with *Methanocalculus halotolerans*.

H_2 (%)	Acetate 2M (μl)	Yeast extract 10% (μl)	Inoculum 10% (mL)
0	250	150	2.5
0	250	150	2.5
10	250	150	2.5
10	250	150	2.5
40	250	150	2.5
40	250	150	2.5
90	250	150	2.5
90	250	150	2.5
10	-	-	-
10	-	-	-
40	-	-	-
40	-	-	-
90	-	-	-
90	-	-	-

3.12   Experiment with Different Pressures

In these experiments, measurements of the pressure and pH were conducted at the beginning and the end, as well as collecting liquid samples. The gas composition was not performed at the start of the experiments with *Desulfohalobium retbaense* because the headspace was filled with 100% H_2. Therefore, the initial gas composition was already known, and only the measurement at the end of the experiments was necessary. However, the gas composition was measured for *Methanocalculus halotolerans* at the start and the end. This was because it was more challenging to obtain precisely 90% H_2 compared to 100% H_2. Only the bottle

with 0.3 barg was measured at the beginning, as it is assumed that all the bottles contained the same gas composition due to the same procedure. All pressures were measured at the end with the microGC. The measurement of acetate was performed at the end of the experiment, as the initial amount is already known from the preparation of the bottles in Table 3.5 and Table 3.6.

Similar to the experiment with H_2 concentrations, each pressure in this study was measured as duplicates for the same reason as stated in Section 3.11.1.

3.12.1 *Desulfohalobium retbaense*

Ten bottles were prepared for this experiment, whereas six were unsterile and four were sterile. The unsterile bottles had injected 300 µL from 2M stock solution acetate, 350 µL vitamin, and 2.5 ml from 10% stock solution inoculum (see Table 3.5).

The experimental setup had three different pressures of 0.3 barg, 1 barg, and 1.7 barg, in addition to duplicates. First, all the bottles were flushed with H_2 for one minute to obtain $100\%H_2$ in the headspace. Then, to achieve the desired pressure, H_2 was manually injected into the headspace using a syringe to the target pressure.

The bottles were stored upside down in the incubator at 37 °C to prevent H_2 leakage.

Table 3.5: Experimental plan for the experiments of different pressures with *Desulfohalobium retbaense*.

H_2 (%)	Acetate 2M (μl)	Vitamin (μl)	Inoculum 10% (mL)	Pressure (barg)
100	300	350	2.5	0.3
100	300	350	2.5	0.3
100	300	350	2.5	1
100	300	350	2.5	1
100	300	350	2.5	1.7
100	300	350	2.5	1.7
100	-	-	-	1
100	-	-	-	1
100	-	-	-	1.7
100	-	-	-	1.7

3.12.2   *Methanocalculus halotolerans*

This experiment had a similar setup as the previous one. However, during this experiment, a problem was encountered. While filling the bottles in the laboratory, the supply of H_2 was depleted. A modification of the original experimental plan was therefore necessary. Seven bottles were prepared for this experiment; five were unsterile, and two were sterile. Due to the modification, the unsterile bottle with 0.5 barg and both sterile bottles with 1.5 barg and 2 barg were not measured as duplicates. The unsterile bottles included 250 µL from 2M stock solution acetate, 150 µL from 10% stock solution yeast extract, and 2.5 ml from 10% stock solution inoculum (see Table 3.6).

This experiment consists of three different pressure setups of 0.5 barg, 1.5 barg, and 2 barg. To achieve a consistent mixture in the headspace of all bottles, a 90% H_2 and 10% CO_2 gas mixture was flushed into them simultaneously. Furthermore, the H_2/CO_2 mixture was injected into the headspace using a syringe to achieve the desired pressure.

The bottles were stored upside down in the incubator at 37 °C to prevent H_2 leakage.

Table 3.6: Experimental plan for the experiments with different pressures with *Methanocalculus halotolerans*.

H_2 (%)	Acetate 2M (μl)	Yeast extract 10% (μl)	Inoculum 10% (mL)	Pressure (bar)
90	250	150	2.5	0.5
90	250	150	2.5	1.5
90	250	150	2.5	1.5
90	250	150	2.5	2
90	250	150	2.5	2
90	-	-	-	1.5
90	-	-	-	2

3.13   Calculations

The ideal gas law was used to relate the properties that define the state of a system. It describes the relationship between the pressure, volume, amount, and temperature of a perfect gas [74]. In this thesis, H_2 can be considered a perfect gas since the pressure was kept at low pressure (below 35 barg) [75]. Hence, the perfect gas law was applied to calculate the number of H_2 moles present in the headspace of the bottle. The partial pressure in the bottle was obtained from the measurements with the pressure transducer. The pressure inside the bottles is relative to the pressure outside, and therefore the absolute pressure was calculated by adding the atmospheric pressure to the partial pressure. The volume of H_2 in the headspace was determined by using the microGC. The total volume of the bottles was 58.35 mL, whereas 28.15 mL was liquid volume and 30.2 mL was gas volume for the SRB. The same volume was for the methanogen, except that composition was 27.9 mL for liquid volume and 30.45 mL for gas volume. The gas volume from the bottles was multiplied with the H_2 volume in the headspace. Since the bottle was stored in the incubator at 37 °C, the same temperature was used in the calculations.

$$PV = nRT \tag{3.1}$$

$$n = \frac{PV}{RT} \tag{3.2}$$

Where P is the pressure [Pa], V is the volume [m^3], n is the number of moles [mol], R is the gas constant [8.314 $m^3 \cdot Pa \cdot K^{-1} \cdot mol^{-1}$], and T is the temperature [K].

During the sampling process, removing the needle from the rubber resulted in pressure loss. To quantify the number of moles lost during the sampling day, the difference between the number of moles of H_2 at the start and at the end was calculated.

$$x_0 - x_n = \Delta x \tag{3.3}$$

Where x_0 is the initial number of moles [moles] H_2, x_n is the final number of moles [moles] H_2, and ΔX is the loss of moles [moles].

The SRB and methanogen consumed the dissolved H_2 in the medium. Therefore, to compare

the total H_2 consumption between the SRB and the methanogen under different H_2 concentrations and pressures, it was necessary to establish a common starting point. Therefore, the total H_2 consumption was on a relative scale, as all the start points were normalized to the initial moles H_2 over time. To calculate the percentage of change over time, the following equation was utilized:

$$(1 - \frac{x_n}{x_0}) * 100\% = \% \tag{3.4}$$

Where x_n is the final value, and x_0 is the initial value.

To determine the maximum consumption rate for the different H_2 concentrations and pressures, the consumption rate was first calculated by determining the slope of the decrease in the amount of H_2 over time. The slope represents the rate of change along the regression line, which is a straight line between two variables [76]. Subsequently, the maximum consumption rate in millimoles per day is the highest absolute value.

$$\text{slope} = \frac{\sum_{i=1}^{n}(x_i - \bar{x})(y_i - \bar{y})}{\sum_{i=1}^{n}(x_i - \bar{x})^2} \tag{3.5}$$

Where the slope is in millimoles per day [mmoles/day], x is day [day] and y is the H_2 consumption [mmoles].

Each H_2 concentration and pressure were measured as duplicates, thus representing the average of two measurements.

$$\bar{x} = \frac{1}{n}\sum_{i=1}^{n} x_i \tag{3.6}$$

Where $\bar{x}$ is the average, x is the value, and n is the number of values.

Acetate was included in the bottles as a carbon source for the microbes. The dilution equation was used to calculate the concentration of the initial amount of acetate included in the medium.

$$C_1 * V_1 = C_2 * V_2 \tag{3.7}$$

$$C_2 = \frac{C_1 * C_1}{V_2} \tag{3.8}$$

Where C_1 is the initial concentration of the solution [mol/m³], V_1 is the initial volume of the solution [m³], C_2 is the final concentration of the solution [mol/m³], and V_2 is the final volume of the solution [m³].

The average deviation determines the variability in a given data set. It calculates the average of the absolute deviations of the data points from their mean [77]. The average deviation was used for the small sample size of two values (Equation 3.9), while the standard deviation population was used for more than two values (Equation 3.10). The deviations were also used to create error bars.

$$AD = \frac{1}{n} \sum_{i=1}^{n} |x_i - \bar{x}| \tag{3.9}$$

Where x is the value, $\bar{x}$ is the mean of the values, and n is the number of values.

$$STDEV.P = \sqrt{\frac{\sum_{i=1}^{n}(x_i - \bar{x})^2}{n}} \tag{3.10}$$

Where x is the value, $\bar{x}$ is the mean of the values, and n is the number of values.

Chapter 4

Uncertainty Assessment

This chapter presents and discusses the sensitivity and uncertainty of the methods in Chapter 3. All the errors and method sensitivity are important for understanding and interpreting the experimental results.

4.1 Error and Uncertainty in the Procedures

There is a potential risk of contamination during the experimental procedure involving microorganisms. Working with anaerobic microorganisms such as *Desulfohalobium retbanse* and *Methanocalculus halotolerans* requires special precautions to avoid contamination of oxygen and others that can alter the results.

To ensure the viability of the microorganisms, the presence of O_2 had to be eliminated from the bottles as they are highly sensitive to it. The anaerobic microorganisms cannot thrive in the presence of O_2, which are toxic and can either inhibit their growth or be fatal [78]. This can be prevented by flushing the syringe with N_2 at least three times before injecting or extracting liquid and gas from the bottles. Furthermore, sodium resazurin was added to the medium to identify oxidation by the change to pink color. Despite the precautions taken to eliminate the presence of O_2 in the bottles, it was observed that a few bottles had been infiltrated with O_2. In cases of underpressure in the bottles, the probability of O_2 infiltrating increases.

A minor pressure loss was observed after removing the needle from the rubber of the bottles. The pressure loss occurred after measurements with the pressure transducer and the

microGC. The pressure loss was accounted for in the experiment with different H_2 concentrations, which were calculated and included in the results. In contrast, the pressure loss was not accounted for in the experiments with different pressures. The procedure for the pressure measurements was the same for all experiments. However, in the experiments with different pressures, the gas composition was only measured at the start and the end of the experiment. This approach's purpose is to avoid altering the pressure level caused by gas leakage from the needle, which could result in an incorrect interpretation of the influence of different pressures on H_2 consumption. Due to the lack of gas composition data, the calculation of H_2 loss in the unsterile bottles was not performed. However, H_2 loss can be calculated by subtracting the number of moles H_2 in the sterile from the unsterile.

The effect of temperature on pressure measurements is an important factor to consider. This is because the pressure is proportional to the temperature according to the perfect gas law in Equation 3.1. In this case, a bottle recently removed from an incubator will have a slightly higher pressure than one allowed to sit at room temperature for some time. This difference in pressure can therefore affect the accuracy of the measurements.

4.2 Error and Uncertainty in the Calculations

As previously mentioned, the pressure loss was not accounted for in the experiments with different pressures. The uncertainty of the apparatuses was also not included in the calculations. This is because the uncertainty of the biological variability of microbial growth and activity is greater than that of the apparatuses. Accounting for factors such as individual microbes and their responses to temperature, pH, and nutrients is challenging.

The bottles were stored in an incubator at 37 °C, and the temperature used in the calculations corresponds to this. However, the temperature in the bottles decreases when the bottles are at room temperature for the pressure measurements. Consequently, the temperature and pressure used in the calculations may not accurately represent the actual conditions and could potentially be lower.

Chapter 5

Results and Discussion

This chapter presents and discusses the results of the experimental laboratory work with the sulfate-reducing bacterium *Desulfohalobium retbaense* and methane-producing archaeon *Methanocalculus halotolerans*. The experiments were divided into two parts to study the influence on H_2 consumption. The first part studied the impact of different H_2 concentrations, while the second part focused on the impact of different pressures.

The chapter consists of three main sections. The first section presents and discusses the results from the experiments with different H_2 concentrations on H_2 consumption by SRB and methanogen separately. The second section presents and discusses the effects of different pressures on H_2 consumption by both microorganisms separately. Finally, a comparison of the results between the previous sections is conducted.

5.1 Impact of Different Hydrogen Concentrations on SRB and Methanogen

The experiments studied the impact of the different H_2 concentrations on the SRB (0%, 10%, 40%, and 100%) and the methanogen (0%, 10%, 40%, and 90%) on microbial H_2 consumption and acitivites. In this thesis, the H_2 consumption rate refers to the microbial consumption of H_2. Meanwhile, H_2 loss refers to several factors, including microbial consumption, pressure loss, and H_2 dissolved in the medium.

5.1.1   Sulfate-reducing bacterium

Desulfohalobium retbaense used H_2 (aq) as a source of electrons to reduce sulfate and produce gaseous H_2S. Figure 5.1 A) illustrates a significant decrease of 0.18, 0.28, and 0.57 millimoles (mmoles) for $10\%H_2$ (purple), $40\%H_2$ (orange), and $100\%H_2$ (red) respectively, in the initial 14 days. Subsequently, the graphs level off and move towards stabilization. The H_2 was fully consumed after 14 days in the bottles with $10\%H_2$. However, the SRB failed to consume all H_2 in concentrations of $40\%H_2$ and $100\%H_2$. The consumption ended at 0.19 and 0.70 mmoles, respectively.

All the bottles contained the same medium, which implies that the initial pH is expected to be similar for all H_2 concentrations. Therefore, the initial pH was not measured for unsterile and sterile $10\%H_2$, nor for sterile $100\%H_2$. The H_2 concentrations in sterile controls (dashed lines) in Figure 5.1 A) are expected to be constant due to no microbial activity. However, between days 28 and 34, a decrease of 0.09 mmoles for sterile $100\%H_2$ was caused by a measurement error. Pressure loss is expected due to pressure and microGC measurements for low-pressure experiments. Therefore, if the pressure levels were below the lower limit (<25 mbarg) required for microGC measurements, the pressure was increased by re-adding N_2. Thus, for long-duration experiments, it was anticipated that gas composition would change due to the re-adding of N_2.
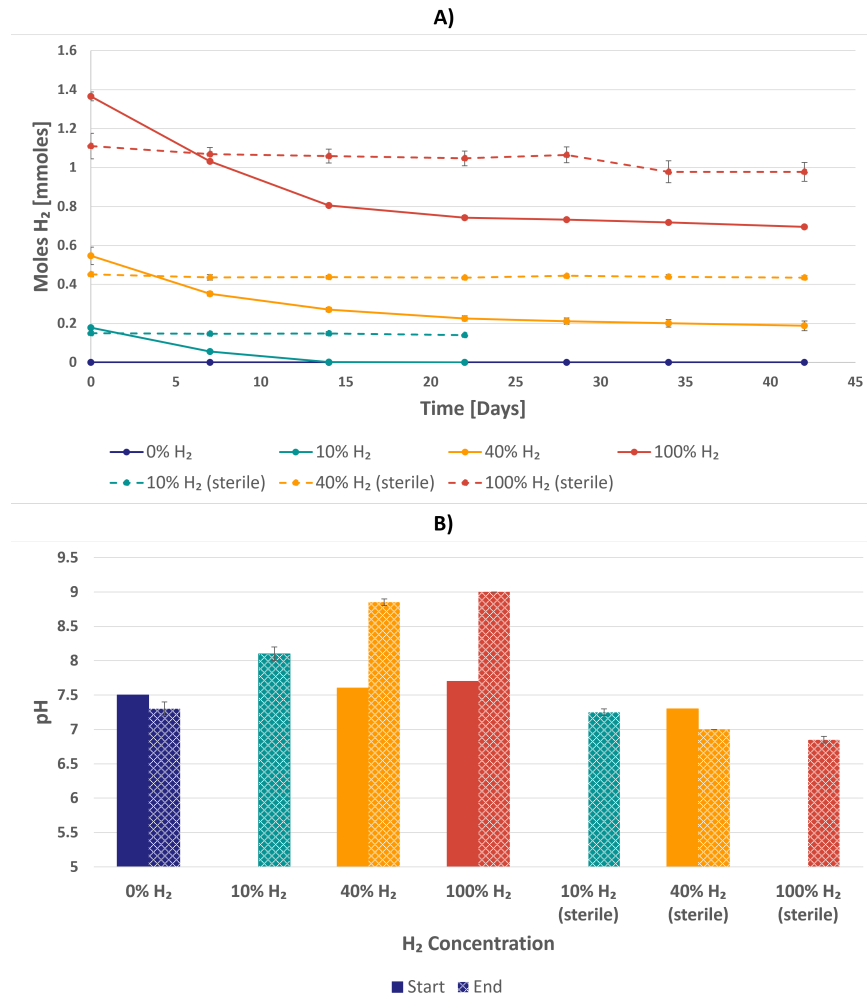
Figure 5.1: **A)** The consumed H_2 number of mmoles by *Desulfohalobium retbaense* in 42 days for four H_2 concentrations; $0\%H_2$, $10\%H_2$, $40\%H_2$ and $100\%H_2$. Each H_2 concentration has a sterile control (i.e., without bacteria cells) represented in dashed lines, except for $0\%H_2$. **B)** The pH at the start and at the end of the experiment with *Desulfohalobium retbaense* for $0\%H_2$, $10\%H_2$, $40\%H_2$, and $100\%H_2$. The initial pH is illustrated in solid colors, while the end pH is patterned.

Figure 5.2 A) illustrates that all the available H_2 was consumed in 14 days by the SRB initially containing $10\%H_2$. For $40\%H_2$ and $100\%H_2$, the microbial H_2 consumption was 65% and 49%, respectively, in the same duration. The following week, the H_2 consumption for $40\%H_2$ and $100\%H_2$ were less than 10%, indicating less microbial activity.

Figure 5.2 B) suggests that the H_2 consumption is faster for the higher H_2 concentrations. This is because the maximum consumption rate follows a linear trend. However, as seen in Figure 5.1 A), the initial quantity of moles was also lower for 10% H_2 concentration as

opposed to the remaining. Therefore, there was less H_2 available for the SRB to consume.

The anomaly in the graph of the sterile control for $100\%H_2$ is previously described in Figure 5.1. The error bars in $40\%H_2$ were larger compared to the other H_2 concentrations due to the variation in gas composition between the duplicate measurements. One of the duplicates had a slightly higher initial H_2 concentration and lower final H_2 concentration than the other sample.
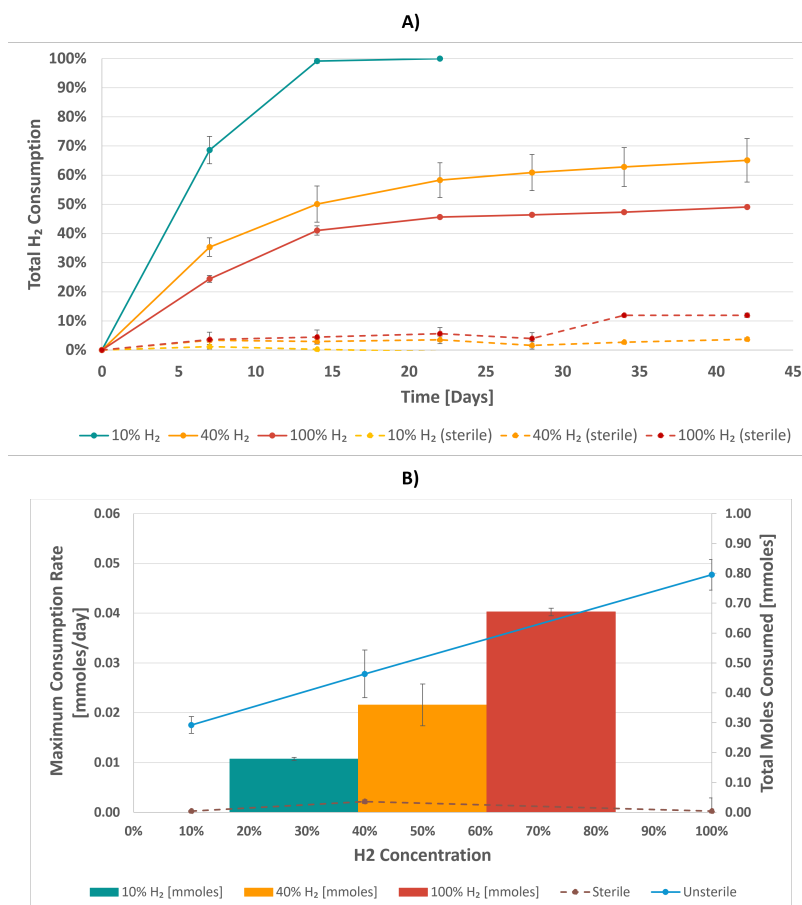
Figure 5.2: **A)** Relative total percentage H_2 consumed by *Desulfohalobium retbaense* over 42 days for the different H_2 concentrations of $10\%H_2$, $40\%H_2$ and $100\%H_2$, including the sterile represented in dashes. This graph is on a relative scale obtained from the data in Figure 5.1 A). For comparison, all the start points were normalized to initial moles H_2 over time. **B)** The relationship between the maximum consumption rate and the number of moles consumed by *Desulfohalobium retbaense* as a function of H_2 concentration (10%, 40%, and 100%). The x-axis is the $\%H_2$ concentrations, while the y-axis is the maximum consumption rate in mmoles/day. The secondary y-axis is the total number of moles consumed by the SRB in mmoles.

The production of H_2S is unfavorable and undesired in UHS due to its toxicity and gas storage composition alteration, as mentioned in Section 2.4.1. As seen in Figure 5.3, the graphs display a minor increase in H_2S concentration for all H_2 concentrations in the first seven days, followed by a decrease. The most prominent was the increase from 0.85% to 1.74% H_2S for 100%H_2 concentration. The sterile controls were also not stable.
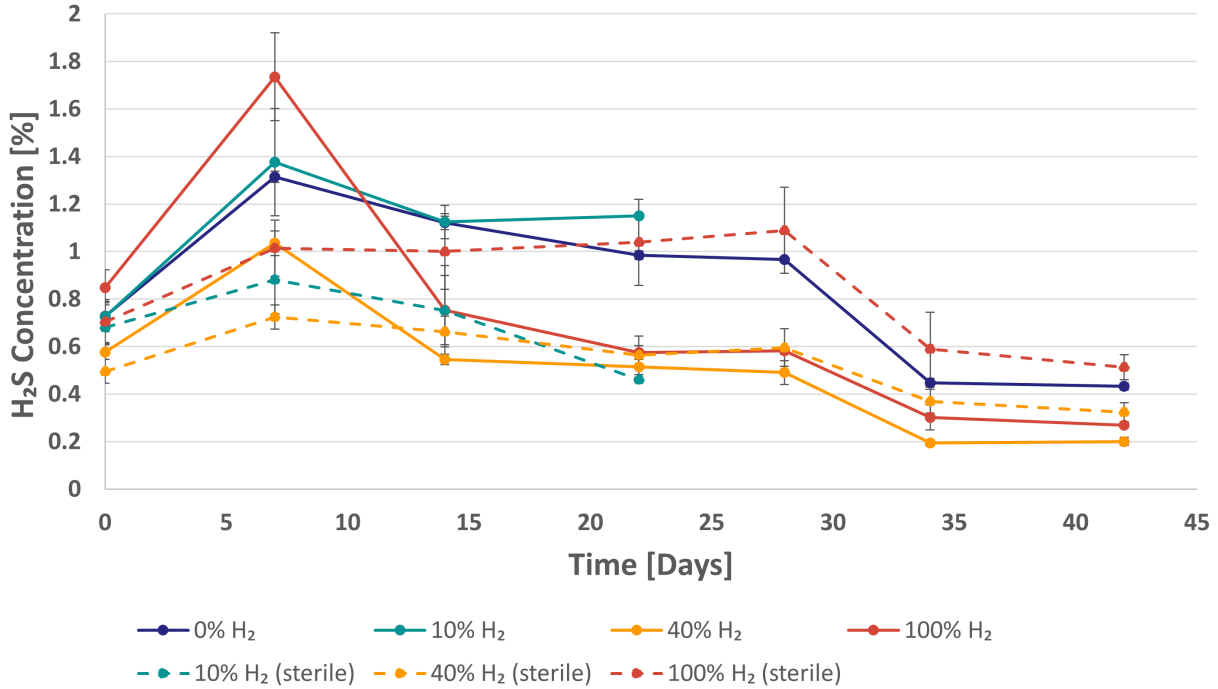
Figure 5.3: H_2S concentration over 42 days by *Desulfohalobium retbaense* for four different H_2 concentrations; 0%H_2, 10%H_2, 40%H_2 and 100%H_2. Each H_2 concentration has a sterile control represented in dashed lines, except for 10%H_2.

The result shows that *Desulfohalobium retbaense* is capable of consuming H_2 at all H_2 concentrations (not 0%H_2), which was expected. This is because the SRB utilized H_2 in their metabolic process as described in literature [73]. In a confined system, however, the consumption rate will decrease over time and reach zero at some point, either due to H_2 depletion or the presence of other factors that may inhibit its metabolism.

The observed effect is likely due to the influence of the pH. The pH value increased from around 7.5 to 9.0 for the H_2 concentrations that did not achieve complete consumption (10%H_2, 40%H_2 and 100%H_2). This may indicate that the high pH, which is close to 9.0, inhibits the bacterium's metabolism. Tran *et al.* [79] found that one of the primary factors that strongly influence metabolic activities and disturb the growth of microbes, among other

things, is the environmental pH. Furthermore, the authors also found that occurrences outside the optimum pH can decrease the growth rate and metabolisms by up to 50%. As earlier mentioned in Section 3.1, the optimal pH for *Desulfohalobium retbaense* growth is between 5.5 and 8.0. At the end of the experiment, the pH for 40%H_2 and 100%H_2 were 8.85 and 9.0, respectively, out of the optimum range. Thereby inhibiting bacterial activities.

Other factors contribute to the dissimilarity of graphs in total H_2 consumption, namely physical and biological factors. For the physical factor, the solubility of H_2 in water is low (0.0014 g H_2/kg water) compared to other gases such as H_2S (approx. 2.5 g H_2S/kg water) [34]. However, it is even lower in brine due to the "salting-out effect" as explained in Section 2.1. Therefore, the microbes can only consume the dissolved H_2(aq). The biological factor is that the amount of H_2 used in these experiments is artificially high and cannot be found naturally. Therefore, the microbes are not used to such high elevated concentrations and can be overburdened. This implies that the microbes can be enabled to perform their metabolic process effectively, resulting in inhibited growth and function.

A possible explanation for the decrease of H_2S concentration is due to the relationship between sulfide and pH, as shown in Figure 2.8. At the neutral pH of 7.0, the fraction of H_2S and HS^- is at equilibrium. The fraction changes as the pH increases or decreases [80]. In this case, the increased pH led to a consequent reduction in the concentration of H_2S. The presence of H_2S is very low, below 0.1 mol fraction, between pH 8.0 and 10.0. This is consistent with the end measurements of the pH in Figure 5.1 B), which were pH 8.1, pH 8.85, and pH 9.0 for 10%H_2, 40%H_2, and 100%H_2, respectively. Thereby, there is no to very little H_2S in the gaseous phase.

5.1.2   Methanogen

Methanocalculus halotolerans use H_2 as an electron donor to reduce CO_2 and produce CH_4, which is a potent greenhouse gas. This is further described in Section 2.4. Figure 5.4 A) shows the number of mmoles decreased over time due to microbial consumption by the methanogen. The methanogen completely consumed all the available H_2 on day 3 for 10%H_2. For the remaining H_2 concentrations, the amounts of H_2 present were consumed on day 7. However, measurements were not conducted during the weekend, which corresponds to day 5 and day 6. This implies that 40%H_2 could have depleted during the weekend but was not measured before day 7. The measured pH values in Figure 5.4 B) are stable at around pH 7.4 at the start and pH 7.5 at the end, indicating no notable increase from the initial measurements.
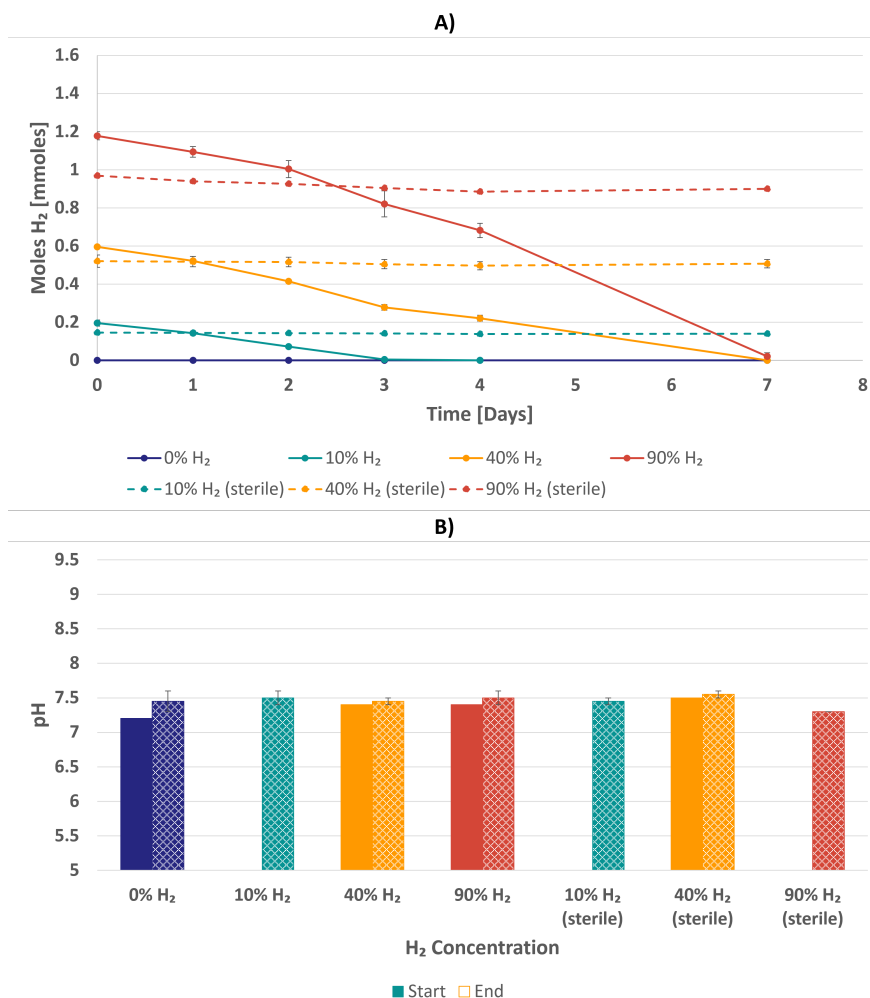
Figure 5.4: **A)** The H_2 amount consumed in mmoles over 7 days by *Methanocalculus halotolerans* for the four different H_2 concentrations of $0\%H_2$, $10\%H_2$, $40\%H_2$, and $90\%H_2$, including the sterile controls represented in dashes (except for $0\%H_2$). **B)** The measured pH at the start and at the end of the experiment with *Methanocalculus halotolerans* for $0\%H_2$, $10\%H_2$, $40\%H_2$, and $90\%H_2$. The initial pH is illustrated in solid colors, while the end is patterned.

The methanogen in $10\%H_2$ consumed 63% of the available H_2 on day 2, as illustrated in Figure 5.5 A). At the same time, the microbial consumption in $40\%H_2$ and $90\%H_2$ was 30% and 15%, respectively. $10\%H_2$ concentration consumed all the available H_2 after four days. The sterile controls (dashed lines) increased overall by less than $10\%H_2$, which implies that the consumption in the unsterile H_2 concentrations was due to microbial activity. Furthermore, the H_2 loss in the sterile controls is due to pressure loss after removing the needle from the bottles during the pressure and microGC measurements.

At higher H_2 concentrations, the maximum consumption rates were relatively higher, as seen in Figure 5.5 B). The maximum consumption rate displayed a linear trend for $10\%H_2$, $40\%H_2$, and $90\%H_2$ with 0.07, 0.14, and 0.22 millimoles per day (mmoles/day), respectively. The number of mmoles consumed also appears to relate to the maximum consumption rate, as it is also linear. This could be due to more available H_2 for consumption for the higher H_2 concentrations.
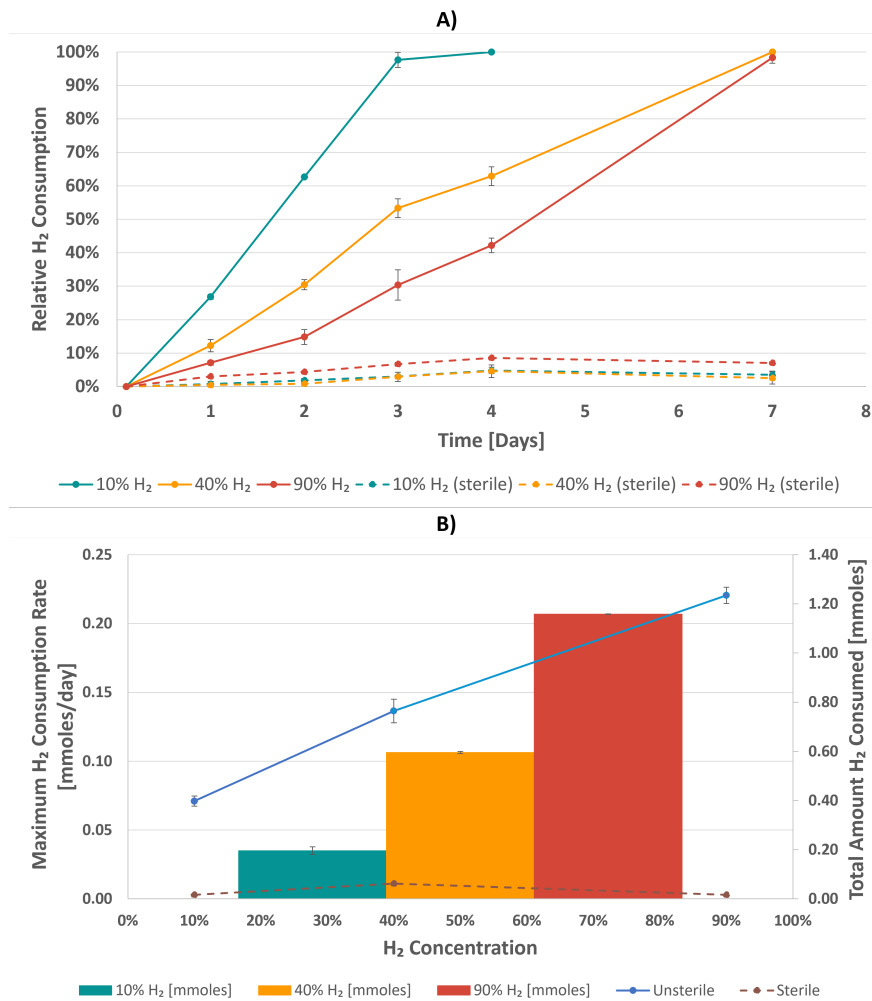
Figure 5.5: **A)** The relative total percentage H_2 consumption over seven days by *Methanocalculus halotolerans* for three different H_2 concentrations of $10\%H_2$, $10\%H_2$, $90\%H_2$, and $90\%H_2$, including the sterile controls represented in dashes (except $10\%H_2$). **B)** The relationship between the maximum consumption rate and the number of moles consumed by *Methanocalculus halotolerans* as a function of H_2 concentration (10%, 40%, and 90%). The x-axis is the $\%H_2$ concentrations, while the y-axis is the maximum consumption rate in mmoles/day. The secondary y-axis is the total number of moles consumed by the methanogen in mmoles.

The production of CH_4 is undesired in UHS because of the alteration of the gas mixture in the subsurface, as described in Section 2.4.2. The graphs in Figure 5.6 illustrate a significant increase in produced CH_4 by the methanogen over seven days, where the observed concentration is more notable for the higher H_2 concentrations. Since $10\%H_2$ was consumed first, the CH_4 was at 2.8% on day 4. Meanwhile, the final measurable concentration of CH_4 was 9.1% and 14.7% for $40\%H_2$ and $90\%H_2$, respectively. No detectable concentration of CH_4 was detected in the sterile controls. This result implies that the CH_4 production in the unsterile experiment is solely due to microbial processes.
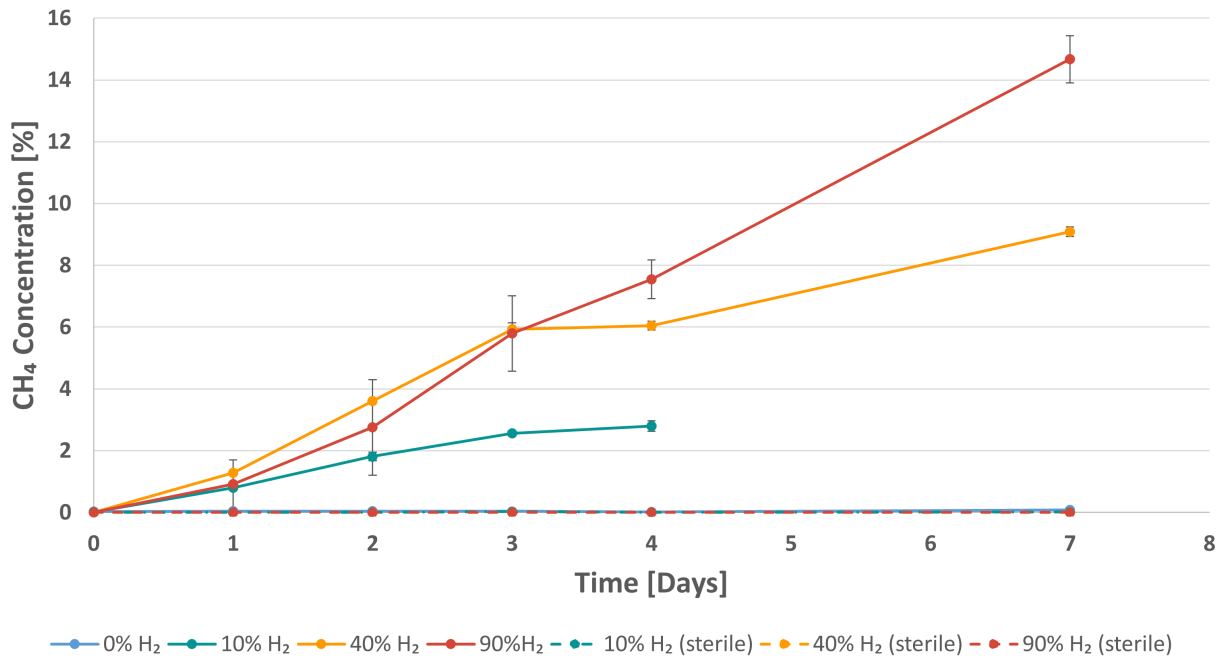
Figure 5.6: CH_4 concentration over 7 days by *Methanocalculus halotolerans* for four different H_2 concentrations; $0\%H_2$, $10\%H_2$, $40\%H_2$ and $90\%H_2$. Each H_2 concentration has a sterile control represented in dashed lines, except for $0\%H_2$.

The results show that the methanogen in $10\%H_2$, $40\%H_2$, and $90\%H_2$ was capable of consuming all the available H_2 within a week, which was expected. The maximum consumption rate is linear, suggesting that the methanogen effectively used the available H_2 in their metabolic processes. The greater availability of the greater H_2 resulted in faster and increased consumption. Conrad *et al.* [81] found that excess H_2 was significantly stimulating for methanogenesis in paddy soil. This could indicate that H_2 concentration is not an inhibiting factor for microbial consumption and activity. Although *Methanocalculus halotolerans* are not commonly found in paddy salt due to the requirement of salt, it could give an indication of the influence.

Despite a minor increase, the measured pH for all H_2 concentrations was stable. Ollivier *et al.* [73] observed that the pH of the medium increased by 0.1 units during growth. However, the medium utilized by the authors was not identical to the medium, as more Na_{Cl}l, $MgCl_2$ x $6\,H_2O$, and $CaCl_2$ x $2\,H_2O$ was added compared to the media in this thesis. The stable pH in Figure 5.4 aligns with the observation by the authors, despite the slightly modified medium. The observed stable pH can be attributed to re-adding 80% N_2 and 20% CO_2 to maintain pressure. In industry, CO_2 is utilized to neutralize the pH in alkaline wastewater [82] [83]. Therefore, the presence of CO_2 may have contributed to maintaining the stable pH.

Methanogenesis requires CO_2 or other carbon sources to produce CH_4. Without CO_2 present, this metabolic process will not occur otherwise [82]. The results in Figure 5.6 are consistent with the results from the study by Yasin *et al.* [82]. Furthermore, the CH_4 concentration appeared linear and was higher for the highest H_2 concentration. This could imply that the microbial activity was efficient and had the potential to continue given enough substrates and nutrients.

The stable pH, fast microbial consumption, and high production of CH_4 collectively suggest that the methanogen was unaffected by the different H_2 concentrations. The metabolic processes were effectively utilized H_2 and produced CH_4. It could also suggest that the consumption could continue given sufficient H_2 and carbon sources present.

5.2   Impact of Different Pressures on SRB and Methanogen

These experiments investigated the impact of different pressures on microbial H_2 consumption and activities. The pressures used in the experiments are significantly lower compared to the actual conditions beneath the surface. The maximum pressure used in this experiment was 2 barg, significantly lower than the 200 bar operational pressure in the subsurface.

5.2.1   Sulfate-reducing bacterium

In Figure 5.7, a notable decline of 279.8, 460.3, and 444.9 mbarg can be observed during the first 14 days for the pressures of 0.3 barg, 1 barg, and 1.7 barg, respectively. The experiment ended on day 36 due to time constraints.

The minor decreasing trend observed in the sterile controls was due to pressure loss in the procedure, as no microbes were present. The procedure for pressure measurement was similar for all, which indicates that the majority of the pressure loss for bottles with SRB was due

to microbial consumption of the dissolved H_2 in the liquid. A pressure decline was observed on day 22 for 1.7 barg (sterile). This observation can be attributed to an increase in pressure in one of the duplicates due to temperature difference, as explained in Section 4.1. This is reflected in the large error bar, which implies a significant difference between the duplicates.
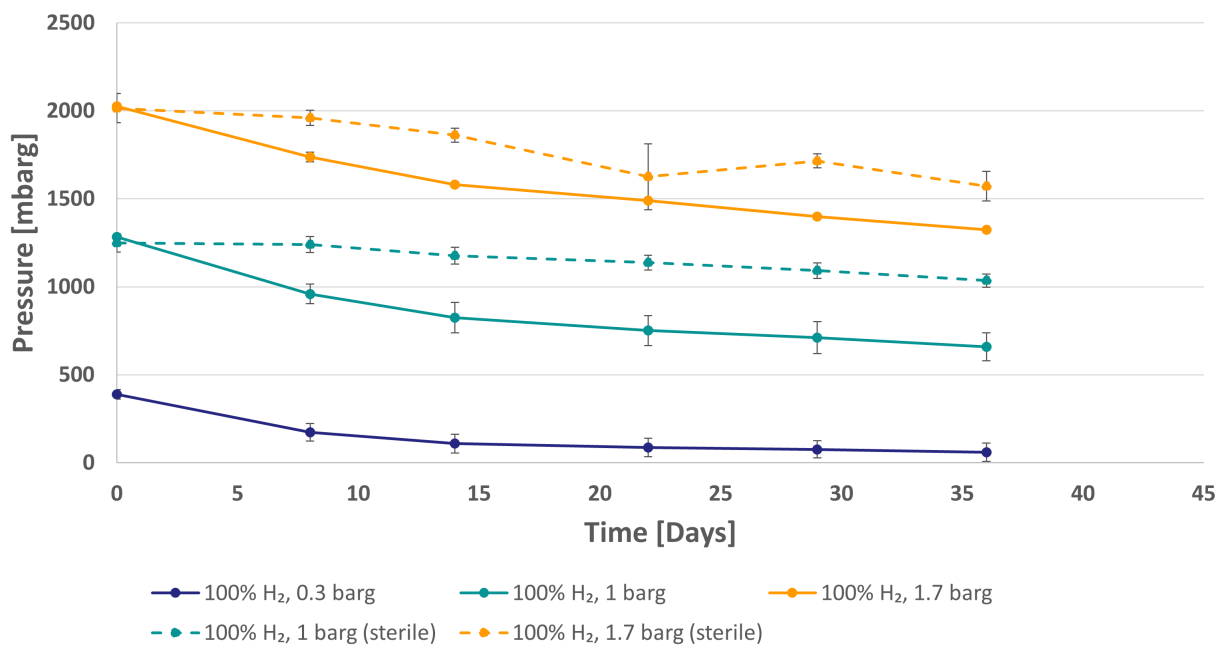
Figure 5.7: The pressure measurements over 36 days of *Desulfohalobium retbaense* for three different pressures of 0.3 barg, 1 barg, and 1.7 barg, including sterile controls for 1 barg and 1.7 barg. The headspace of the bottles was initially 100% gas-saturated with H_2.

During the first 14 days in Figure 5.8, the SRB consumed 20% of the available H_2 in both 0.3 barg and 1 barg. The consumption was 14.6% for 1.7 barg within the same duration. In comparison, the sterile controls of 1 barg and 1.7 barg increased to 3.2% and 5%, respectively. The pressures of 0.3 barg and 1 barg consumed a higher percentage of the available H_2 than 1.7 barg. The consumption ended at 34.3% for 0.3 barg, 27.2% for 1 barg, and 23.1% for 1.7 barg.

The increase in H_2 consumption in the first 14 days implies a higher activity by the SRB, followed by a reduction in microbial activity. The pressures of 0.3 barg and 1 barg, relatively, consumed more of the total H_2 available compared to the highest pressure of 1.7 barg. All the bottles containing the SRB increased from pH 7.33 to around pH 9. However, due to the lack of data on pH development, it is difficult to determine when 1.7 barg reached pH 9. The pH development could potentially explain the behavior of slow and lower H_2 consumption in

1.7 barg compared to the lower pressures.

The sterile controls showed a H_2 consumption up to 15%, which is inaccurate as it was expected to be stable due to the absence of microbial cells. This observation can be explained by the pressure loss from the measurement with the pressure transducer, as described in Section 4.1. The loss is similar for all the measurements due to the same procedure. In addition, the loss could also include gas leakage of the highly volatile H_2 or dissolution of H_2 in the medium. The error bars in 5.8 were larger for 0.3 barg and sterile 1.7 barg (dashed lines) than the rest. One of the bottles with 0.3 barg had a larger decrease in both the pressure and gas composition of H_2 at the end compared to the duplicate. On day 22, the graph of 1.7 barg has a large error bar because one of the duplicates increased in pressure. One of the duplicates had a higher temperature than the other, as the temperature can influence pressure, as seen in Equation 3.1.
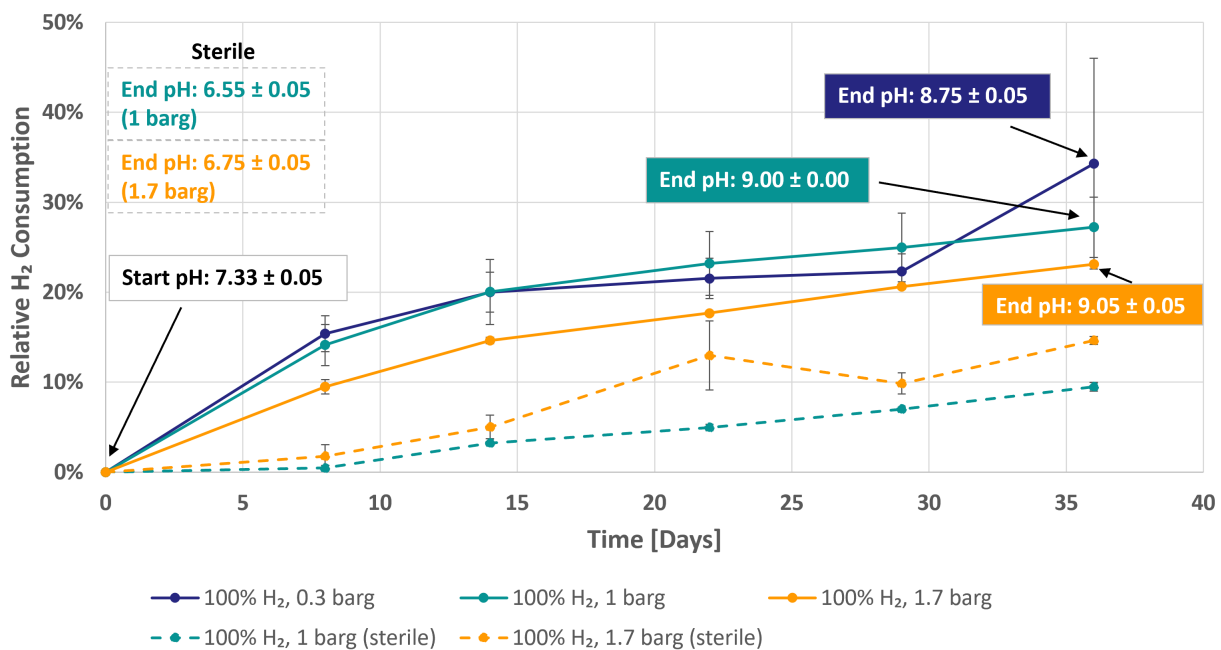
Figure 5.8: Relative percentage of the total H_2 consumed by *Desulfohalobium retbaense* over 42 days for the different pressures of 0.3 barg, 1 barg, and 1.7 barg, including the sterile represented in dashes for the two latter. This graph is on a relative scale obtained from Figure B.1 in Appendix B.1. For comparison, all the start points were normalized to initial moles H_2.

The highest maximum consumption rate is observed for 1 barg in Figure 5.9. Upon considering the error bars, the three rates are similar. This result was unexpected as the highest pressure would yield a higher maximum rate. The total number of moles consumed appears

to increase with increasing pressure. However, none of the graphs consumed all the available H_2, as seen in Figure 5.8.

Figure 5.9: The relationship between the maximum consumption rate and the number of moles consumed by *Desulfohalobium retbaense* as a function of the pressure. The x-axis is the pressure in mbarg, while the y-axis is the maximum consumption rate in mmoles/day. The secondary y-axis is the total number of moles consumed by the SRB in mmoles.

The measurable H_2S in the headspace for the three pressures of 0.3 barg, 1 barg, and 1.7 barg is seen in Table 5.1. Due to unknown reasons, the uncertainty in 0.3 barg is large due to one of the duplicates containing a significantly higher amount of H_2S.

Table 5.1: The measurable H_2S concentration in the headspace at the end of the experiment for the three pressures of 0.3 barg, 1 barg, and 1.7 barg.

Pressure [barg]	H_2S concentration the end [%]	$\pm$
0.3	3.42	3.07
1	0.37	0.02
1.7	0.32	0.00

The unexpectedly similar maximum consumption rate for the three pressures of 0.3 barg, 1 barg, and 1.7 barg implies that the SRB does not consume H_2 any faster at higher pressure.

The higher pressures resulted in greater availability of H_2 due to dissolution in the medium, as explained in Section 2.1 and Figure 2.4. The maximum consumption rate was the same for all pressure considering the error bars, indicating that the H_2 was not a limiting factor for consumption. Since the higher pressure was expected to yield a higher consumption rate, other factors were limiting microbial activity. These factors could potentially include insufficient numbers of bacterial cells and deficiency of vitamin or sulfate. The absence of essential nutrients and sulfate inhibits the microbial activity of the SRB [11], [24]. Dohrmann and Krüger [24] experienced in their study that the SRB depended strongly on the availability of the sulfate. The high pH could be the limiting factor based on the obtained results. The pH increase is a result of the metabolic process of SRB, where they utilize H^+ in their metabolism, as seen in Equation 2.3. The high pH of around 9.0 in the end measurements, as seen in Figure 5.8, may have been inhibiting microbial activity. Consequently, the maximum consumption rate reached a certain threshold where the SRB could not consume faster.

5.2.2   Methanogen

All unsterile bottles with pressures of 0.5 barg, 1.5 barg, and 2 barg reached 0 barg on day 7, day 8, and day 14, respectively (seen in Figure 5.10). The reduction was greater for 1.5 barg and 2 barg over the weekend, from day 4 to day 7. The pressure loss of the sterile controls for 1.5 barg and 2 barg was less than the unsterile and was caused by the needle removal during the pressure measurements. The measuring procedure was similar for all, which implies a consistent pressure loss. This suggests that the unsterile bottles experienced lost the majority of the pressure due to the dissolution of H_2 in the liquid and microbial H_2 consumption.
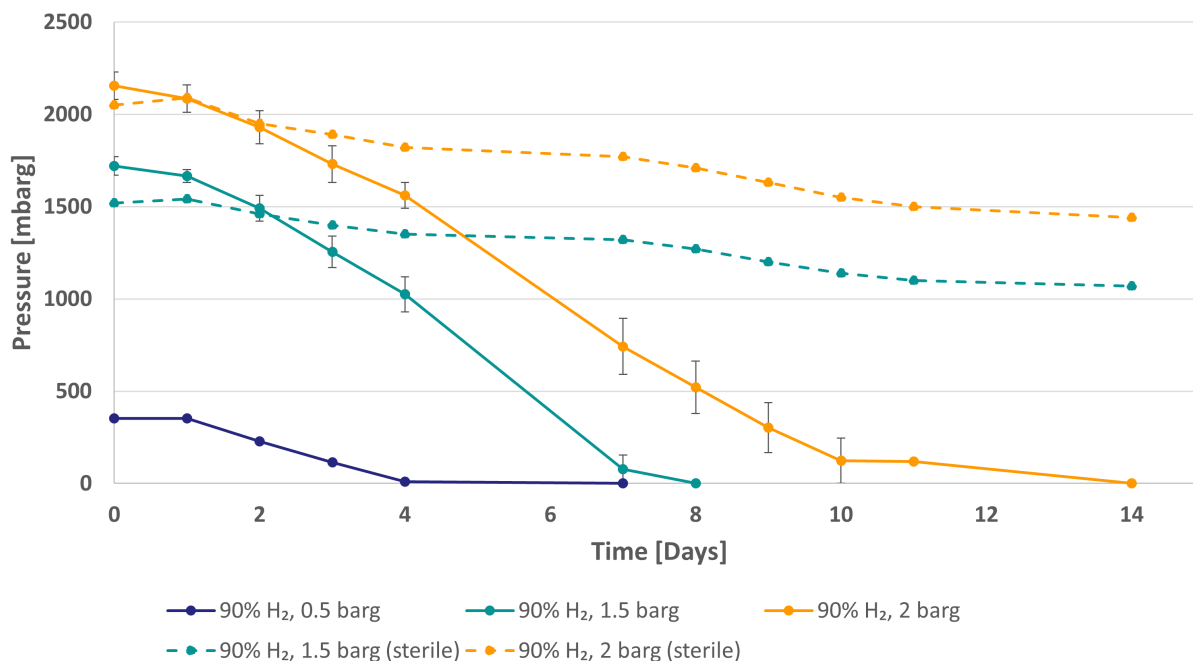
Figure 5.10: The pressure measurements over 14 days of *Methanocalculus halotolerans* for three different 0.5 barg, 1.5 barg, and 2 barg, including sterile controls for the latter two. The headspace contained 90% H_2 and 10% CO_2.

Figure 5.11 shows that the relative consumption was 25% for 0.5 barg and 1.5 barg after the initial four days, while 2 barg was slightly lower at 19%. The microbial consumption was slower for all pressures during the initial four days than the following days. The pressures of 0.5 barg and 2 barg consumed all of the available H_2 on day 7 and day 14, respectively. Meanwhile, 1.5 barg only partially consumed the present H_2. However, the error bar on day 7 for 1.5 barg is larger than the others in the same graph. This is a result of the considerable deviation observed between the duplicates because the depletion of pressure occurred on different days. Thus, it is also possible to assume that 1.5 barg reached complete consumption due to the large error bar. The same applies to 2 barg with a large error bar on day 10. The H_2 consumption by the sterile controls was inaccurate as there were no methanogens present. This was caused by pressure loss during measurements and was not accounted for in the results.

The end measurement of the pH for all pressures and both sterile and unsterile experiments increased from close to pH 7.0 to around pH 8.0 (see Figure 5.11). The highest increase in end pH was observed for 1.5 barg, followed by two barg and 0.5 barg. In comparison, the pH of the sterile controls increased to pH 8. Therefore, the increased pH does not appear to

affect the consumption.
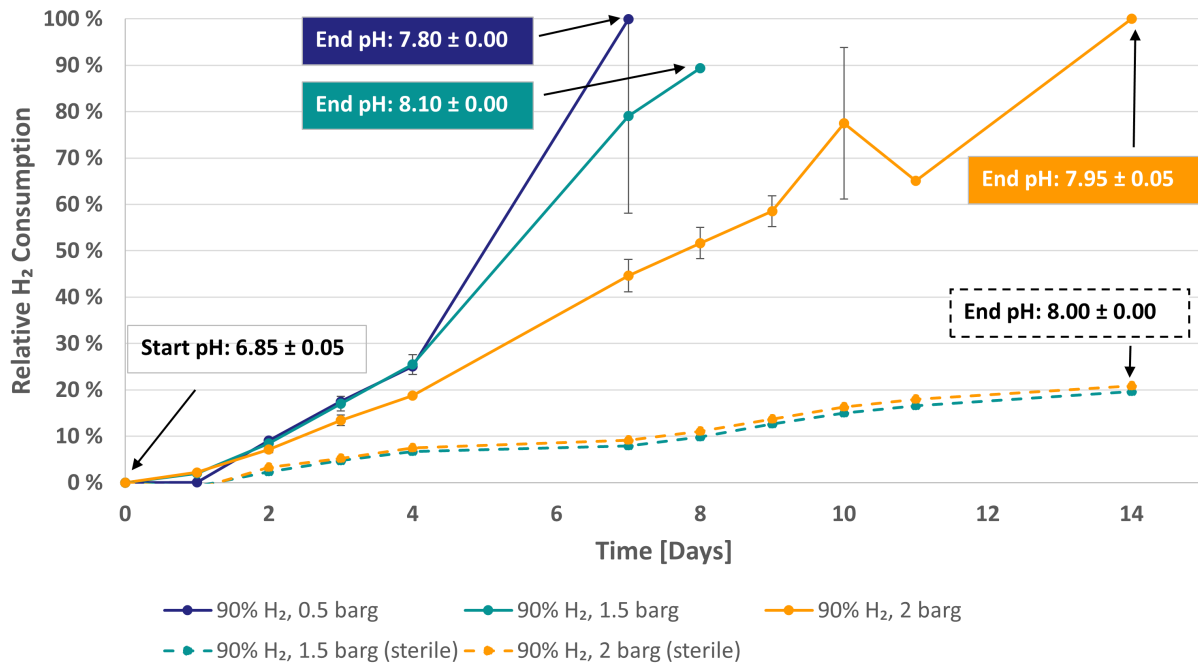
Figure 5.11: The total relative percentage H_2 consumed by *Methanocalculus halotolerans* over 14 days was calculated for three different pressures of 0.5 barg, 1.5 barg, and 2 barg, including sterile controls for the latter two. The graph is on a relative scale obtained from Figure B.2 in Appendix B.1. The average of the initial pH is included, and the end pH is in the same colors as the respective pressure graphs.

The highest maximum consumption rate was 0.66 mmoles/day in 1.5 barg, as seen in Figure 5.12. The maximum consumption rate was expected to follow a linear trend with increasing pressure. The large error bars observed for 2 barg for both maximum consumption rate and total amount consumed result from the duplicates finished on different days. Considering the large error bar in 2 barg, the maximum consumption rate for 2 barg may be equivalent to or even higher than in 1.5 barg. Although the experiment with 0.5 barg ended first, it also had the lowest maximum rate with 0.3 mmoles/day and the total amount of H_2 of 1.19 mmoles. Assuming complete H_2 consumption for all, the bars in Figure 5.12 show that the higher pressures contained a higher amount of dissolved H_2 available for the methanogen to consume.
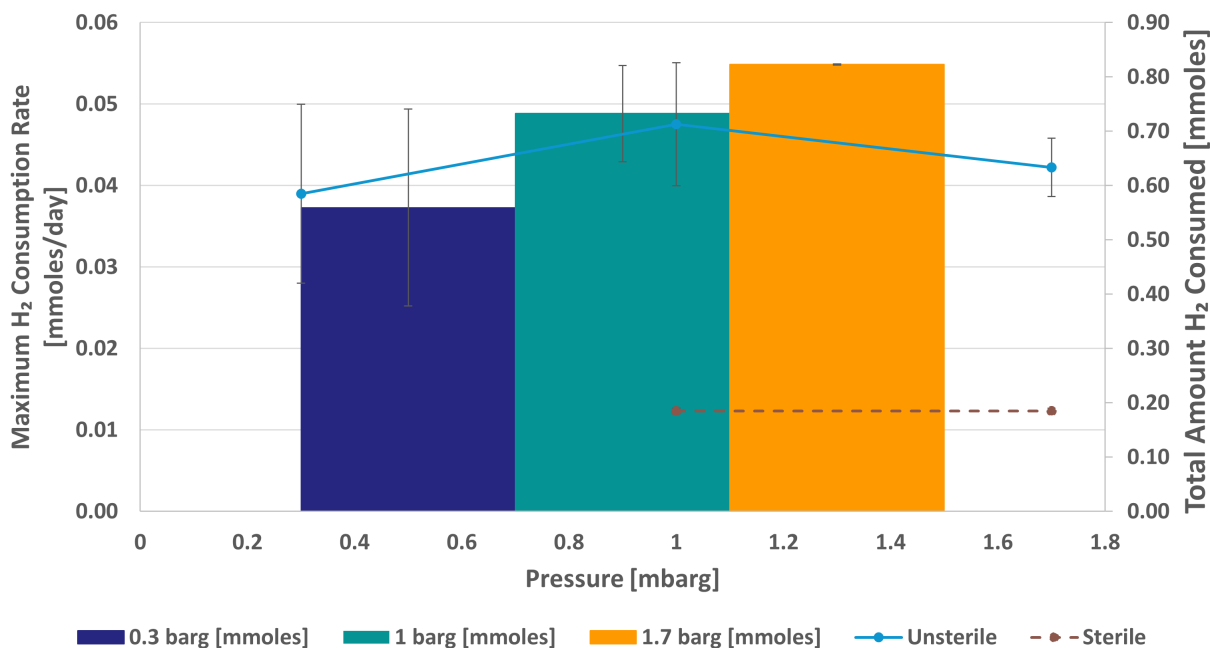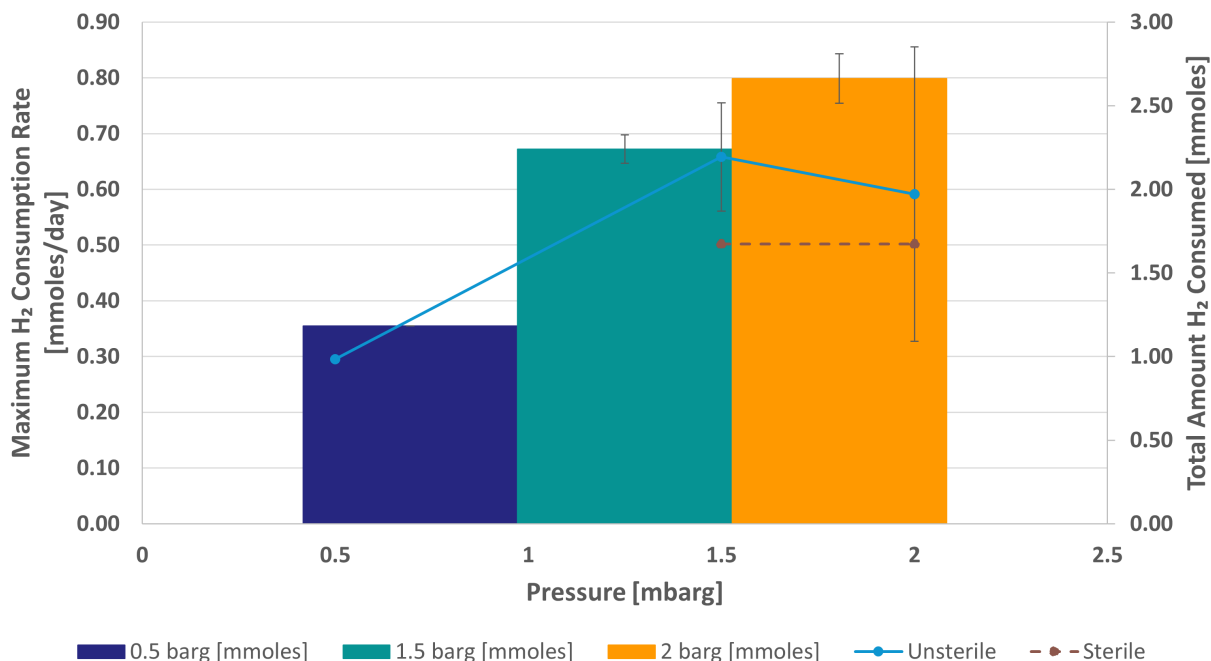
Figure 5.12: The relationship between the maximum consumption rate and the number of moles consumed by *Methanocalculus halotolerans* as a function of the pressure. The x-axis is the pressure in mbarg, while the y-axis is the maximum consumption rate in mmoles/day. The secondary y-axis is the total number of moles consumed by the methanogen in mmoles.

Table 5.2 presents the CH_4 concentration, which increased with increasing pressure. The significant amount of CH_4 indicates an effective microbial activity by the methanogen.

Table 5.2: The measurable CH_4 concentration in the headspace at the end of the experiment for the three pressures 0.5 barg, 1.5 barg, and 2 barg.

Pressure [barg]	CH_4 concentration at the end [%]	$\pm$
0.5	15.06	0.00
1.5	24.20	0.10
2	29.92	2.58

As expected, all the pressures reached 0 mbarg, indicating that the methanogen consumed all the available H_2. Considering the large error bars in Figure 5.11 of the relative H_2 consumption, it can be assumed that the methanogen consumed all the available H_2. Furthermore, it can also be assumed that the maximum consumption rate for 2 barg in Figure 5.12 could be higher or equivalent to 1.5 barg due to the error bars. Assuming a higher maximum consump-

tion rate at 2 barg compared to 1.5 barg would suggest a linear trend in the consumption rate for the methanogen. The linear trend implies that there were no limiting factors inhibiting microbial activity. However, assuming the equivalent maximum consumption rate would imply that there could be a limiting factor for microbial activity at higher pressures. In this experiment, no CO_2 was re-added, resulting in a slight increase in pH of around 1.0. Despite the small increase, the pH remained within the range of 7.0 to 8.4. Therefore, the observed pH increase did not inhibit the microbial activity, indicating that pH was not a limiting factor. Furthermore, the methanogen produced a significant amount of CH_4, indicating an efficient microbial metabolic process.

5.3   Comparison of the Impact of Different Hydrogen Concentration and Pressure on SRB and Methanogen

The duration of the experiment to study the impact of different H_2 concentrations with *Desulfohalobium retbaense* was 42 days, while *Methanocalculus halotolerans* lasted for seven days. The methanogen managed to achieve complete H_2 consumption for all H_2 concentrations, while the SRB accomplished the same for only $10\%H_2$. The experiments on the impact of different pressures lasted 36 days for the SRB and 14 days for the methanogen. During the mentioned periods, the different pressures with the SRB of 0.3 barg, 1 barg, and 1.7 barg did not reach 0 barg. A depletion of pressure could indicate complete consumption. In contrast, the methanogen in the different pressures of 0.5 barg, 1.5 barg, and 2 barg managed to do so within a shorter time frame. Furthermore, none of the pressures with the SRB consumed all the available H_2. Conversely, the methanogen achieved complete consumption for 0.5 barg and 2 barg.

Table 5.3: Overview of the most important data from the experiments with different H_2 concentrations for the SRB and the methanogen.

	H₂ Concentration		
	SRB		
	10%H_2	40%H_2	100%H_2
Max. Consumption Rate [mmoles/day]	0.02 ± 0.00	0.03 ± 0.00	0.05 ± 0.00
Loss of H_2 [mmoles]	0.18 ± 0.01	0.36 ± 0.07	0.68 ± 0.01
Initial pH	7.53 ± 0.15		
End pH	8.10 ± 0.10	8.85 ± 0.05	9.00 ± 0.00
Produced H_2S in the end [%]	1.15 ± 0.00	0.20 ± 0.02	0.27 ± 0.01
	Methanogen		
	10%H_2	40%H_2	90%H_2
Max. Consumption Rate [mmoles/day]	0.07 ± 0.00	0.14 ± 0.01	0.22 ± 0.01
Loss of H_2 [mmoles]	0.20 ± 0.02	0.60 ± 0.00	1.16 ± 0.00
Initial pH	7.38 ± 0.11		
End pH	7.50 ± 0.10	7.45 ± 0.05	7.50 ± 0.10
Produced CH_4 in the end [%]	2.28 ± 0.16	9.10 ± 0.16	14.70 ± 0.76

Table 5.4: Measurement of the amount of acetate at the start and at the end of the experiments for the different H_2 concentrations.

SRB			
	Start	End	$\pm$	
0%H_2	1428	1507	66	mg/L
10%H_2	1428	1751	158	mg/L
100%H_2	1428	1439	99	mg/L
Methanogen			
0%H_2	1216	1283	23	mg/L
10%H_2	1216	1326	78	mg/L
90%H_2	1216	1336	74	mg/L

The pH can be used as a proxy for estimating the microorganisms' activity because it directly affects microbial metabolism. The results in Table 5.3 show a substantial difference between the SRB and the methanogen regarding the measured end-values of the pH and H_2 consumption. Specifically, the SRB had significant increases in pH up to 9.0, whereas the measurements for the methanogen were stable at around pH 7.50. In addition, the end pH was higher for the highest H_2 concentration in the case of the SRB. The high pH inhibited

the microbial activity of the SRB, resulting in a lower H_2 consumption compared to the methanogen. However, the pH values were obtained only at the beginning and end of the experiment. This poses a challenge to compare and fully understand the relationship between consumption and pH without the measurements during the experiments. For instance, questions such as when the end pH was reached and the progression over time would be interesting to study.

The pH also directly impacted the H_2S concentration. The decreasing H_2S concentration was due to less fraction of H_2S compared to HS^- in an alkaline environment, suggesting that less H_2S was available in the gaseous phase. Meanwhile, CH_4 concentration of the methanogen increased with higher H_2 concentrations, resulting in the highest to be up to 14.70% CH_4. This suggests an efficient metabolic process with no limiting factors for the methanogen compared to the limiting factor of high pH for the SRB.

The maximum consumption rate for both SRB and methanogen showed a linear trend. This implies that the higher H_2 concentrations consumed the available H_2 faster. The H_2 consumption rate by the SRB was considerably lower than by the methanogen. According to Dopffel *et al.* [11], sulfate reduction is a very process that indicates that there was a limiting factor, which in this case was the high pH.

Table 5.4 shows that the amount of acetate did not decrease during the experiment with the different H_2 concentrations, which implies that neither SRB nor methanogen used acetate in their metabolic processes. Therefore, the acetate was not a limiting factor for the H_2 consumption. This was unexpected as it was described in the literature that acetate was required for microbial activity [72], [73]. A possible explanation for the stable acetate amount could be that the SRB and methanogen had sufficient energy reserves from the preculture, making the acetate utilization redundant. It is not within the metabolic capability of the SRB to produce acetate, as the primary metabolic byproduct is sulfide (shown in Equation 2.3). Therefore, the error may be attributed to the procedure where the injection of acetate in the bottles was not identical.

Table 5.5: Overview of the most important data for the experiments with different pressures for the SRB and the methanogen.

	Pressure		
	SRB		
	0.3 barg	1 barg	1.7 barg
Max. Consumption Rate [mmoles/day]	0.04 ± 0.01	0.05 ± 0.01	0.04 ± 0.00
Loss of H_2 [mmoles]	0.57 ± 0.18	0.74 ± 0.09	0.83 ± 0.00
Initial pH	7.33 ± 0.05		
End pH	8.75 ± 0.05	9.00 ± 0.00	9.05 ± 0.05
Produced H_2S in the end [%]	3.42 ± 3.07	0.37 ± 0.02	0.32 ± 0.00
	Methanogen		
	0.5 barg	1.5 barg	2 barg
Max. Consumption Rate [mmoles/day]	0.30 ± 0.00	0.66 ± 0.10	0.59 ± 0.27
Loss of H_2 [mmoles]	1.18 ± 0.00	2.24 ± 0.08	2.66 ± 0.15
Initial pH	6.85 ± 0.05		
End pH	7.8 ± 0.00	8.10 ± 0.00	7.95 ± 0.05
Produced CH_4 in the end [%]	15.6 ± 0.00	24.20 ± 0.10	29.92 ± 2.58

Table 5.6: Measurement of acetate at the start and at the end of the experiments for the different pressures.

SRB			
	Start	End	$\pm$	
1 bar	1529	1438	48	mg/L
1.7 bar	1529	1480	62	mg/L
Methanogen			
1.5 bar	1221	1212	59	mg/L
2 bar	1221	1191	32	mg/L

Based on the observed results in Table 5.5, the pressure affects the solubility of the H_2 in the medium and the microbial H_2 consumption, which resulted in greater availability of H_2 in the aqueous phase for microbial consumption. As shown in Figure 2.4, increased pressure in the headspace forces the molecules to dissolve into the medium until a dynamic equilibrium is achieved. By observing the greater H_2 loss in the SRB and methanogen under higher pressures and comparing the H_2 loss in Table 5.3, it is evident that the solubility of H_2 is affected by the pressure, despite its low solubility.

Despite the higher amount of available H_2, the maximum consumption rate for the SRB was similar for all pressures. In contrast, the rate by the methanogen followed a linear trend. Higher pressures were expected to yield a higher maximum consumption rate. As discussed earlier, the limiting factor for the SRB was primarily the increased pH. However, additional factors such as low microbial cell numbers or deficiencies in vitamin or sulfate could also contribute. The methanogen also increased slightly to around pH 8, which was not the case in the different H_2 concentrations experiment. As discussed in Section 5.2.2, the pH increase was due to not re-adding CO_2 and was too small to affect the microbial activity as it was still within the pH range of the methanogen. Consequently, the threshold for the maximum consumption rate was higher for the methanogen than the SRB, mainly due to the limiting factors.

As described in Section 5.2.1, the high pH influenced the gaseous H_2S concentration. The H_2S concentrations for the different pressures are stable, disregarding the large uncertainty for 0.5 barg. The CH_4 concentrations were higher for the higher pressures and greater compared to the experiment with different H_2 concentrations. This implies that the metabolic processes of the methanogen were active without limiting factors.

Both the methanogen and the SRB utilized a minor amount of acetate as a carbon source in their metabolic processes, as seen in Table 5.6. The SRB used more acetate compared to the methanogen. Given the uncertainty, the utilization is not significant. Cell numbers were not measured in this thesis due to time constraints, leading to uncertainty regarding the observed utilization. Therefore, whether the observed utilization resulted from procedure error or actual utilization by the microbes is not certain.
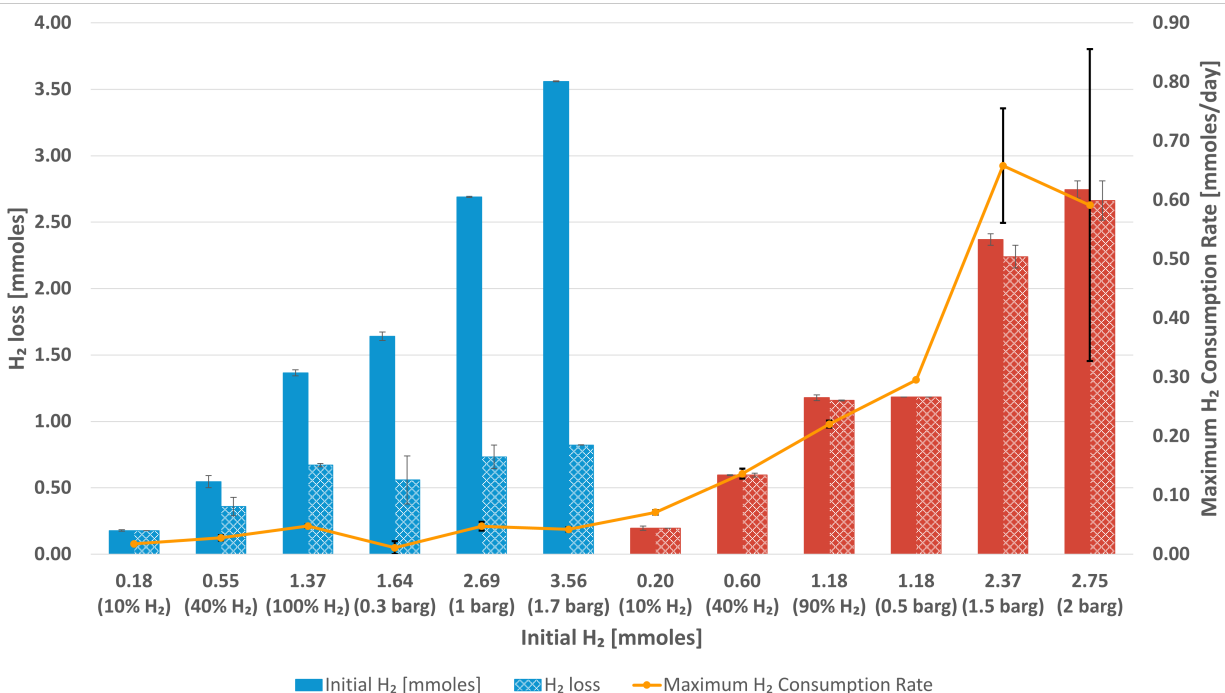
Figure 5.13: Comparison of the maximum consumption rate (mmoles/day) and H_2 loss (mmoles) for different the H_2 concentrations and different pressures by the SRB and methanogen. The SRB data is represented in blue color, while the red color is for the methanogen. The solid colors illustrate the total amount of initial H_2 (mmoles), the patterned colors are the total H_2 loss (mmoles) and the orange graph is the maximum consumption rate for the respective H_2 concentrations and pressures.

Figure 5.13 compares the maximum consumption rate by the SRB and methanogen for the different H_2 concentrations and pressures. The increasing initial H_2 indicates that the quantity of available H_2 was affected by the pressure, solubility, and H_2 concentration. The methanogen also contained CO_2 in the headspace of the bottles as mentioned in Section 3.11, therefore the initial H_2 was lower than for the SRB. Nevertheless, the SRB did not utilize as much of the H_2 as the methanogen. The microbial activity by the SRB corresponds with the limiting factor of pH. The microbial activity of the methanogen was not inhibited, and therefore the maximum consumption rate was significantly higher than for the SRB.

Based on the obtained data, the methanogen has a higher threshold of maximum consumption rate than the SRB. The SRB inhibited its microbial activity; therefore, the methanogen can be more of a concern in UHS. Regarding the safety of UHS, the SRB poses a lower risk since the pH affected the composition of sulfides, and less of the toxic gaseous H_2S was available.

5.4 Hydrogen consumption in Porous Media (Micromodel)

Microbial H_2 consumption in porous media of subsurface reservoirs can differ from our bottle experiments. Microbial growth in the bottles occurs in a well-mixed environment, where nutrients can easily diffuse and be transported. However, the environment in porous media is more heterogeneous, and the transportation and diffusion of nutrients can be influenced by pore geometry. Dr. Na Liu conducted the micromodel experiment to achieve a comprehensive understanding of microbial behavior in porous media. The objective of the experiment was to study the H_2 consumption by microorganisms in a microfluidic pore network saturated with H_2 and SRB *Desulfohalobium retbaense*.

Figure 5.14: Image of the microfluidic setup in the laboratory captured by Malin Haugen.

The experimental setup is seen in Figure 5.14, and the procedure is described in Appendix C. To directly observe the microbial-induced sulfate reduction, a silicon-wafer micromodel with pore patterns from a natural sandstone was utilized. The experiment was conducted at 35 barg and 37 °C, replicating the environment of a shallow aquifer or gas-water transition zone within a depleted gas field [84], [85].
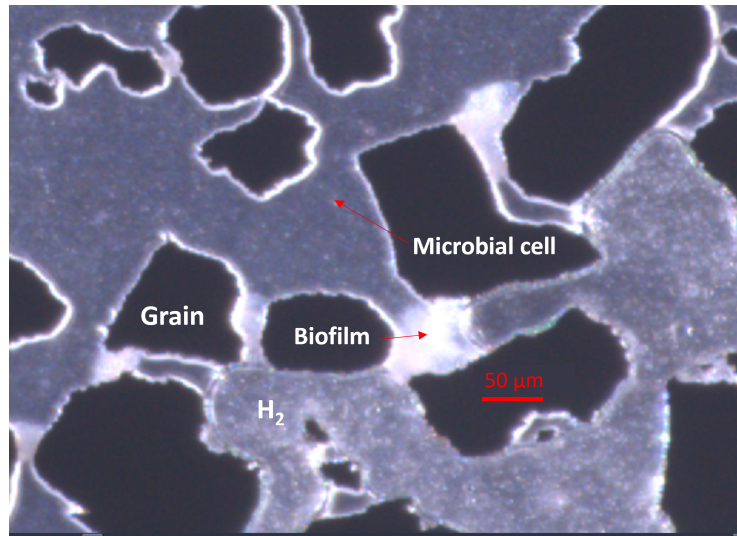
Figure 5.15: Close-up image of the microbial cells, H_2 and biofilms in the pore space. Image provided by Dr. Na Liu.

A close-up image of the micromodel obtained from the experiment is seen in Figure 5.15, which illustrates the various components present. The small white dots in the aqueous phase (dark grey) is the microbial cells, the gaseous phase (light grey) is the H_2, and the silicon grains are the black structures. The microbial growth of the SRB resulted in biofilm formation, seen as the white clusters in Figure 5.15. This accumulation of biofilms can cause clogging in the pores, which can lead to changes in the physical property of porosity and permeability [86], [87], [88].
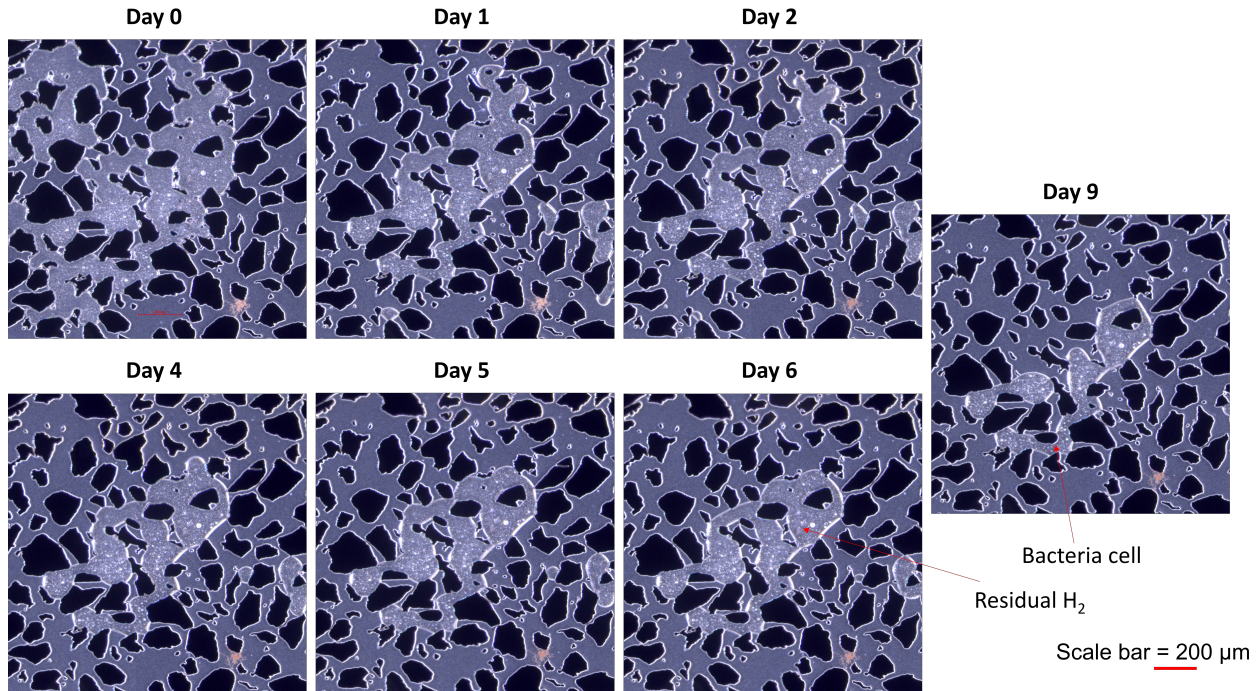
Figure 5.16: Images of H_2 consumption by *Desulfohalobium retbaense* in porous media over 9 days. The microbial H_2 consumption rate was $1.23 \cdot 10^{-6}$ mmoles/day. Images provided by Dr. Na Liu.

Figure 5.16 shows the H_2 consumption by the SRB over nine days. Initially, the majority of the area in the image was occupied by gaseous H_2. However, after a day, the microbes consumed a significant amount of H_2 located at the image's upper left region and lower bottom left region. The following day, the microbial H_2-consumption was barely perceptible. However, the H_2-consumption after day 2 was more prominent than on day 1 and day 2.

The experimental duration between the experiments in the bottles and the micromodel varied. Specifically, the experiment conducted in the porous media lasted nine days, while the experiment with different H_2 concentrations in bottles lasted for 42 days. Additionally, the experiment studying the effects of different pressures spanned 36 days. Furthermore, the SRB had a consumption rate of $1.23 \cdot 10^{-6}$ mmoles/day within the porous media (See calculation in Appendix D). In the experimental setups using bottles with different H_2 concentrations, the consumption rates were 0.02 mmoles/day for 10%H_2, 0.03 mmoles/day for 40%H_2, and 0.05 mmoles/day for 100%H_2. In the experiments conducted with bottles of different pressures, the consumption rates were calculated to be 0.4 mmoles/day for 0.3 barg and 1.7 barg and 0.05 mmoles/day for 1 barg. The activity and growth of the microbes were, therefore, more rapid in the bottle compared to porous media. It was expected that the larger sur-

face area in the porous media would result in an increased contact area for interconnection between the microbes and H_2. The lower H_2 consumption rate in the micromodel could be due to the pore geometry, volume of bacterial solution, and unfavorable environments in the micromodel. However, the observed consumption rates in the bottles and micromodel may not be directly comparable due to the difference in scale.

The irregular structure and pores in the porous media can create physical barriers for the microbes' movement towards H_2 bubbles, limiting the H_2 consumption rate and microbial growth. The environment in the bottles is not structured as in the porous media. Thus the microbes had more accessible H_2. Furthermore, the micromodel contained fewer microbial cells compared to the bottles. The volume of bacterial solution in the micromodel was approximately 9.46 µL (Appendix D), significantly smaller than the 25 mL in the bottles. The microbial growth in the confined micromodel can lead to the accumulation of byproducts and toxins in the aqueous phase, thus reducing microbial activity. For example, the production of the toxic H_2S by the SRB can diffuse into the cell membrane and damage the proteins, resulting in respiratory inhibition [22], [89], [90]. As seen in Figure 5.16, the microbial activity is reduced after two days, resulting in a low H_2 consumption rate in the micromodel.

The surface area affects the biofilm formation. The microbes adhere to the surface and develop biofilm, an accumulation of microbial cells enclosed in a matrix of exopolymeric substances secreted by the microbes [11], [91]. This community provides protection for the microbes against environmental stress such as pH change [84], [92]. The development of biofilms can cause clogging of the pore space or pipelines. The biofilms can also interfere with the H_2 flow and occupy available pore space, resulting in reduced porosity and permeability [11], [22], [84], [93]. Furthermore, corrosion often occurs under the biofilm, which can damage the equipment of the installation [11]. As seen in Figure 5.16, there was an expected development of biofilms by the SRB. However, Liu *et al.* [84], who conducted the experiment with the SRB, did not observe a large amount of biofilm. The biofilm formation after 18 hours in the inlet area was less than 0.1% of the pore space. Hence, the SRB *Desulfohalobium retbaense* has limited development of biofilms [84].

Chapter 6

Conclusion

Experimental laboratory work has been conducted in this thesis to study the impact of different H_2 concentrations and pressures on the H_2 consumption by SRB and methanogen. The objective was to quantify and study the H_2 consumption for a better understanding of the microbes' behavior and the implications in UHS. Specifically, the behavior of the SRB *Desulfohalobium retbaense* and the methanogen *Methanocalculus halotolerans.* Similar types are commonly found in saline environments, including saline aquifers and salt caverns, which are considered suitable for UHS.

The results showed that the SRB slowly consumed the available H_2, where the highest maximum rate was at $100\%H_2$ with 0.05 mmoles/day compared to 0.22 mmoles/day at $90\%H_2$ for the methanogen. However, the SRB did not manage to consume all the available H_2 except in $10\%H_2$ concentration. The SRB utilized H^+ in their metabolic process, which caused the pH to increase. As the pH approached 9.0, the H_2 consumption declined due to the unfavorable environment. The pH also affected the measurable percentage of H_2S concentration in the headspace at the end. The increased pH lead to less H_2S and more HS^-. Furthermore, the H_2 concentrations also affected the consumption of the available H_2. The observed trend suggests that the highest H_2 concentration had a higher pH. Hence, the H_2 concentrations do affect the H_2 consumption of the SRB.

The methanogen consumed all the available H_2 for all H_2 concentrations, indicating an absence of limitations. The pH was stable and showed a minimal increase of around 0.1 compared to the SRB. At the highest H_2 concentration, the methanogen consumed more of the available H_2, and the maximum consumption rate was higher. Furthermore, the CH_4 con-

centration in the headspace at the end was notably higher compared to H_2S. Thus, the methanogen had a sufficient amount of nutrients and adequate conditions for their metabolic process.

As the pH increased to 9.0, the metabolic processes of SRB were inhibited and did not manage to consume all the available H_2 for any of the pressures. However, the H_2 consumption was greater compared to the experiments with different H_2 concentrations. The same trend was also observed for the methanogen. The higher pressures resulted in greater availability of H_2 in the aqueous phase for microbial consumption. Thus, the pressure did not affect the microbes directly, but it affected the solubility of the H_2 in the medium.

The results obtained from the micromodel of the SRB showed a significantly lower consumption rate of $1.23 \cdot 10^{-6}$ mmoles/day compared lowest of 0.02 mmoles/day in the bottle experiments. The lower consumption rate can be attributed to three main factors. Firstly, the pore geometry created structural barriers for the microbes' movement for H_2 consumption and microbial growth. Secondly, fewer microbial cells were present in the micromodel due to the difference in the bacterial volume of around 9.46 µL compared to 25 mL in the bottles. Finally, the accumulated byproducts and toxins produced by the SRB can cause an unfavorable environment for microbial activity. The pH could also be an inhibiting factor, as observed in the experiments with the bottles. However, measuring the pH of the micromodel experiment is not possible. However, due to the difference in scale, the consumption rate may not be comparable.

The presence of SRB and methanogen can result in implications for UHS, including the alteration of gas mixtures in the storage due to the productions of H_2S and CH_4. Among these, CH_4 appears to be of greater concern due to the more prominent production compared to H_2S. Higher H_2 concentrations also resulted in a greater percentage of CH_4 production by the methanogen. Contrarily, the increased pH to 9.0 by the SRB led to a reduction of the amount of H_2S. The metabolic processes of the SRB were inhibited at higher H_2 concentrations. In terms of UHS, this is favorable and constitutes a positive outcome. Furthermore, the micromodel experiment revealed that the formation of biofilms was not substantial for the *Desulfohalobium retbaense*. This finding suggests a reduced likelihood of clogging and corrosion associated with biofilm formation.

Microorganisms can pose a risk to UHS, even under high salinity conditions. The SRB was observed to limit its microbial activity, while no such limitations were evident for the methanogen. Therefore, further research is necessary to comprehensively understand and

control microbial activity to ensure safe, stable, and economically feasible large-scale storage that facilities the acceleration of the energy transition.

Chapter 7

Future Work

During the experimental study conducted in this thesis, several suggestions emerged for improvement of the results and for enhancing our knowledge of microbial activities and their implications on UHS. The following recommendations for future work are:

- For more realistic microbial behavior, a higher pressure of up to 200 bars would be appropriate to apply to mimic the storage conditions.

- The pH had a higher importance than anticipated before conducting the experiments. Hence, it is recommended to conduct measurements of the pH development as a function of consumption rate to capture the relationship between the pH and H_2 consumption.

- The pH was a limiting factor for the microbial activity for the SRB. To better understand other limiting factors, the pH should be kept stable in the future to isolate any other limiting factors.

- Due to time constraints, the measurements of cell numbers were not conducted in this thesis. By doing so, the cell numbers will provide the number of cells in the different experiments and information on microbial growth. In addition, study the relationship between the cell numbers and microbial H_2 consumption.

- To enhance the validity of the results, conducting experiments with more than duplicates is recommended. Multiple replicates allow the elimination of potential outliers, addressing random behavior and identifying procedural errors.

- To study and compare the H_2 consumption and biofilm formation by the methanogen to other H_2 consuming microbial processes in porous media, it is suggested to conduct micromodel experiments.

- The next natural step would be to study the microbial activity on the core scale to get a better insight into the H_2 consumption, microbial growth, and chemical reactions to subsurface rocks.

- There is a need for more data on microbial activity on the field scale, which is important to understand microbial behavior in their natural habitat.

Appendices

Appendix A

HPLC Procedure

The procedure to measure the amount of acetate in the liquid samples was provided and written by Dr. Abduljelil Kedir at NORCE. Furthermore, he performed the experiment and supplied the data for this thesis. Figure A.1 and Figure A.2 were not explicitly used in this thesis, but Dr. Kedir used the curves to determine the acetate amount. The procedure is given below.

Liquid samples were analyzed by using liquid chromatography of Agilent 1260II HPLC which is equipped with a quaternary pump, temperature control column compartment integrated with autosampler, 1260 Refractive Index Detector (RID), and 1260 Diode Array Detectors HS (DAD HS). A guard column (i.e., Hi-Plex H 50X7.7 mm) and an analytical column (i.e., Hi-Plex H 300 x 7.7 mm, 8 μm) were used for the separation of the analytes. Milli-Q water was used to prepare the mobile phase, solutions, and samples after filtering it through a 0.22 μm Millipak filter. A mobile phase of 14 mM H_2SO_4 solution was prepared from HPLC grade stock solution and run in isocratic elution mode. Samples are diluted by using mobile phase solution (i.e., 14 mM H_2SO_4) and filtered through using a 0.45 μm RC syringe filter. A 20 μL of the sample was injected and the total run time was between 40 to 75 min depending on analyte interest. The autosampler compartment was controlled at 22°C while the column temperature was maintained at 60°C.

The organic acids were monitored using DAD and RID while sugars and alcohols were monitored using RID. The DAD recorded the absorbance at a wavelength of 210 nm beside the spectrum between 190-400 nm. The RID optical unit temperature was set to 55°C with positive polarity mode and the reference cell was purged with the mobile phase before start-

ing the analysis. The column was conditioned at 0.2 mL/min and 60°C with Milli-Q water overnight and regenerated with 14mM H2SO4 for 2 hours after every batch of analysis. This protocol is to extend the durability of the analytical column besides using the guard column. The Agilent OpenLAB CDS Software was used for data acquisition and data processing. All analytes were identified and quantified based on retention time and the respective reference standard calibration curves.
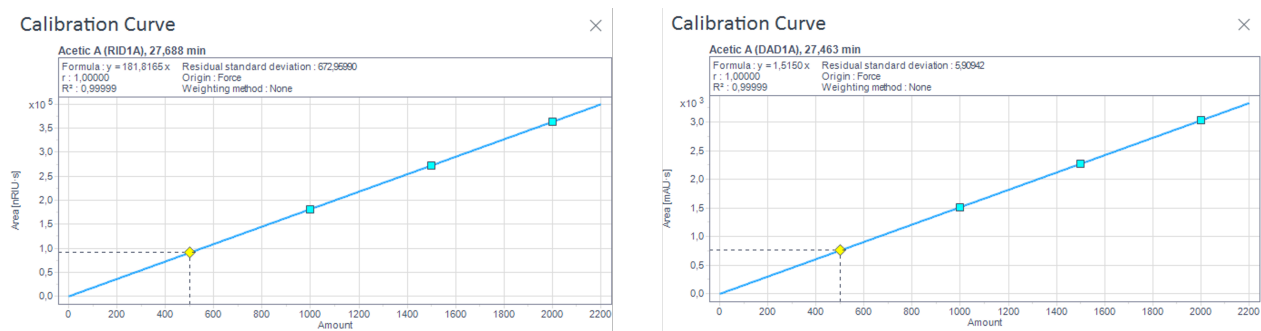
Figure A.1: Calibration curve of acetic acid, DAD and RID detectors
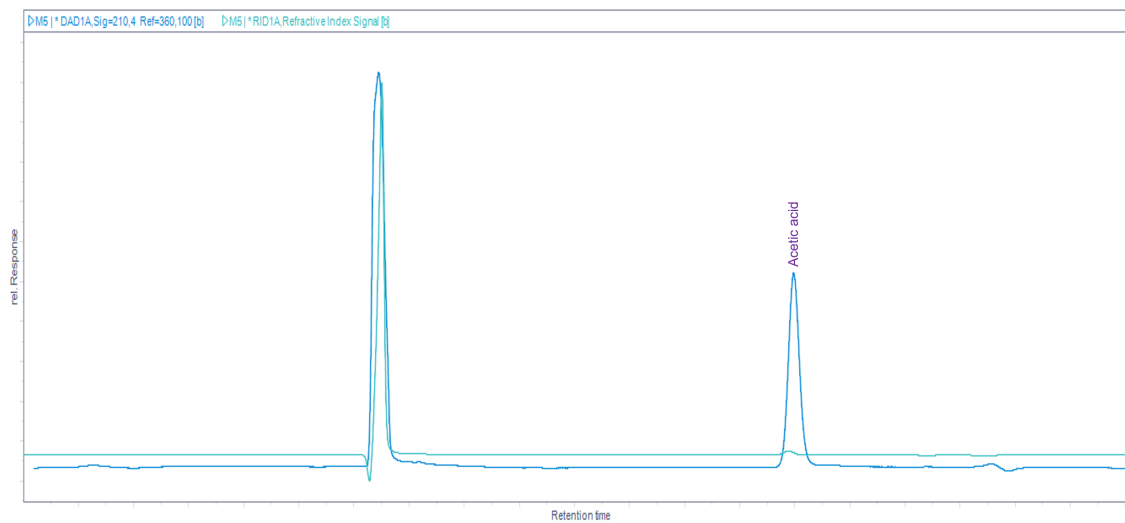
Figure A.2: Chromatogram of acetic acid

Appendix B

Results and Discussion

B.1 Experiments with Different Pressures

The data in Figure B.1 was the foundation for the calculation of total relative H_2 consumption by the SRB in Figure 5.8. Similarly, the total relative H_2 consumption by the methanogen in Figure 5.11 was derived from the data in Figure B.2.
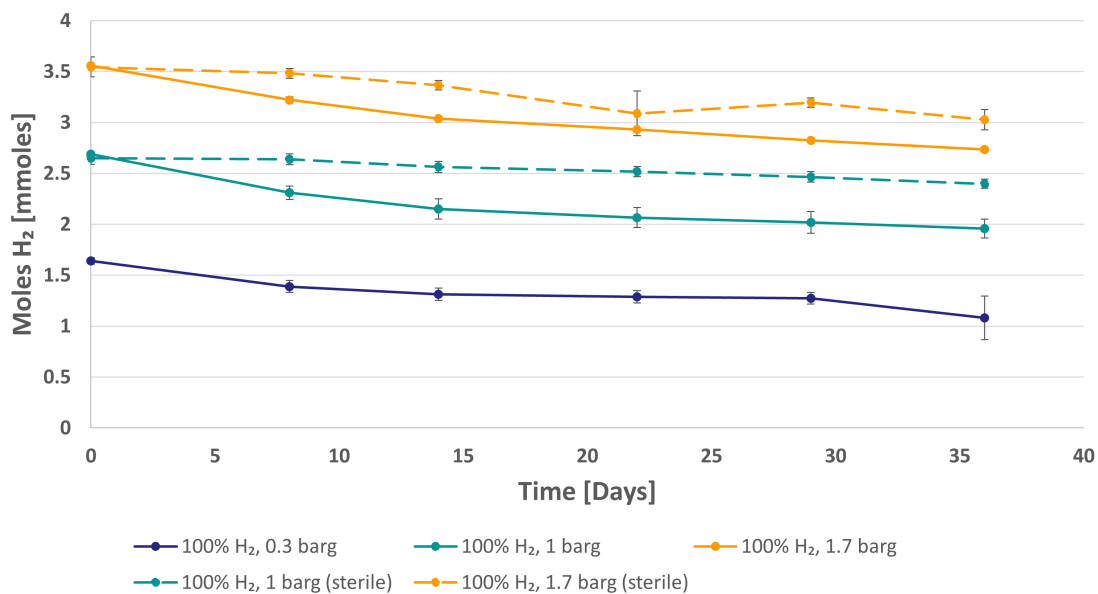
Figure B.1: The consumed H_2 amount (mmoles) by *Desulfohalobium retbaense* in 42 days for three pressures of 0.3 barg, 1 barg, and 1.7 barg. The last two pressures had a sterile control (i.e., without bacteria cells) represented in dashed lines.
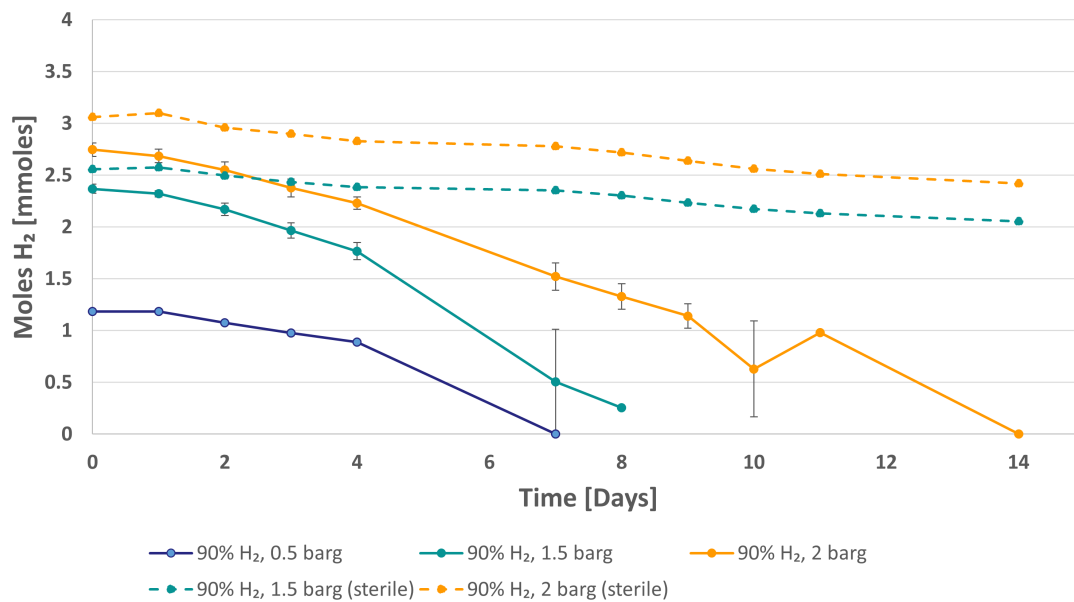
Figure B.2: The consumed H_2 amount (mmoles) by *Methanocalculus halotolerans* in 14 days for three pressures of 0.5 barg, 1 barg, and 2 barg. The last two pressures had a sterile control represented in dashed lines.

Appendix C

Micromodel Procedure

Dr. Na Liu at the Department of Physics and Technology at the University of Bergen conducted the experiment on microbial behavior in porous media. The procedure for the micromodel experiment with the same SRB as in this thesis is explained in Liu *et al.* [84]. Figure C.1 of the pore network properties was provided by Dr. Liu.

Parameter	Value
Width	27.0 mm
Length	21.4 mm
Depth	30 μm
Porosity	0.61
Pore volume	11.1 μL
Permeability	2.97 D
Repetition of pattern	36
Grain size	0.5 - 78 366 μm^2
Pore throat length	0.7 - 194 μm
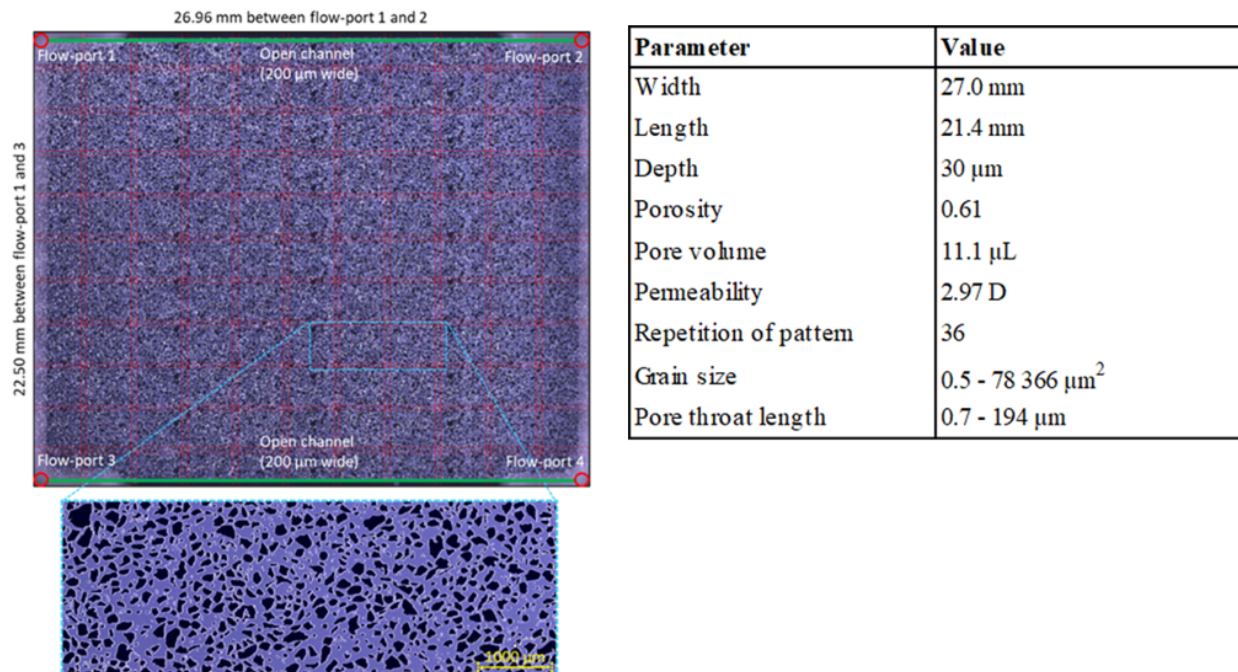
Figure C.1: The pore network properties of the micromodel

Appendix D

Calculations in Micromodel experiment

Table D.1 was provided by Dr. Na Liu of the H_2 consumption by the SRB in the micromodel. The value of approx. 9.46 µL of microbial solution was also provided by Dr. Liu. Table D.2 is the relevant H_2 properties used in the calculation. The volume μL^3 in Table D.1 was found by multiplying μL^2 with the depth from Figure C.1.

Table D.1: Table with H_2 consumption provided from Dr. Na Liu.

Hours	μL^2	μL^3
0h	410886	12326580
25h	252057	7561710
45h	250926	7527789
88h	241062	7231870
112h	217703	6531089
135h	206370	6191100
189h	168279	5048370
Volume change:		7278210

Table D.2: H_2 properties for calculation in the micromodel experiment. The density for H_2 at 35 bar and 37 °C was found in NIST Chemistry WebBook (Isothermal Properties for Hydrogen).

Density of H_2 at 35 bar and 37 °C	0.002682 g/mL
Molar weight of H_2	2.016 g/mol

$$\text{Rate: } \frac{7278210 \text{ μm}^3}{180 \text{ h}} = 38509 \text{ μm}^3/\text{h} \tag{D.1}$$

$$38509 \text{ μm}^3/\text{h} \cdot 10^{-12} = 3.851 \cdot 10^{-8} \text{ mL/h} \tag{D.2}$$

$$3.851 \cdot 10^{-8} \text{ mL/h} \cdot 24 \text{ h} = 9.242 \cdot 10^{-7} \text{ mL/day} \tag{D.3}$$

Used the value of the density of H_2 at 35 bar and 37 °C from Table D.2.

$$\text{Mass: } 9.242 \cdot 10^{-7} \text{ mL/day} \cdot 0.002682 \text{ g/mL} = 2.48 \cdot 10^{-9} \text{ g/day} \tag{D.4}$$

Used the molar weight of H_2 from Table D.2 to calculate the consumption rate.

$$\frac{2.48 \cdot 10^{-9}}{2.016 \text{ g/mol}} = 1.23 \cdot 10^{-9} \text{ moles/day} \tag{D.5}$$

$$\text{Microbial } H_2 \text{ consumption rate: } 1.23 \cdot 10^{-6} \text{ mmoles/day} \tag{D.6}$$

Bibliography

[1] International Energy Agency (IEA), "Energy technology perspectives 2023," International Energy Agency, Tech. Rep., 2023, License: CC BY 4.0. [Online]. Available: `https://www.iea.org/reports/energy-technology-perspectives-2023`.

[2] International Energy Agency (IEA), "World energy outlook 2022," 2022, License: CC BY 4.0. [Online]. Available: `https://www.iea.org/reports/world-energy-outlook-2022`.

[3] V. Masson-Delmotte, P. Zhai, H.-O. Pörtner, *et al.*, "Global warming of 1.5°c. an ipcc special report on the impacts of global warming of 1.5°c above pre-industrial levels and related global greenhouse gas emission pathways, in the context of strengthening the global response to the threat of climate change, sustainable development, and efforts to eradicate poverty," Cambridge, UK and New York, NY, USA, 2018, pp. 3–24. DOI: `10.1017/9781009157940.001`. [Online]. Available: `https://doi.org/10.1017/9781009157940.001`.

[4] Intergovernmental Panel on Climate Change (IPCC), "Climate change 2021: Mitigation of climate change," Intergovernmental Panel on Climate Change (IPCC), Tech. Rep., 2021, Accessed on: May 20, 2023. [Online]. Available: `https://www.ipcc.ch/report/ar6/wg3/downloads/report/IPCC_AR6_WGIII_FullReport.pdf`.

[5] Intergovernmental Panel on Climate Change (IPCC), "Climate change 2021: Impacts, adaptation and vulnerability," Intergovernmental Panel on Climate Change (IPCC), Tech. Rep., 2021, Accessed on: May 20, 2023. [Online]. Available: `https://report.ipcc.ch/ar6/wg2/IPCC_AR6_WGII_FullReport.pdf`.

[6] International Renewable Energy Agency (IRENA), "Renewable power generation costs in 2020," International Renewable Energy Agency, Tech. Rep., 2021. [Online]. Available: `https://www.irena.org/publications/2021/Jun/Renewable-Power-Costs-in-2020`.

[7] P. Preuster, A. Alekseev, and P. Wasserscheid, "Hydrogen storage technologies for future energy systems," *Annual Review of Chemical and Biomolecular Engineering*, vol. 8, no. 1, pp. 445–471, 2017, PMID: 28592172. DOI: `10.1146/annurev-chembioeng-060816-101334`. [Online]. Available: `https://doi.org/10.1146/annurev-chembioeng-060816-101334`.

[8] International Energy Agency (IEA), "Global hydrogen review 2022," International Energy Agency, Tech. Rep. 2022. [Online]. Available: `https://www.iea.org/reports/global-hydrogen-review-2022`.

[9] O. Kruk, R. Prelicz, and T. Rudolph, "Assessment of the potential, the actors and relevant business cases for large scale and seasonal storage of renewable electricity by hydrogen underground storage in europe -overview of all known underground storage technologies," HyUnder, Technical report, 2013. [Online]. Available: `https://hyunder.eu/wp-content/uploads/2016/01/D3.1_Overview-of-all-known-underground-storage-technologies.pdf`.

[10] R. Tarkowski, "Underground hydrogen storage: Characteristics and prospects," *Renewable and Sustainable Energy Reviews*, vol. 105, pp. 86–94, 2019, ISSN: 1364-0321. DOI: `https://doi.org/10.1016/j.rser.2019.01.051`. [Online]. Available: `https://www.sciencedirect.com/science/article/pii/S1364032119300528`.

[11] N. Dopffel, S. Jansen, and J. Gerritse, "Microbial side effects of underground hydrogen storage – knowledge gaps, risks and opportunities for successful implementation," *International Journal of Hydrogen Energy*, vol. 46, no. 12, pp. 8594–8606, 2021, ISSN: 0360-3199. DOI: `https://doi.org/10.1016/j.ijhydene.2020.12.058`. [Online]. Available: `https://www.sciencedirect.com/science/article/pii/S0360319920345936`.

[12] D. R. Lovley and S. Goodwin, "Hydrogen concentrations as an indicator of the predominant terminal electron-accepting reactions in aquatic sediments," *Geochimica et Cosmochimica Acta*, vol. 52, no. 12, pp. 2993–3003, 1988, ISSN: 0016-7037. DOI: `https://doi.org/10.1016/0016-7037(88)90163-9`. [Online]. Available: `https://www.sciencedirect.com/science/article/pii/0016703788901639`.

[13] M. Berta, F. Dethlefsen, M. Ebert, D. Schäfer, and A. Dahmke, "Geochemical effects of millimolar hydrogen concentrations in groundwater: An experimental study in the context of subsurface hydrogen storage," *Environmental Science & Technology*, vol. 52, no. 8, pp. 4937–4949, 2018, PMID: 29527891. DOI: `10.1021/acs.est.7b05467`. eprint: `https://doi.org/10.1021/acs.est.7b05467`. [Online]. Available: `https://doi.org/10.1021/acs.est.7b05467`.

[14] S. P. Gregory, M. J. Barnett, L. P. Field, and A. E. Milodowski, "Subsurface microbial hydrogen cycling: Natural occurrence and implications for industry," *Microorganisms*, vol. 7, no. 2, p. 53, 2019, ISSN: 2076-2607. DOI: `https://doi.org/10.3390/microorganisms7020053`. [Online]. Available: `http://www.mdpi.com/2076-2607/7/2/53`.

[15] S. H. Yousefi, R. Groenenberg, J. Koornneef, J. Juez-Larré, and M. Shahi, "Techno-economic analysis of developing an underground hydrogen storage facility in depleted gas field: A dutch case study," *International Journal of Hydrogen Energy*, 2023, ISSN: 0360-3199. DOI: `https://doi.org/10.1016/j.ijhydene.2023.04.090`. [Online]. Available: `https://www.sciencedirect.com/science/article/pii/S0360319923018256`.

[16] J. Simon, A. Ferriz, and L. Correas, "Hyunder – hydrogen underground storage at large scale: Case study spain," *Energy Procedia*, vol. 73, pp. 136–144, 2015, 9th International Renewable Energy Storage Conference, IRES 2015, ISSN: 1876-6102. DOI: `https://doi.org/10.1016/j.egypro.2015.07.661`. [Online]. Available: `https://www.sciencedirect.com/science/article/pii/S1876610215014290`.

[17] R. Tarkowski, "Perspectives of using the geological subsurface for hydrogen storage in poland," *International Journal of Hydrogen Energy*, vol. 42, no. 1, pp. 347–355, 2017, ISSN: 0360-3199. DOI: `https://doi.org/10.1016/j.ijhydene.2016.10.136`. [Online]. Available: `https://www.sciencedirect.com/science/article/pii/S036031991633230X`.

[18] R. Tarkowski and G. Czapowski, "Salt domes in poland – potential sites for hydrogen storage in caverns," *International Journal of Hydrogen Energy*, vol. 43, no. 46, pp. 21 414–21 427, 2018, ISSN: 0360-3199. DOI: `https://doi.org/10.1016/j.ijhydene.2018.09.212`. [Online]. Available: `https://www.sciencedirect.com/science/article/pii/S0360319918331410`.

[19] W. Liu, Z. Zhang, J. Chen, *et al.*, "Feasibility evaluation of large-scale underground hydrogen storage in bedded salt rocks of china: A case study in jiangsu province," *Energy*, vol. 198, p. 117 348, 2020, ISSN: 0360-5442. DOI: `https://doi.org/10.1016/j.energy.2020.117348`. [Online]. Available: `https://www.sciencedirect.com/science/article/pii/S0360544220304552`.

[20] D. Zivar, S. Kumar, and J. Foroozesh, "Underground hydrogen storage: A comprehensive review," *International Journal of Hydrogen Energy*, vol. 46, no. 45, pp. 23 436–23 462, 2021, Hydrogen Separation, Production and Storage, ISSN: 0360-3199. DOI:

https://doi.org/10.1016/j.ijhydene.2020.08.138. [Online]. Available: `https://www.sciencedirect.com/science/article/pii/S0360319920331426`.

[21]   N. Heinemann, J. Alcalde, J. M. Miocic, *et al.*, "Enabling large-scale hydrogen storage in porous media – the scientific challenges," *Energy Environ. Sci.*, vol. 14, pp. 853–864, 2 2021. DOI: `10.1039/D0EE03536J`. [Online]. Available: `http://dx.doi.org/10.1039/D0EE03536J`.

[22]   E. M. Thaysen, S. McMahon, G. J. Strobel, *et al.*, "Estimating microbial growth and hydrogen consumption in hydrogen storage in porous media," *Renewable and Sustainable Energy Reviews*, vol. 151, p. 111 481, 2021, ISSN: 1364-0321. DOI: `https://doi.org/10.1016/j.rser.2021.111481`. [Online]. Available: `https://www.sciencedirect.com/science/article/pii/S1364032121007620`.

[23]   C. Fournier, Y. Le Gallo, and J. Tremosa, "Modelling of microbial H_2 reactivity at lab and reservoir scale," 2023, A part of WP3 of the Hystories project. [Online]. Available: `https://hystories.eu/wp-content/uploads/2023/04/Hystories_D3.3-0_Modelling-of-microbial-H2-reactivity-at-lab-and-reservoir-scale.pdf`.

[24]   A. B. Dohrmann and M. Krüger, "Microbial H_2 consumption by a formation fluid from a natural gas field at high-pressure conditions relevant for underground H_2 storage," *Environmental Science & Technology*, vol. 57, no. 2, pp. 1092–1102, 2023, PMID: 36599497. DOI: `10.1021/acs.est.2c07303`. eprint: `https://doi.org/10.1021/acs.est.2c07303`. [Online]. Available: `https://doi.org/10.1021/acs.est.2c07303`.

[25]   H. B. Navaid, H. Emadi, and M. Watson, "A comprehensive literature review on the challenges associated with underground hydrogen storage," *International Journal of Hydrogen Energy*, vol. 48, no. 28, pp. 10 603–10 635, 2023, ISSN: 0360-3199. DOI: `https://doi.org/10.1016/j.ijhydene.2022.11.225`. [Online]. Available: `https://www.sciencedirect.com/science/article/pii/S0360319922055446`.

[26]   International Energy Agency (IEA), "The future of hydrogen," Paris, Technical Report IEA, 2019, License: CC BY 4.0. [Online]. Available: `https://www.iea.org/reports/the-future-of-hydrogen`.

[27]   Volvo Group. "Hydrogen: A fuel for future markets." Accessed: February 7, 2023, Volvo Group. (n.d.), [Online]. Available: `https://www.volvogroup.com/en/sustainable-transportation/sustainable-solutions/hydrogen-fuel-cells.html`.

[28]   A. Willige. "The colors of hydrogen: Expanding ways of decarbonization." Accessed: February 7, 2023, Mitsubishi Heavy Industries Group. (2021), [Online]. Available: `https://spectra.mhi.com/the-colors-of-hydrogen-expanding-ways-of-decarbonization`.

[29]   K. Mazloomi and C. Gomes, "Hydrogen as an energy carrier: Prospects and challenges," *Renewable and Sustainable Energy Reviews*, vol. 16, no. 5, pp. 3024–3033, 2012, ISSN: 1364-0321. DOI: `https://doi.org/10.1016/j.rser.2012.02.028`. [Online]. Available: `https://www.sciencedirect.com/science/article/pii/S1364032112001220`.

[30]   O. R. Hansen, "Liquid hydrogen releases show dense gas behavior," *International Journal of Hydrogen Energy*, vol. 45, no. 2, pp. 1343–1358, 2020, International Hydrogen and Fuel Cell Conference 2018, Trondheim, Norway, ISSN: 0360-3199. DOI: `https://doi.org/10.1016/j.ijhydene.2019.09.060`. [Online]. Available: `https://www.sciencedirect.com/science/article/pii/S0360319919333749`.

[31]   R. Belford, *University of Arkansas at Little Rock: Chem 1403 General Chemistry II*. LibreTexts, Figure 2.4 is taken from this book from Chapter 13.4.

[32]   S. Chabab, P. Théveneau, C. Coquelet, J. Corvisier, and P. Paricaud, "Measurements and predictive models of high-pressure H_2 solubility in brine H_2O+NaCl for underground hydrogen storage application," *International Journal of Hydrogen Energy*, vol. 45, no. 56, pp. 32 206–32 220, 2020, ISSN: 0360-3199. DOI: `https://doi.org/10.1016/j.ijhydene.2020.08.192`. [Online]. Available: `https://www.sciencedirect.com/science/article/pii/S0360319920332195`.

[33]   K. Maebashi, K. Iwadate, K. Sakai, *et al.*, "Toxicological analysis of 17 autopsy cases of hydrogen sulfide poisoning resulting from the inhalation of intentionally generated hydrogen sulfide gas," *Forensic Science International*, vol. 207, no. 1, pp. 91–95, 2011, ISSN: 0379-0738. DOI: `https://doi.org/10.1016/j.forsciint.2010.09.008`. [Online]. Available: `https://www.sciencedirect.com/science/article/pii/S0379073810004421`.

[34]   Engineering Toolbox. "Solubility of gases in water vs. temperature." Accessed: May 5, 2023. Figure 2.3 is taken from this website. (2008), [Online]. Available: `https://www.engineeringtoolbox.com/gases-solubility-water-d_1148.html`.

[35]   F. Zhang, P. Zhao, and J. Maddy, "The survey of key technologies in hydrogen energy storage," *International Journal of Hydrogen Energy*, vol. 41, no. 33, pp. 14 535–14 552, 2016, ISSN: 0360-3199. DOI: `https://doi.org/10.1016/j.ijhydene.2016.05.293`.

[Online]. Available: https://www.sciencedirect.com/science/article/pii/S0360319916318171.

[36] H. Noh, K. Kang, and Y. Seo, "Environmental and energy efficiency assessments of offshore hydrogen supply chains utilizing compressed gaseous hydrogen, liquefied hydrogen, liquid organic hydrogen carriers and ammonia," *International Journal of Hydrogen Energy*, vol. 48, no. 20, pp. 7515–7532, 2023, ISSN: 0360-3199. DOI: https://doi.org/10.1016/j.ijhydene.2022.11.085. [Online]. Available: https://www.sciencedirect.com/science/article/pii/S0360319922052983.

[37] M. Aziz, "Liquid hydrogen: A review on liquefaction, storage, transportation, and safety," *Energies*, vol. 14, no. 18, 2021, ISSN: 1996-1073. DOI: 10.3390/en14185917. [Online]. Available: https://www.mdpi.com/1996-1073/14/18/5917.

[38] E. Rivard, M. Trudeau, and K. Zaghib, "Hydrogen storage for mobility: A review," *Materials*, vol. 12, no. 12, 2019, ISSN: 1996-1944. DOI: 10.3390/ma12121973. [Online]. Available: https://www.mdpi.com/1996-1944/12/12/1973.

[39] J. Andersson and S. Grönkvist, "Large-scale storage of hydrogen," *International Journal of Hydrogen Energy*, vol. 44, no. 23, pp. 11 901–11 919, 2019, ISSN: 0360-3199. DOI: https://doi.org/10.1016/j.ijhydene.2019.03.063. [Online]. Available: https://www.sciencedirect.com/science/article/pii/S0360319919310195.

[40] M. R. Usman, "Hydrogen storage methods: Review and current status," *Renewable and Sustainable Energy Reviews*, vol. 167, p. 112 743, 2022, ISSN: 1364-0321. DOI: https://doi.org/10.1016/j.rser.2022.112743. [Online]. Available: https://www.sciencedirect.com/science/article/pii/S1364032122006311.

[41] A. Klerke, C. H. Christensen, J. K. Nørskov, and T. Vegge, "Ammonia for hydrogen storage: Challenges and opportunities," *Journal of Materials Chemistry*, vol. 18, no. 20, pp. 2285–2392, 2008, ISSN: 0959-9428. DOI: 10.1039/B720020J. [Online]. Available: http://dx.doi.org/10.1039/B720020J.

[42] M. Aziz, A. T. Wijayanta, and A. B. D. Nandiyanto, "Ammonia as effective hydrogen storage: A review on production, storage and utilization," *Energies*, vol. 13, no. 12, 2020, ISSN: 1996-1073. DOI: 10.3390/en13123062. [Online]. Available: https://www.mdpi.com/1996-1073/13/12/3062.

[43] O. H. Hansen, "Hydrogen and ammonia infrastructure - safety and risk information and guidance," Tech. Rep., 2020, [Accessed: 28.02.2023]. [Online]. Available: https://static1.squarespace.com/static/5d1c6c223c9d400001e2f407/t/5eb553d755f94d75be877403/158894183.

[44] J. Taylor, J. Alderson, K. Kalyanam, A. Lyle, and L. Phillips, "Technical and economic assessment of methods for the storage of large quantities of hydrogen," *International Journal of Hydrogen Energy*, vol. 11, no. 1, pp. 5–22, 1986, ISSN: 0360-3199. DOI: `https://doi.org/10.1016/0360-3199(86)90104-7`. [Online]. Available: `https://www.sciencedirect.com/science/article/pii/0360319986901047`.

[45] A. Aftab, A. Hassanpouryouzband, Q. Xie, L. L. Machuca, and M. Sarmadivaleh, "Toward a fundamental understanding of geological hydrogen storage," *Industrial & Engineering Chemistry Research*, vol. 61, no. 9, pp. 3233–3253, 2022. DOI: `10.1021/acs.iecr.1c04380`. eprint: `https://doi.org/10.1021/acs.iecr.1c04380`. [Online]. Available: `https://doi.org/10.1021/acs.iecr.1c04380`.

[46] D. Tiab and E. C. Donaldson, "Chapter 3 - porosity and permeability," in *Petrophysics (Third Edition)*, D. Tiab and E. C. Donaldson, Eds., Third Edition, Boston: Gulf Professional Publishing, 2012, pp. 85–219, ISBN: 978-0-12-383848-3. DOI: `https://doi.org/10.1016/B978-0-12-383848-3.00003-7`. [Online]. Available: `https://www.sciencedirect.com/science/article/pii/B9780123838483000037`.

[47] R. Tarkowski and B. Uliasz-Misiak, "Towards underground hydrogen storage: A review of barriers," *Renewable and Sustainable Energy Reviews*, vol. 162, p. 112 451, 2022, ISSN: 1364-0321. DOI: `https://doi.org/10.1016/j.rser.2022.112451`. [Online]. Available: `https://www.sciencedirect.com/science/article/pii/S1364032122003574`.

[48] N. S. Muhammed, M. B. Haq, D. A. Al Shehri, *et al.*, "Hydrogen storage in depleted gas reservoirs: A comprehensive review," *Fuel*, vol. 337, p. 127 032, 2023, ISSN: 0016-2361. DOI: `https://doi.org/10.1016/j.fuel.2022.127032`. [Online]. Available: `https://www.sciencedirect.com/science/article/pii/S001623612203856X`.

[49] A. Raza, M. Arif, G. Glatz, *et al.*, "A holistic overview of underground hydrogen storage: Influencing factors, current understanding, and outlook," *Fuel*, vol. 330, p. 125 636, 2022, ISSN: 0016-2361. DOI: `https://doi.org/10.1016/j.fuel.2022.125636`. [Online]. Available: `https://www.sciencedirect.com/science/article/pii/S0016236122024668`.

[50] S. R. Thiyagarajan, H. Emadi, A. Hussain, P. Patange, and M. Watson, "A comprehensive review of the mechanisms and efficiency of underground hydrogen storage," *Journal of Energy Storage*, vol. 51, p. 104 490, 2022, ISSN: 2352-152X. DOI: `https://doi.org/10.1016/j.est.2022.104490`. [Online]. Available: `https://www.sciencedirect.com/science/article/pii/S2352152X22005114`.

[51]   L. Louis, "Four ways to store large quantities of hydrogen," Dec. 2021. DOI: 10.2118/208178-MS.

[52]   J.-J. Dong, J.-Y. Hsu, W.-J. Wu, *et al.*, "Stress-dependence of the permeability and porosity of sandstone and shale from TCDP Hole-A," *International Journal of Rock Mechanics and Mining Sciences*, vol. 47, no. 7, pp. 1141–1157, 2010, ISSN: 1365-1609. DOI: https://doi.org/10.1016/j.ijrmms.2010.06.019. [Online]. Available: https://www.sciencedirect.com/science/article/pii/S1365160910001164.

[53]   M. Perera, "A review of underground hydrogen storage in depleted gas reservoirs: Insights into various rock-fluid interaction mechanisms and their impact on the process integrity," *Fuel*, vol. 334, p. 126 677, 2023, ISSN: 0016-2361. DOI: https://doi.org/10.1016/j.fuel.2022.126677. [Online]. Available: https://www.sciencedirect.com/science/article/pii/S0016236122035013.

[54]   N. Heinemann, J. Scafidi, G. Pickup, *et al.*, "Hydrogen storage in saline aquifers: The role of cushion gas for injection and production," *International Journal of Hydrogen Energy*, vol. 46, no. 79, pp. 39 284–39 296, 2021, ISSN: 0360-3199. DOI: https://doi.org/10.1016/j.ijhydene.2021.09.174. [Online]. Available: https://www.sciencedirect.com/science/article/pii/S0360319921037277.

[55]   A. Sainz-Garcia, E. Abarca, V. Rubi, and F. Grandia, "Assessment of feasible strategies for seasonal underground hydrogen storage in a saline aquifer," *International Journal of Hydrogen Energy*, vol. 42, no. 26, pp. 16 657–16 666, 2017, ISSN: 0360-3199. DOI: https://doi.org/10.1016/j.ijhydene.2017.05.076. [Online]. Available: https://www.sciencedirect.com/science/article/pii/S0360319917319420.

[56]   J. Williams, M. Jin, M. Bentham, G. Pickup, S. Hannis, and E. Mackay, "Modelling carbon dioxide storage within closed structures in the uk bunter sandstone formation," *International Journal of Greenhouse Gas Control*, vol. 18, pp. 38–50, 2013, ISSN: 1750-5836. DOI: https://doi.org/10.1016/j.ijggc.2013.06.015. [Online]. Available: https://www.sciencedirect.com/science/article/pii/S1750583613002636.

[57]   J. Michalski, U. Bünger, F. Crotogino, *et al.*, "Hydrogen generation by electrolysis and storage in salt caverns: Potentials, economics and systems aspects with regard to the german energy transition," *International Journal of Hydrogen Energy*, vol. 42, no. 19, pp. 13 427–13 443, 2017, Special Issue on The 21st World Hydrogen Energy Conference (WHEC 2016), 13-16 June 2016, Zaragoza, Spain, ISSN: 0360-3199. DOI: https://doi.org/10.1016/j.ijhydene.2017.02.102. [Online]. Available: https://www.sciencedirect.com/science/article/pii/S0360319917306109.

[58]   A. Rouabhi, G. Hévin, A. Soubeyran, P. Labaune, and F. Louvet, "A multiphase multicomponent modeling approach of underground salt cavern storage," *Geomechanics for Energy and the Environment*, vol. 12, pp. 21–35, 2017, ISSN: 2352-3808. DOI: `https://doi.org/10.1016/j.gete.2017.08.002`. [Online]. Available: `https://www.sciencedirect.com/science/article/pii/S2352380817300242`.

[59]   A. Lemieux, K. Sharp, and A. Shkarupin, "Preliminary assessment of underground hydrogen storage sites in ontario, canada," *International Journal of Hydrogen Energy*, vol. 44, no. 29, pp. 15 193–15 204, 2019, ISSN: 0360-3199. DOI: `https://doi.org/10.1016/j.ijhydene.2019.04.113`. [Online]. Available: `https://www.sciencedirect.com/science/article/pii/S0360319919315423`.

[60]   A. Oren, "Diversity of halophilic microorganisms: Environments, phylogeny, physiology, and applications," *Journal of Industrial Microbiology and Biotechnology*, vol. 28, no. 1, pp. 56–63, Jan. 2002, ISSN: 1367-5435. DOI: `10.1038/sj/jim/7000176`. eprint: `https://academic.oup.com/jimb/article-pdf/28/1/56/34742876/jimb0056.pdf`. [Online]. Available: `https://doi.org/10.1038/sj/jim/7000176`.

[61]   T. Hoehler and B. Jørgensen, "Microbial life under extreme energy limitation," *Nature reviews. Microbiology*, vol. 11, pp. 83–94, Feb. 2013. DOI: `10.1038/nrmicro2939`.

[62]   A. Oren, *Diversity of Halophiles*, K. Horikoshi, Ed. Tokyo: Springer Japan, 2011, pp. 309–32, ISBN: 978-4-431-53898-1. DOI: `10.1007/978-4-431-53898-1_14`. [Online]. Available: `https://doi.org/10.1007/978-4-431-53898-1_14`.

[63]   A. Oren, *Life at High Salt Concentrations*, E. Rosenberg, E. F. DeLong, S. Lory, E. Stackebrandt, and F. Thompson, Eds. Berlin, Heidelberg: Springer Berlin Heidelberg, 2013, pp. 421–440, ISBN: 978-3-642-30123-0. DOI: `10.1007/978-3-642-30123-0_57`. [Online]. Available: `https://doi.org/10.1007/978-3-642-30123-0_57`.

[64]   Z. Zhang, C. Zhang, Y. Yang, *et al.*, "A review of sulfate-reducing bacteria: Metabolism, influencing factors and application in wastewater treatment," *Journal of Cleaner Production*, vol. 376, p. 134 109, 2022, ISSN: 0959-6526. DOI: `https://doi.org/10.1016/j.jclepro.2022.134109`. [Online]. Available: `https://www.sciencedirect.com/science/article/pii/S0959652622036812`.

[65]   F. J. Millero, S. Hubinger, M. Fernandez, and S. Garnett, "Oxidation of H$_2$S in seawater as a function of temperature, ph, and ionic strength," *Environmental science & technology*, vol. 21, no. 5, pp. 439–443, 1987.

[66]   H. Wang, F. Chen, S. Mu, *et al.*, "Removal of antimony (Sb(V)) from Sb mine drainage: Biological sulfate reduction and sulfide oxidation–precipitation," *Bioresource Technology*, vol. 146, pp. 799–802, 2013, ISSN: 0960-8524. DOI: `https://doi.org/10.1016/j.biortech.2013.08.002`. [Online]. Available: `https://www.sciencedirect.com/science/article/pii/S0960852413012315`.

[67]   I. Kushkevych, D. Dordević, and M. Vítězová, "Analysis of pH dose-dependent growth of sulfate-reducing bacteria," *Open Medicine*, vol. 14, no. 1, pp. 66–74, 2019. DOI: `doi:10.1515/med-2019-0010`. [Online]. Available: `https://doi.org/10.1515/med-2019-0010`.

[68]   J. Sun, S. Hu, K. R. Sharma, B.-J. Ni, and Z. Yuan, "Stratified microbial structure and activity in sulfide- and methane-producing anaerobic sewer biofilms," *Applied and Environmental Microbiology*, vol. 80, no. 22, pp. 7042–7052, 2014. DOI: `10.1128/AEM.02146-14`. [Online]. Available: `https://journals.asm.org/doi/abs/10.1128/AEM.02146-14`.

[69]   A. E. Lewis, "Review of metal sulphide precipitation," *Hydrometallurgy*, vol. 104, no. 2, pp. 222–234, 2010, ISSN: 0304-386X. DOI: `https://doi.org/10.1016/j.hydromet.2010.06.010`. [Online]. Available: `https://www.sciencedirect.com/science/article/pii/S0304386X10001775`.

[70]   Z. Lyu, N. Shao, T. Akinyemi, and W. B. Whitman, "Methanogenesis," *Current Biology*, vol. 28, no. 13, R727–R732, 2018, ISSN: 0960-9822. DOI: `https://doi.org/10.1016/j.cub.2018.05.021`. [Online]. Available: `https://www.sciencedirect.com/science/article/pii/S0960982218306237`.

[71]   A. Oren, "Thermodynamic limits to microbial life at high salt concentrations," *Environmental Microbiology*, vol. 13, no. 8, pp. 1908–1923, 2011. DOI: `https://doi.org/10.1111/j.1462-2920.2010.02365.x`. [Online]. Available: `https://ami-journals.onlinelibrary.wiley.com/doi/abs/10.1111/j.1462-2920.2010.02365.x`.

[72]   B. Ollivier, C. E. Hatchikian, G. Prensier, J. Guezennec, and J.-L. Garcia, "Desulfohalobium retbaense gen. nov., sp. nov., a halophilic sulfate-reducing bacterium from sediments of a hypersaline lake in senegal," *International Journal of Systematic and Evolutionary Microbiology*, vol. 41, no. 1, pp. 74–81, 1991, ISSN: 1466-5034. DOI: `https://doi.org/10.1099/00207713-41-1-74`. [Online]. Available: `https://www.microbiologyresearch.org/content/journal/ijsem/10.1099/00207713-41-1-74`.

[73] B. Ollivier, M.-L. Fardeau, J.-L. Cayol, *et al.*, "Methanocalculus halotolerans gen. nov., sp. nov., isolated from an oil-producing well," *International Journal of Systematic and Evolutionary Microbiology*, vol. 48, no. 3, pp. 821–828, 1998. DOI: `https://doi.org/10.1099/00207713-48-3-821`. [Online]. Available: `https://www.microbiologyresearch.org/docserver/fulltext/ijsem/48/3/ijs-48-3-821.pdf?expires=1678104848&id=id&accname=guest&checksum=87B8B4C75164BF741F98E8E8DCEB4D7C`.

[74] P. Atkins and J. de Paula, *Atkins' Physical chemistry*, eng, 10th ed. Oxford: Oxford University Press, 2014, ISBN: 9780199697403.

[75] R. R. Ratnakar, B. Dindoruk, and A. Harvey, "Thermodynamic modeling of hydrogen-water system for high-pressure storage and mobility applications," *Journal of Natural Gas Science and Engineering*, vol. 81, p. 103 463, 2020, ISSN: 1875-5100. DOI: `https://doi.org/10.1016/j.jngse.2020.103463`. [Online]. Available: `https://www.sciencedirect.com/science/article/pii/S1875510020303176`.

[76] Microsoft. "Slope function." Accessed online: May 12, 2023, Microsoft. (n.d.), [Online]. Available: `https://support.microsoft.com/en-us/office/slope-function-11fb8f97-3117-4813-98aa-61d7e01276b9`.

[77] Microsoft. "Avedev function." Accessed online: May 12, 2023, Microsoft. (n.d.), [Online]. Available: `https://support.microsoft.com/en-us/office/avedev-function-58fe8d65-2a84-4dc7-8052-f3f87b5c6639`.

[78] D. J. Hentges, "Anaerobes: General characteristics," in *Medical Microbiology*, S. Baron, Ed., 4th, Galveston (TX): University of Texas Medical Branch at Galveston, 1996, ch. 17. [Online]. Available: `https://www.ncbi.nlm.nih.gov/books/NBK7638/`.

[79] T. T. T. Tran, K. Kannoorpatti, A. Padovan, and S. Thennadil, "Sulphate-reducing bacteria's response to extreme ph environments and the effect of their activities on microbial corrosion," *Applied Sciences*, vol. 11, no. 5, 2021, ISSN: 2076-3417. DOI: `10.3390/app11052201`. [Online]. Available: `https://www.mdpi.com/2076-3417/11/5/2201`.

[80] C. Hemme and W. van Berk, "Potential risk of H_2S generation and release in salt cavern gas storage," *Journal of Natural Gas Science and Engineering*, vol. 47, pp. 114–123, 2017, ISSN: 1875-5100. DOI: `https://doi.org/10.1016/j.jngse.2017.09.007`. [Online]. Available: `https://www.sciencedirect.com/science/article/pii/S1875510017303761`.

[81] R. Conrad, H. Schütz, and M. Babbel, "Temperature limitation of hydrogen turnover and methanogenesis in anoxic paddy soil," *FEMS Microbiology Letters*, vol. 45, no. 5, pp. 281–289, 1987, ISSN: 0378-1097. DOI: `https://doi.org/10.1016/0378-1097(87)90005-X`. [Online]. Available: `https://www.sciencedirect.com/science/article/pii/037810978790005X`.

[82] N. H. M. Yasin, T. Maeda, A. Hu, C.-P. Yu, and T. K. Wood, "CO_2 sequestration by methanogens in activated sludge for methane production," *Applied Energy*, vol. 142, pp. 426–434, 2015, ISSN: 0306-2619. DOI: `https://doi.org/10.1016/j.apenergy.2014.12.069`. [Online]. Available: `https://www.sciencedirect.com/science/article/pii/S0306261914013269`.

[83] S. Choi, K. Ko, H. Chun, and J. Kim, "- utilization of carbon dioxide for neutralization of alkaline wastewater," in *Greenhouse Gas Control Technologies - 6th International Conference*, J. Gale and Y. Kaya, Eds., Oxford: Pergamon, 2003, pp. 1871–1874, ISBN: 978-0-08-044276-1. DOI: `https://doi.org/10.1016/B978-008044276-1/50318-4`. [Online]. Available: `https://www.sciencedirect.com/science/article/pii/B9780080442761503184`.

[84] N. Liu, A. R. Kovscek, M. Fernø, and N. Dopffel, "Pore-scale study of microbial hydrogen consumption and wettability alteration during underground hydrogen storage," 2023.

[85] M. Lysyy, G. Ersland, and M. Fernø, "Pore-scale dynamics for underground porous media hydrogen storage," *Advances in Water Resources*, vol. 163, p. 104 167, 2022, ISSN: 0309-1708. DOI: `https://doi.org/10.1016/j.advwatres.2022.104167`. [Online]. Available: `https://www.sciencedirect.com/science/article/pii/S0309170822000434`.

[86] N. Liu, T. Skauge, D. Landa-Marbán, *et al.*, "Microfluidic study of effects of flow velocity and nutrient concentration on biofilm accumulation and adhesive strength in the flowing and no-flowing microchannels," *Journal of Industrial Microbiology and Biotechnology*, vol. 46, no. 6, pp. 855–868, Jun. 2019, ISSN: 1367-5435. DOI: `10.1007/s10295-019-02161-x`. [Online]. Available: `https://doi.org/10.1007/s10295-019-02161-x`.

[87] M. E. Davey, D. Gevertz, W. A. Wood, J. B. Clark, and G. E. Jenneman, "Microbial selective plugging of sandstone through stimulation of indigenous bacteria in a hypersaline oil reservoir," *Geomicrobiology Journal*, vol. 15, no. 4, pp. 335–352, 1998. DOI: `10.1080/01490459809378087`. [Online]. Available: `https://doi.org/10.1080/01490459809378087`.

[88] J. Vilcáez, L. Li, D. Wu, and S. S. Hubbard, "Reactive transport modeling of induced selective plugging by leuconostoc mesenteroides in carbonate formations," *Geomicrobiology Journal*, vol. 30, no. 9, pp. 813–828, 2013. DOI: 10.1080/01490451.2013.774074. eprint: `https://doi.org/10.1080/01490451.2013.774074`. [Online]. Available: `https://doi.org/10.1080/01490451.2013.774074`.

[89] Y. Chen, J. J. Cheng, and K. S. Creamer, "Inhibition of anaerobic digestion process: A review," *Bioresource Technology*, vol. 99, no. 10, pp. 4044–4064, 2008, ISSN: 0960-8524. DOI: `https://doi.org/10.1016/j.biortech.2007.01.057`. [Online]. Available: `https://www.sciencedirect.com/science/article/pii/S0960852407001563`.

[90] E. Ntagia, I. Chatzigiannidou, A. J. Williamson, J. B. A. Arends, and K. Rabaey, "Homoacetogenesis and microbial community composition are shaped by pH and total sulfide concentration," *Microbial Biotechnology*, vol. 13, no. 4, pp. 1026–1038, 2020. DOI: `https://doi.org/10.1111/1751-7915.13546`. eprint: `https://ami-journals.onlinelibrary.wiley.com/doi/pdf/10.1111/1751-7915.13546`. [Online]. Available: `https://ami-journals.onlinelibrary.wiley.com/doi/abs/10.1111/1751-7915.13546`.

[91] R. M. Donlan, "Biofilms: Microbial life on surfaces," *Emerging infectious diseases*, vol. 8, no. 9, p. 881, 2002. DOI: `https://doi.org/10.3201/eid0809.020063`. [Online]. Available: `https://wwwnc.cdc.gov/eid/article/8/9/02-0063_article`.

[92] H.-C. Flemming and J. Wingender, "The biofilm matrix," *Nature reviews microbiology*, vol. 8, no. 9, pp. 623–633, 2010. DOI: `https://doi.org/10.1038/nrmicro2415`. [Online]. Available: `https://www.nature.com/articles/nrmicro2415#citeas`.

[93] S. W. Taylor and P. R. Jaffé, "Biofilm growth and the related changes in the physical properties of a porous medium: 1. experimental investigation," *Water Resources Research*, vol. 26, no. 9, pp. 2153–2159, 1990. DOI: `https://doi.org/10.1029/WR026i009p02153`. eprint: `https://agupubs.onlinelibrary.wiley.com/doi/pdf/10.1029/WR026i009p02153`. [Online]. Available: `https://agupubs.onlinelibrary.wiley.com/doi/abs/10.1029/WR026i009p02153`.